Prolinases from *Lactobacillus plantarum* WCFS1: Cloning, Purification and Characterization of the Recombinant Enzymes

A Thesis Submitted to the College of Graduate Studies and Research
in Partial Fulfillment of the Requirements for the Degree of
Master of Science in the Department of
Food and Bioproduct Sciences
University of Saskatchewan
Saskatoon

By
Yanyu Huang
2014

PERMISSION TO USE STATEMENT

In presenting this thesis in partial fulfillment of the requirements for a Master of Science degree from the University of Saskatchewan, I agree that the Libraries of this University may make it freely available for inspection. I further agree that permission for copying this thesis in any manner, in whole or in part, for scholarly purposes may be granted by the professor or professors who supervised my thesis work or, in their absence, by the Head of the Department or the Dean of the College in which my thesis work was done. It is understood that any copying or publication or use of this thesis or parts thereof for financial gain shall not be allowed without written permission. It is also understood that due recognition shall be given to me and to the university of Saskatchewan in any scholarly use which may be made of any material in my thesis.

Requests for permission to copy or to make other use of material in this thesis in whole or part should be addressed to:

Head of the Department of Food and Bioproduct Sciences
University of Saskatchewan
Saskatoon, Saskatchewan S7N 5A8

ABSTRACT

Lactobacillus plantarum WCSF1 has two putative prolinases (PepR1 and PepR2), and they share only 48.5% amino acid sequence identity. To investigate the differences in enzymatic characters between two enzymes, the genes are cloned and expressed in *E. coli* using non-tagged pKK223-3 and His-tagged pET32b(+) systems. Culture conditions of overexpressed recombinant prolinases (r-PepR1 and r-PepR2) are optimized as pH7.0-7.5 LB media at 16°C with 1 mM IPTG induction. Recombinant prolinases with His-tag give higher yields and are more cost-efficient over non-tagged recombinant prolinases. After purification, these recombinant enzymes show similar hydrolysis activities towards Pro-Gly substrate, proving their nature as prolinases. Structural analyses using CD spectrum and computer modelling show that r-PepR1 and r-PepR2 share structural similarity in their secondary structure having the highest β-sheets over other components; and dynamic light scattering and gel filtration chromatography analyses indicate their quaternary structure being homotetrameric. Structural similarity can be linked to enzyme function feature. The two enzymes have the same enzymatic functionality may be due to their structural similarity. Despite for their structural similarities and the same enzymatic functionality, they show differences in their substrate specificity, optimum temperature and pH, kinetic parameters (K_m and k_{cat} values), thermal stability, and proteolysis mode. r-PepR1 has its optimal activity at 25°C pH7.5 against substrate Pro-Met, whereas r-PepR2 is most active at 30°C pH8.0 against Pro-Gly. r-PepR1 has a low thermal stability with a T_M (the midpoint temperature of the unfolding transition) at 29°C, whereas r-PepR2 has a higher T_M at 48°C. However, r-PepR1 is aggregated and inactivated at near physiological temperature (42°C). The catalytic mode of r-PepR1 could be a metallo-protease since its activity reduces by 38% with a metal-chelating agent EDTA; while the activity of r-PepR2 is inhibited by 47% with a serine protease inhibitor PMSF, suggesting it is a serine protease. These isozymes cooperatively and complementarily work together to hydrolyze proline-containing peptides, showing broader specificity, broader range of working pH and temperature, and higher efficiency, suggesting that the proline recycling are mediated through these two enzymes to adapt a wide rage of environmental conditions.

TABLE OF CONTENTS

ACKNOWLEDGEMENTS

My first and sincere appreciation goes to Dr. Takuji Tanaka, without whose support, encouragement and patience this accomplishment would not have been possible. I would like to thank him for all I have learned from him, for his continuous enlightening instructions in all stages of this thesis, and for his help to build up my self-discipline, self-motivation and self-confidence.

I also thank my advisory committees with my deep gratitude and respect to Dr. Robert Tyler, Dr. Xiao Qiu for their precious academic advices on my thesis.

I thank Dr. Scott Napper for graciously acting as my external examiner, and his feedback in the final stages of my thesis editing was invaluable.

Special thanks to my dear lab mates, Tae Sun Kang, Oarabile Michael Kgosisejo, Timothy Howdeshell, and Douglas Grahame for advise, friendship and good conversation made my time in the lab most enjoyable.

I am grateful to Ann Harley and Patricia Olesiuk for their help on personal and administrative works.

I am also indebted to my family for their constant love, encouragement and support.

LIST OF TABLES

LIST OF FIGURES

LIST OF ABBREVIATIONS

APP	aminopeptidase P
BSA	bovine serum albumin
CD	circular dichroism
CPP	carboxypeptidase P
DPP II	dipeptidyl peptidase II
DPP IV	dipeptidyl peptidase IV
DTT	Dithiothreitol
DLS	dynamic light scattering
dNTP	deoxynucleotide triphosphate
EDTA	ethylene diamine tetra acetic acid
IPTG	isopropyl β-D-1-thiogalactopyranoside
kD	Kilodalton
K_m	Michaelis-Menten constant
LAB	lactic acid bacteria
LB	Luria-Bertani broth
MAL	2,5-pyrroledione
MW	molecular weight
p-value	the probability of obtaining a result
PCR	polymerase chain reaction
PDB	Protein Data Bank
PCP	prolyl carboxypeptidase
PepI	proline iminopeptidase
PepL	Aminopeptidase
*pep*R	prolinase coding gene
PepR	Prolinase
pHMB	*p*-hydroxymercuribenzoate
PMSF	Phenylmethanesulfonylfluoride
PrtP	cell envelope-associated proteinase
R_{caf}	the ratio to caffeine

rpm	revolutions per minute
r-PepR	recombinant prolinase
SAP	shrimp alkaline phosphatase
SDS-PAGE	sodium dodecyl sulphate polyacrylamide gel electrophoresis
TEMED	N, N, N', N'-tetramethylethylenediamine
TH.V	threshold value
T_M	the midpoint temperature of unfolding transition
v	Velocity
V_{max}	maximum velocity
Xaa	amino acid

1 INTRODUCTION

Cheese flavor is developed as a consequence of enzymatic processes involving proteolysis. Proteolysis is the most important primary biochemical event that occurs in the most cheeses during ripening (McSweeney, 2004). Proteolysis in cheese manufacture leads to hydrolysis of casein (the most abundant milk protein) generating a mixture of small peptides and amino acids. This proteolysis contributes to the softening of texture, and conferring taste and mouth feel characteristics on cheese. However, proteolysis also introduces unfavourable bitter peptides, proline-containing peptides in particular since proline residues compose about 10.5% in casein, which is twice as much as the average in other proteins.

The role of proline residues in the bitter taste of peptides has been investigated by Ishibashi *et al*. (1987 and 1988). Proline-containing peptides deliver bitterness depending on the conformational alternation in the peptide molecule folding the peptide skeleton due to the unique cyclic structure of proline residues. The cyclic structure is formed with its side chain being bonded to both its nitrogen and α-carbon as an imino ring. Due to the limited rotation of proline caused by the cyclic attribute, proline is the only amino acid incompatible with α-helix or β-sheet secondary structures (Damina *et al*., 1997). This distinguished structure has proline residues within polypeptides acting as structural elements restraining the susceptibility of polypeptide chain to proteolysis. It allows proline residues to protect biologically active peptides against enzymatic degradation (Damina *et al*., 1997). In fermented food, restrained susceptibility of hydrolyzing proline-containing peptides leads to gathering of bitterness as a result from accumulation of the proline-containing peptides. In cheese manufacturing, bitterness from proline-containing peptides can be alleviated with prolinase, which involves in final hydrolysis of proline-containing peptides (iminodipeptides with N-terminal proline or hydroxyproline: i.e. Pro-Xaa).

Moreover, prolinase can also be utilized as clinical treatment to compensate prolidase activity in prolidase deficient disease which is a rare inherited metabolic disorder. The disorder

leads to considerable loss of free proline and hydroxyproline in urine (Milligan *et al.,* 1989). Investigations have been done to screen for deficient activity of prolidase and estimate the activity of prolinase. Prolinase activity is reported to increase in the plasma of prolidase-deficient patients (Myara and Stalder, 1986) and in prolidase-deficient fibroblasts (Miech *et al.,* 1988). Prolinase activity is higher in prolidase-deficient cells than in normal control cells (Miech *et al.*, 1988) because prolinase is one of two major enzymes (prolinase and prolidase) that produce free proline. Prolinase has an ability to maintain the same level of proline in prolidase-deficient fibroblast as in normal cells. Prolinase is, therefore, not only beneficial for debittering in fermented food manufacturing, but also providing assistance towards the patients with prolidase deficiency.

Investigations on prolinase characteristic features are necessary for the potential of applying this peptidase in debittering process as well as to understand fundamental differences of this proline specific peptidase from other peptidases. This research aimed to clone the prolinase genes *pep*R1 and *pep*R2 from *Lactobacillus plantarum* WCFS1, and to characterize the enzyme features including substrate specificity, pH dependence, temperature dependency, thermal stability, enzyme kinetics, proteolysis mode, protein secondary, tertiary (also known as three-dimensional structure) and quaternary structures.

2 LITERATURE REVIEW

2.1 Applications of prolinase in cheese proteolysis for debittering

2.1.1 Proteolysis in cheese ripening

Cheese is a fermented food derived from milk, which is massively consumed all over the world. Cheese is with high commercial values because it enriches human diet by providing and preserving quantities of nutrient (such as fat, protein, calcium, and phosphorus) in a wide diversity of flavour, aromas and texture (Steinkraus, 1994). Cheese ripening consists of a series of events: chemical, enzymatic and microbiological events. These events are the results of biochemical activity occurring in cheese and contribute to the diversity of cheese products. Three primary biochemical reactions contribute to cheese ripening: glycolysis, lipolysis and proteolysis (Cogan and Beresford, 2002). Glycolysis is the conversion of lactose to lactic acid during the growth of microorganisms. Lipolysis leads to hydrolysis of the milk fat and production of glycerol and free fatty acids, many of which, particularly short-chain ones, have strong characteristic flavour. Proteolysis breaks down protein network that affects the texture, and generates short peptides and free amino acids, which imparts flavour to cheese.

Among these biochemical reactions, proteolysis is considered to be the most complex and the key aspect of cheese manufacture (Cogan and Beresford, 2002; McSweeney, 2004). Because of the significance of proteolysis, proteolysis and the enzymes responsible for this process have been reviewed comprehensively over the past three decades (Grappin *et al*., 1985; Rank *et al*., 1985; Fox, 1989; Fox and Law, 1991; Fox and McSweeney 1996, 1997; Sousa *et al*., 2001; Upadhyay *et al.*, 2004). Proteolysis directly contributes to generation of short peptides and amino acids by hydrolysis of casein (the most abundant milk protein) and indirectly contributes to softening of texture, development of the typical cheese flavour during cheese ripening.

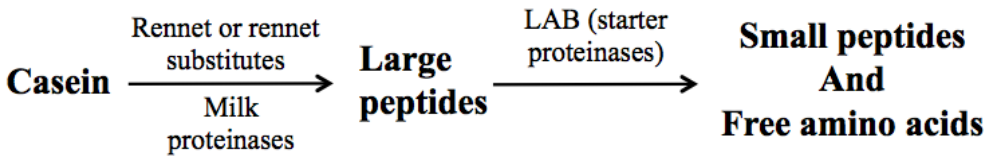

Fig. 2-1 Proteolytic agents in cheese during ripening.

In cheese proteolysis, three main groups of agents are responsible for the degradation of casein: rennet or rennet substitutes (i.e., chymosin, pepsin), indigenous milk enzymes (plasmin and other somatic cell proteinases, such as cathepsins B, D, G, H, L and elastase), enzymes from starter bacteria (lactic acid bacteria (LAB), such as *Lactococcus, Lactobacillus, Streptococcus*) (McSweeney and Sousa, 2000; Fox, 1989; Visser, 1977) (Fig. 2-1). Among rennet or rennet substitutes, chymosin (EC 3.4.23.4) is the dominant proteinase with 88-94% of milk clotting activity, and the remainder being pepsin (EC 3.4.23.1) with 6-12% of milk clotting activity (Rothe *et al.*, 1977). Rennet or rennet substitutes initially hydrolyze casein through attacking a specific Phe-Met bond of the micelle-stabilized casein during coagulation of milk. The major indigenous milk proteinase, plasmin (EC 3.4.21.7) is also associated with casein micelles. Plasmin and other somatic cell proteinases continue on hydrolyzing casein to a lesser extent, resulting in formation of large-sized water-insoluble and intermediate-sized water-soluble peptides. These peptides are subsequently degraded by proteinases and peptidases from starter bacteria. The starter LAB has a complex proteolytic system with a composition of a cell envelope-associated proteinase (PrtP) and a range of intracellular proteinases and, more importantly, peptidases. The proteinases and peptidases of LAB are indispensible for cheese ripening since these enzymes eventually release small peptides and free amino acids. For cheese varieties, secondary starters are added to supply extra proteolytic actions. The secondary starters have diverse ranges of functions depending on the organisms used, leading to the variety of cheese. The variety of cheese is characterized by the final products of proteolysis: liberation of different peptides, various concentrations of free amino acids, and their transformation to metabolic end-products (volatile flavour compounds and fatty acids).

2.1.2 Proline structural aspects

Proline is unique among the 20 amino acids because it has no primary amino group but a cyclic structure called imino ring. The imino ring is formed with the side chain of proline being bonded to both its nitrogen and α-carbon atom. With the limited rotation of proline caused by the cyclic structure, proline leads to a fixed bend into the peptide chain that is a potent repeated structure breaker, and tends to change the direction of peptide chains (Cunningham and O'Connor, 1997). Therefore, proline is the only amino acid not compatible with α-helix secondary structures, but it can be compatible with β-sheets (Damina *et al*., 1997). This distinguished structural characteristic of proline imposes many restrictions on the conformation aspects of proline-containing peptides and proteins, and confers particular biological properties. One of biological properties is offering protection against enzymatic degradation. Proline residues within polypeptide can act as structural elements restraining the susceptibility of polypeptide chain to proteolytic hydrolysis. In brief, the unique ring structure of proline distinguishes it from other amino acids in terms of rigidity, chemical stability, and biochemical reactions.

2.1.3 Richness of proline in milk proteins

Casein is one of proline-rich proteins and is most abundant milk protein, making up 80% of the protein in bovine milk (Andrews, 1983). Casein contains 10.5% of proline residues two-times more than other residues (Tristram, 1946; Dunn *et al.*, 1949). Proteolysis of proline-rich proteins results in the release of proline-containing peptides (Table 2-1). However, further hydrolysis of proline-containing peptides is restricted, owing to the particular conformation of proline residues.

Table 2-1 Amount of proline residue in proline-rich proteins, (adapt from Troll and Lindsley, 1955)

Proteins	Amount of proline residue
Bovine serum albumin	4.95 ± 0.03[a]
Casein	11.2 ± 0.05[a]
Bovine Achilles tendon	12.8 ± 0.0[a]
Horse Achilles tendon	12.9 ± 0.1[a]
Carp ichthyocol	11.1 ± 0.1[a]
Plasma	4.12 ± 0.03[b]
Hydrolyzed urine	69.9 ± 0.2[c]

[a] g in per 100 g of protein
[b] g in per 100 mL
[c] g of excreted per day

2.1.4 Bitterness of proline-containing peptides in casein

Bitterness is regarded as a flavour defect and limits acceptance of cheese, which may lead to an economic problem in cheese manufacture. Bitterness is encountered frequently in Cheddar and Gouda cheeses, and results from the accumulation of bitter-tasting peptides produced by proteolysis of casein (Lemieux and Simard, 1991). Generally, large peptides in casein do not contribute directly to cheese flavour, but are imperative to the development of cheese texture. However, large peptides can be hydrolyzed by proteinases to shorter and flavoured peptides, which includes bitterness. Bitterness of peptides has been investigated in peptides ranging in size from 2 to 23 residues. It has been shown that dipeptides containing neutral amino acids with either large alkyl groups ($\geq C_3$) or a combination of large and small ($\leq C_2$) alkyl groups, neutral and aromatic amino acids are bitter (Kirimura *et al.*, 1969). The bitter peptides are assumed to have a ratio of aliphatic to acidic amino acids of 0.8-1.3 (Edwards and Kosikowski, 1983). Lemieux and Simard showed that formation of bitterness could be due to peptides containing a high proportion of hydrophobic side-chains, proline for instance (1969). However, hydrophobicity of proline does not fully explain the bitterness in casein (Manning and Nursten, 1985). It is confirmed by synthesizing di- and tripeptides containing proline residues that a proline residue promotes bitter taste intensity of peptides only when they have both proline and amino acid containing more than 5 carbons (Shiraishi *et al.*, 1973; Shinoda *et al.*, 1986). It

indicates that the most significant role of a proline residue in peptide bitterness does not rely on its hydrophobic character. Instead, bitterness is exhibited as a result of the conformational alteration of the folding peptide backbone caused by the imino ring of proline molecule. As casein is rich in proline residue, the intensive amount of proline residues acts as a bitter taste determinant in casein lysate (Ishibashi *et al*., 1998). A list of bitter peptides containing proline residues have been isolated and identified from casein lysate and characterized for their bitterness (Table 2-2 and Table 2-3). In these tables, TH.V represents the taste threshold value which is a quantitative factor of taste. For instance, caffeine has a distinct bitter taste with a TH.V of 1.0 mM, indicating that caffeine delivers bitterness with a concentration more than 1.0 mM (Keast and Roper, 2007). R_{caf} is the ratio of peptide bitterness to caffeine. R_{caf} is obtained by dividing the threshold value (TH.V) of caffeine (1.0) by those of peptides. For example, caffeine needs 0.03 parts of Pro-Phe to show an equivalent bitter taste (Tamura *et al.*, 1990). Most of the bitter peptides shown in these tables are derived from the middle portion of β-casein, and some others from the C-terminal portions of α_{s1}- and β-caseins. These bitter peptides slowly accumulate in cheese and contribute to bitter taste in time. Characterization of bitter peptides facilitates alleviation of bitterness from cheese by further enzymatic hydrolysis.

Table 2-2. Bitterness of proline-containing peptides from casein fractions (adapted from Lemieux and Simard, 1992).

Origin	Peptide sequence	TH. V[1] (mM)	R_{caf}[2]	Ref
β-casein: 60-66	Tyr-Pro-Phe-Pro-Gly-Pro-Ile	----	6.3	Kanehisa *et al*., 1984 Shinoda *et al*., 1985;1986
β-casein: 61-66	Pro-Phe-Pro-Gly-Pro-Ile	0.44	2.3	Shinoda *et al*., 1985; 1986
β-casein: 61-67	Pro-Phe-Pro-Gly-Pro-Ile-Pro	0.25	4.0	Kanehisa *et al*., 1984
β-casein: 82-88	Val-Val-Val-Pro-Pro-Phe-Leu	0.14	7.1	Shinoda *et al*., 1985; 1986
β-casein: 82-90	Val-Val-Val-Pro-Pro-Phe-Leu-Gln-Pro	0.38	2.6	Shinoda *et al*., 1985;
β-casein: 196-201	Pro-Val-Leu-Gly-Pro-Val	0.50	2.0	Shinoda *et al*., 1985; 1986
β-casein: 196-209	Pro-Val-Leu-Gly-Pro-Val-Arg-Gly-Pro-Phe-Pro-Ile-Ile-Val	0.0149	67.0	Shinoda *et al*., 1985; 1986
β-casein: 200-209	Pro-Val-Arg-Gly-Pro-Phe-Pro-Ile-Ile-Val	0.004	250.0	Shinoda *et al*., 1985; 1986
β-casein: 202-209	Arg-Gly-Pro-Phe-Pro-Ile-Ile-Val	0.004	250.0	Shinoda *et al*., 1985; 1986
β-casein: 203-209	Gly-Pro-Phe-Pro-Ile-Ile-Val	0.17-0.34	5.88-2.94	Hashimoto *et al*., 1980
β-casein: 204-209	Pro-Phe-Pro-Ile-Ile-Val	0.125	8.0	Shinoda *et al*., 1985
β-casein[3]	Arg-Gly-Pro-Pro-Phe-Ile-Val (BPI-a)	0.05	20.0	Fukui *et al*., 1983; Miyake *et al*., 1983; Otagiri *et al*., 1983; 1985; Nosho *et al*., 1985
β-casein	Arg-Pro-Phe-Phe[4]	0.04	25.0	Nosho *et al*., 1985
β-casein	Arg-Gly-Pro-Pro-Phe-Ile	0.025	40.0	Shinoda *et al*., 1986

[1] TH. V = threshold value;
[2] R_{caf} = the ratio to caffeine;
[3] possibly from the C-terminal sequence of β-casein (Ribadeau-Dumas *et al*., 1972);
[4] this tetrapeptide produces a bitter taste that corresponds to that of PBI-a; however, its molecular weight is only about half that of BPI-a.

Table 2-3 Bitterness of short peptides containing proline residue (adapted from Kirimura *et al.*, 1969; Fujimaki *et al.*, 1970; Matoba *et al*., 1970).

Peptide	Taste	TH. V (mM)[1]	R_{caf}[2]
Pro-Gly	Flat	----	----
Pro-Phe	Bitter	38	0.03
Pro-Lys	Bitter	6	0.17
Pro-Pro	Bitter	4.5	0.22
Pro-Arg	Bitter	3	0.33
Tyr-Pro	Bitter	19	0.05
Gly-Pro	Bitter	6	0.17
Lys-Pro	Bitter	3	0.33
Phe-Pro	Bitter	1.5	0.67
Orn-Pro	Bitter	1.2	0.83
Arg-Pro	Bitter	0.8	1.25
Pro-Gly-Arg	Bitter	25	0.04
Gly-Pro-Gly	Bitter	20	0.05
Arg-Gly-Pro	Bitter	13	0.08
Gly-Gly-Pro	Bitter	9.5	0.11
Pro-Gly-Pro	Bitter	9.5	0.11
Pro-Pro-Gly	Bitter	9.5	0.11
Pro-Gly-Gly	Bitter	4.5	0.22
Phe-Pro-Pro	Bitter	4.5	0.22
Phe-Pro-Lys	Bitter	3	0.33
Lys-Pro-Lys	Bitter	3	0.33
Val-Tyr-Pro	Bitter	3.0	0.33
Pro-Gly-Ile	Bitter	2.3	0.43
Pro-Pro-Phe	Bitter	2.3	0.43
Pro-Pro-Pro	Bitter	2.0	0.50
Arg-Pro-Gly	Bitter	0.8	1.25
Gly-Arg-Pro	Bitter	0.8	1.25
Pro-Phe-Pro	Bitter	0.4	2.50
Phe-Pro-Phe	Bitter	0.4	2.50
Lys-Pro-Phe	Bitter	0.4	2.50
Tyr-Pro-Phe	Bitter	0.3	3.30
Pro-Phe-Pro-Pro	Bitter	4.5	0.22
Phe-Phe-Pro-Pro	Bitter	3.0	0.33
Gly-Pro-Pro-Phe	Bitter	3.0	0.33

[1] TH. V = threshold value;
[2] R_{caf} = the ratio to caffeine.

2.1.5 Proline specific peptidases for hydrolysis of proline-containing peptides

The unique cyclic imino structure of proline not only influences the conformation of peptide backbone, but also restricts the access of peptidases. Hydrolysis of proline-containing peptides can only be achieved by proline-specific peptidases. A variety of proline-specific peptidases has been reported from various sources, such as prolyl oligopeptidase (EC 3.4.21.26), PepF (EC: 3.4.24.70), PepO (not yet received an enzyme classification number (Christensson *et al.*, 2002)), dipeptidyl peptidase IV (DPP IV, EC 3.4.14.5), dipeptidyl peptidase II (DPP II, EC 3.4.14.2), aminopeptidase P (APP, EC 3.4.11.9), PepN (EC 3.4.13.18), PepA (EC 3.4.11.1), PepC (EC 3.4.22.40), proline iminopeptidase (PepI, EC 3.4.11.5), prolyl carboxypeptidase (PCP, EC 3.4.16.2), carboxypeptidase P (CPP, EC 3.4.16.2/EC 3.4.17.16), PepX (EC 3.4.14.5), prolidase (EC 3.4.13.9), and prolinase (EC 3.4.13.8).

Prolyl oligopeptidase is an endopeptidase targeted the carboxyl side of proline residues within peptides (Koida and Walter, 1976). Prolyl oligopeptidase cleaves Pro-Xaa bonds in peptides that consist of an acyl-Yaa-Pro-Xaa sequence (Xaa can be any amino acid, Yaa is an aliphatic amino acid) (Wilk, 1983; Nomura, 1986). Cleavage cannot be completed if a free α-amine exists in the N-terminal sequence Yaa-Pro-Xaa or Pro-Xaa. PepF is generally responsible for degradation of peptides containing between 7 and 17 amino acids with a rather wide substrate specificity (Monnet *et al.*, 1994). PepO is reported to hydrolyze peptides in length range from 5 to 35 residues (Tan *et al.*, 1991; Pritchard *et al.*, 1994; Stepaniak and Fox 1995; Lian *et al.*, 1996). Dipeptidyl peptidase IV (DPP IV) removes dipeptides from substrates consisting of three or more amino acid residues or dipeptides bonded to C-terminal chromogenic or fluorogenic compounds, such as 2-naphthylamides or methylcoumarin amides (Yaron and Naider, 1993). DPP IV prefers a proline residue at the P_1 position, but it could be substituted by alanine or hydroxyproline with lower enzyme activities. However, the bond between P_1 proline and P_1' proline cannot be cleaved with DPP IV (Puschel *et al.*, 1982; Fischer *et al.*, 1983). Dipeptidyl peptidase II (DPP II) is similar to DPP IV, removing N-terminal dipeptides from substrates, but the substrate can be a general sequence consisting of Xaa-Pro-Xaa. DPP II has the highest enzyme activity against tripeptides, decreased activity towards tetrapeptides and without any activity against substrates with more than four residues (Fukasawa *et al.*, 1983; Eisenhauer *et al.*, 1986). Aminopeptidase P (APP) is an exopeptidase for the specific cleavage of N-terminal amino acid (P_1) and penultimate proline (P_1') peptide bonds in both short and long peptides (Yaron and

Berger, 1970). The N-terminal amino acid must have a free amino group, and the penultimate residue must be proline. PepN can cleave N-terminal amino acid from a broad range of peptides. Substrates of PepN from *L. lactis* can be oligo-, di- and tripeptides (Baankreis and Exterkate, 1991; Miyakawa *et al.*, 1992; Tan and Konings, 1990). PepA can trim off N-terminal amino acid from peptides with two to six residues. PepA has preference for L-amino acids at the P_1 position (Matheson *et al.*, 1970). PepC hydrolyzes a wide range of *p*-nitroaniline derivatives, dipeptides and several tripeptides containing basic amino acids (Arg, Lys), Pro, Met, Leu, Phe residues at the N-terminal position (De Palencia, 2000). Proline iminopeptidase (PepI) is a specific exopeptidase exclusively releasing the N-terminal proline residue from peptides of any length. PepI has a high specificity against di- or tripeptides with the N-terminal proline residue, but it is incapable of hydrolyzing peptides with a N-terminal hydroxyl proline residue (Sarid *et al.*, 1962). Prolyl carboxypeptidase (PCP) cleaves the last amino acid at the C-terminal part of peptides if the substrate contains a proline at the ultimate (P_1) position (Kumamoto, 1981). PCP may belong to prolyl oligopeptidase family according to sequence comparisons conducted by Tan and Morris (1993). Carboxypeptidase P (CPP) is similar to PCP, removing the last C-terminal residue from peptides with a preference for proline residue at the P_1 position. CPP has relatively broader substrate specificity than PCP. CPP hydrolyzes peptides with alanine or glycine substitution of proline at P_1 position (Hedeager-Sorensen and Kenny, 1985). PepX cleaves dipeptidyl residues from peptides by hydrolyzing the peptide bond at the carboxyl side of the proline residue when proline is the penultimate N-terminal residue (Vesanto *et al.*, 1995). The smallest proline-containing peptides (i.e. dipeptides) are hydrolyzed by two enzymes: prolidase and prolinase. Prolidase hydrolyzes dipeptides in which the C-terminal residue is proline and the N-terminal residue is an amino acid with a free α-amino group (Xaa-Pro). Prolinase splits iminodipeptides with N-terminal proline or hydroxyproline (i.e. Pro-Xaa). Both prolidase and prolinase hydrolyze dipeptides containing proline or hydroxyproline, but their specificities are distinguished by proline or hydroxyproline position in the peptide chain, and they are responsible to liberate proline for recycling (Fig. 2-2). The substrate specificities of these proline specific peptidases are summarized in Table 2-4.

Table 2-4 Different proline specific peptidases and their hydrolysis position in proline-containing peptides.

Peptidases[1]	Cleavage site	Other residues accepted Pro	Other residues accepted Xaa*	Chain length (No. of residues)
Enodopeptidases				
Prolyl endopeptidase (PepF)	-**Pro**-|-Xaa*- or -Xaa*-|-**Pro**-	----	≠Pro	4-17
Oligopeptidase PepO				5-30
Exopeptidases				
Prolyl aminopeptidase	**Pro**-|-Xaa*-	----	Hydrophobic	2-4
Aminopeptidases P (APP), PepN, PepA, PepC	Xaa*-|-**Pro**-	Hyp	≠Pro	3-9
Dipeptidyl peptidase II	Xaa-**Pro**-|-Xaa*-	Ala	Any	3-11
Dipeptidyl peptidase IV	Xaa-**Pro**-|-Xaa*-	Ala, Hyp	≠Pro ≠ Hyp	3-200
Proline iminopeptidase (PepI)	**Pro**-|-Xaa-Xaa			
Prolyl carboxypeptidase (PCP)	-**Pro**-|-Xaa*	----	≠Pro, hydrophobic	≥3
carboxypeptidase P (CPP)	-**Pro**-|-Xaa*	Ala, Gly, Hyp	≠Pro	2-7
X-prlydipeptidyl aminopeptidase (PepX)	Xaa-**Pro**-|-Xaa-Xaa-			
Dipeptidases				
Prolidase (PepQ)	Xaa*-|-**Pro**	Hyp	Any	2
Prolinase (PepR)	**Pro**-|-Xaa*	Hyp	≠Pro	2

[1] This table (adapted from Cunnngham and O'Connor, 1997; Upadhyay *et al.*, 2004; Mentlein, 1988) demonstrates hydrolysis sites in proline-containing peptides or proteins by different enzymes.

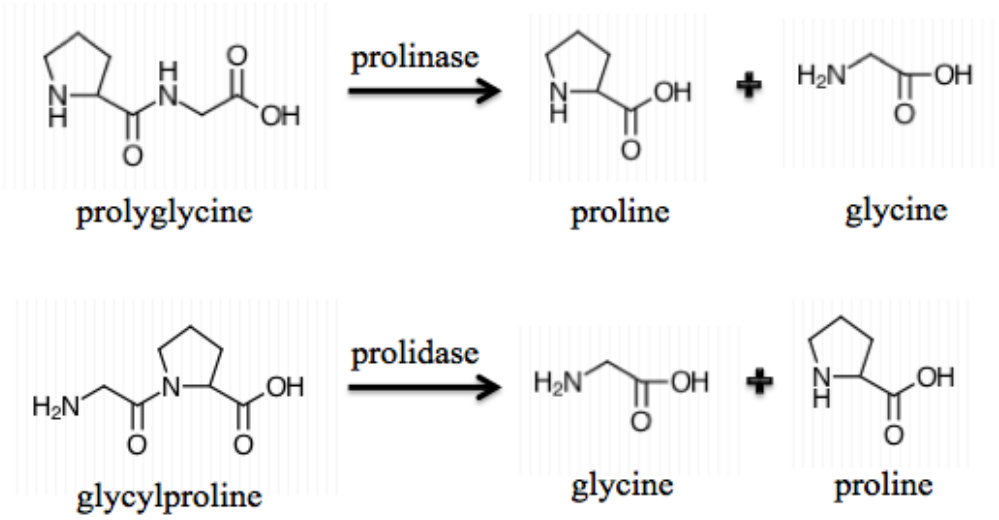

Fig. 2-2 Hydrolytic reactions of prolinase and prolidase by using Pro-Gly and Gly-Pro as substrates respectively

2.2 Characteristics of prolinase

2.2.1 General characteristic

2.2.1.1 Identification

Prolinase is found in yeast (Grassmann *et al.*, 1929), in glycerol extracts of several animal tissues (Grassmann *et al.*, 1932), in aqueous extracts of muscle tissue (Berger and Johnson, 1940), swine kidney (Sarid *et al.*, 1962), bovine kidney (Akrawi and Bailey, 1976), human kidney (Priestman and Butterworth, 1985), human plasma (Myara and Stalder, 1986), human skin fibroblasts (Priestman and Butterworth, 1982; Miech *et al.*, 1988), human prostate (Masuda *et al.*, 1994). Recombinant forms of prolinase (PepR) have been purified and characterized from *Lactobacillus helveticus* CNRZ32 (Shao *et al.*, 1997), *Lactobacillus helveticus* strain 53/7 (Luoma, 2001), *Lactobacillus rhamnosus* (Varmanen *et al.*, 1998). Prolinase is regarded as a cytoplasm protein because there is no essential signal element such as trans-membrane or membrane-associated helices or hydrophobic segments (Pekka *et al*., 1998).

Prolinase is encoded by gene *pepR*. The gene *pepR* (912 bp) from *Lactobacillus helveticus* expresses a 35.1-kDa protein. This protein shares amino acid sequence similarities of 37%, 40% and 40% with iminopeptidases (PepI) from *Bacillus coagulans* (Varmanen *et al.*, 1996),

Lactobacillus delbrueckii subsp. *bulgaricus* (Kitazono *et al.*, 1992; Atlan *et al.*, 1994) and *Lactobacillus delbrueckii* subsp. *lactis* (Klein *et al.*, 1994), respectively. PepR from *Lactobacillus helveticus* CNRZ32 exhibits a molecular mass of 33 kDa (Shao *et al.*, 1996). The native molecular mass of this PepR has been determined to be 125 kDa by gel filtration. It indicates that this PepR is a tetramer. Gene *pepR* (903 bp) from *Lactobacillus rhamnosus* (Varmanen *et al.*, 1998) encodes a 34.2-kDa protein with 68% identity to the PepR protein from *Lactobacillus helveticus.* The *Lactobacillus rhamnosus pepR* is expressed both as mono- and dicistronic transcriptional units. PepR from *Lactobacillus helveticus* CNRZ32 is observed to have optimum activity between 45 to 50°C and pH 6.0 to 6.5, its isoelectric point is determined to be 4.5 (Shao *et al.*, 1996). PepR from bovine kidney (Akrawi and Bailey, 1976) has optimum activity at pH 8.75 and an isoelectric point of 4.25. PepR from swine kidney (Dehm and Nordwig, 1970) shows its pI at 4.3 on isoelectric focusing and optimum activity at pH 8.0. The pI value of human kidney PepR is 5.4 (Butterworth and Priestman, 1984). Prolinase from various sources are purified and characterized into different degrees and some of the characteristics (including: native molecular weight, subunit molecular weight, isoelectric point (pI), the optimum pH, the optimum temperature) are summarized in Table 2-5. The table shows that prolinases share similar pI values but vary in size and optimum pH.

Prolinase is found in many bacteria and mammals. Interestingly the occurrence of prolinases differs between mammals and microorganisms. Mammals have at least two forms of prolinases, such as found in human prostate (Masuda *et al.*, 1994), human skin fibroblasts (Butterworth and Priestman, 1982), human erythrocyte (Wang *et al.*, 2004), human leukocytes (Kodama *et al.*, 1989), and bovine kidneys (Neuman and Smith, 1951; Sarid *et al.*, 1962); whereas two forms of prolinases in microorganism have not been reported or investigated yet except *Lactobacillus plantarum* WCFS1. The genome sequence of *Lactobacillus plantarum* WCFS1 shows two putative prolinase genes. They (*Lactobacillus plantarum pep*R1 and *pep*R2) share 55.5% of DNA identity and their deduced amino acid sequence shared 48.5% identity, implicating their distance. Despite their differences, they both conserve high peptide sequence homology with prolinases in other lactobacilli prolinases (pepR). *L. plantarum* PepR1 has 84%, 84%, and 83% identities with PepR from *L. zeae* ATCC393 (Accession Number: BAF85818.1), *L. rhamnosus* ATCC14957 (Accession Number: BAF85816.1), *L. zeae* DSM20178 (Accession Number: BAF85817.1), respectively; while PepR2 shows 51% with the above three PepR. Thus both

*pep*R1 and *pep*R2 are assumed to code prolinases. The amino acid sequence alignment of *pep*R1 and *pep*R2 is shown in Fig. 2-3, and they share 67% similarity.

2.2.2 Substrate specificity

Prolinase (PepR) of *L.s helveticus* is a strict iminodipeptidase with no or limited hydrolytic activity against tri- and larger peptides. Prolinase is unable to hydrolyze peptides Pro-Gly-Gly, Pro-Pro-Pro, Pro-Phe-Gly-Lys, or Pro-His-Pro-Phe-His-Phe-Phe-Val-Tyr-Lys (Sarid *et al.*, 1962; Varmanen *et al.*, 1996). Prolinase has significant activity against Pro-Leu (~95%), Pro-Met (~90%), Thr-Leu (~90%), Pro-Phe (80%), Gly-Leu (55%), and Met-Ala (30%) (Varmanen *et al.*, 1998). Hydrolysis activities against different substrates have been tested to show these peptides are hydrolyzed by prolinase. The hydrolysis activities are compared in Table 2-6, using control strain (*L. helveticus* CNRZ32) and prolinase-deficient strain (*L. helveticus* JLS221) (Shao *et al.*, 1997). The activity of control-PepR positive strain against each substrate is normalized to 100% and compared with the activity of the PepR negative strain. For instance, PepR negative strain only show 6.73% ± 1.02% activity towards Pro-Leu. It implicates the lack of PepR leading to a significant reduced hydrolysis activity of Pro-Leu.

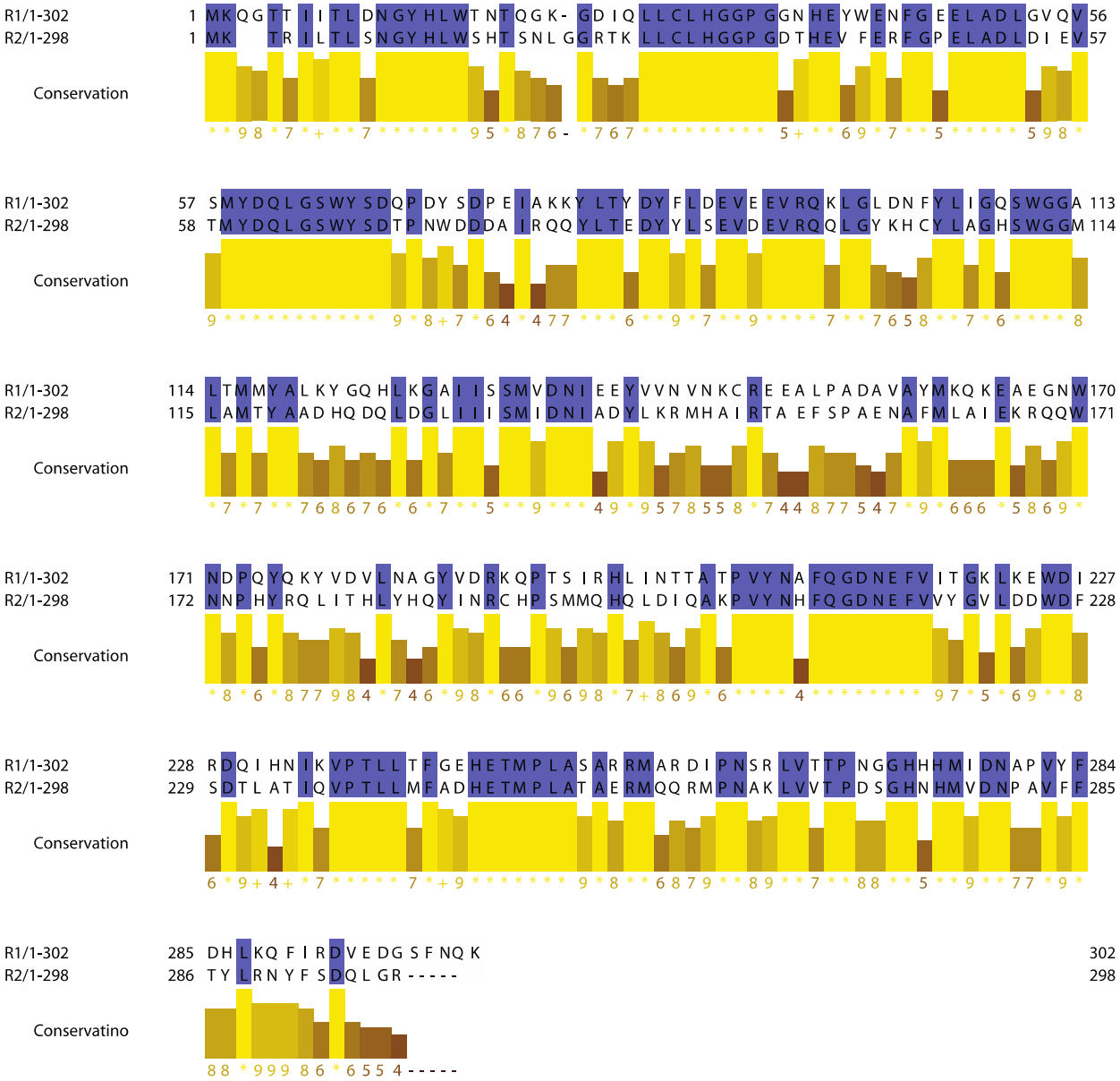

Fig. 2-3 Amino acid sequence alignment of PepR1 and PepR2. Identical amino acids between two genes are highlighted with purple boxes. Conservation represents the amino acid similarity. The higher the number in conservation, the higher the amino acid similarity.

Table 2-5 Summary of the properties of prolinases from various sources.

Enzyme Source[1]	Native MW[2] (kDa)	Subunit MW[3] (kDa)	Optimum pH	Optimum temperature (°C)	pI	Reference
L. helveticus[3]	----[4]	35.1	----	----	4.5	Varmanen *et al.*, 1996
L. helveticu CNRZ32[3]	125	33	6.0-6.5	45-50	4.5	Shao *et al.*, 1996
L. rhamnosus[3]	----	34.2	6.5	37	----	Varmanen *et al.*, 1998
Bovine kidney[4]	----	100	8.75	----	4.25	Akrawi and Bailey, 1976
Swine kidney[4]	----	100	8.0	----	4.3	Dehm and Nordwig, 1970
Human kidney[4]	----	100	----	----	4.5	Butterworth and Priestman, 1984

[1] The enzyme data from bacterial sources (*L. helveticus*, *L. helveticus* CNRZ32, and *L. rhamnosus*) are obtained from pure prolinases; whereas data from mammalian sources (bovine, swine, and human kidneys) are obtained from partially purified prolinases.
[2] Native molecular weights are determined using gel filtration chromatography.
[3] Subunit molecular weights are determined using SDS-PAGE.
[4] Not all of characteristics of prolinase are investigated.

Prolinase not only cleaves N-terminal imino dipeptides but also hydrolyzes a relatively broad range of dipeptides, such as Met-(Ala, Leu, Phe), Leu-(Arg, Ser), Ser-Phe, and Thr-Leu (Shao *et al.*, 1997), Leu-βNA (Pro-β-naphthylamide), Phe-βNA (Varmanen *et al.*, 1998), Pro-βNA, Pro-*p*NA (Varmanen *et al.*, 1996). Prolinase activities against different substrates are shown in Table 2-7 (prolinase from human kidney) and Table 2-8 (recombinant prolinase from *L. helveticus* CNRZ32). The activity of human kidney prolinase (Table 2-7) is normalized to 100% against substrate Gly-Leu, and the relative activities of the enzyme against other substrates are calculated accordingly. Similarly in Table 2-8, the activity of bacterial prolinase is normalized to 100% using Pro-Leu as substrate. Results from the two substrate-specificity studies demonstrate that the two prolinases exhibit high prolinase activity towards Pro-Xaa dipeptides, and dipeptides having neutral as well as nonpolar amino acid residues at the N-terminal, but no prolidase activity towards Xaa-Pro dipeptides. The two prolinases are unable to

hydrolyze tripeptides Pro-Gly-Gly and have low activities against tested tripeptides (Gly-Phe-Leu, Leu-Gly-Gly, Leu-Leu-Leu, Leu-Ser-Phe, Met-Ala-Ser, Phe-Phe-Phe). The results agree that prolinase is selective for dipeptides as substrates in a previous study (Sarid *et al.*, 1962). However, prolinases from different sources have different substrate specificities. For instance, bacterial prolinase has high activities on Pro-Leu and Pro-Phe, while human kidney has little activities on these two dipeptides.

In summary, prolinase displays a wide dipeptidase specificity as well as limited activity for tri- or larger peptides and Pro-(ρNA, βNAP) substrates. Prolinase hydrolyzes dipeptides (Pro-Xaa) with proline or hydroxyproline at N-terminal, and with various amino acids at C-terminal, such as hydrophobic/uncharged (-Ala, -Ile, -Leu, -Val), aromatic (-Phe), and sulfur containing (-Met). Specificities of prolinases vary among the sources.

Table 2-6 Comparison of substrate specificities of two recombinant prolinases from *Lactobacillus helveticus* CNRZ32 and *Lactobacillus helveticus* JLS221, adapted from Shao *et al* (1997).

Substrate	**Relative activity (%)**[1]	
	PepR positive[2]	PepR negative[3]
Pro-Leu	100	6.73 ± 1.02
Pro-Met	100	8.25 ± 0.40
Pro-Phe	100	19.95 ± 0.86
Met-Ala	100	70.56 ±2.14
Thr-Leu	100	12.36 ± 0.77
Gly-Leu	100	44.59 ± 2.99

[1] The activity of PepR positive against each dipeptide substrate is normalized to 100%.
[2] PepR positive is from *L. helveticus* CNRZ32.
[3] PepR negative is from *L. helveticus* JLS221.

Table 2-7 Substrate specificity of prolinase from human kidney, adapted from Priestman and Butterworth (1985).

Substrate	Relative activity (%)[1]
Pro-Leu	48
Pro-Phe	44
Pro-Val	40
Pro-Ala	13
Pro-Gly	9
Gly-Leu	100
Ser-Leu	40
Val-Leu	30
Ala-Leu	28
Phe-Ala	10
Leu-Gly-Gly	4
Hyp-Gly	4
Gly-Pro, Phe-Pro, Phe-Gly, Pro-Gly-Gly	BQL

[1] The activity of prolinase toward Gly-Leu is normalized to 100%.
[2] BQL, below quantifiable limit.

Table 2-8 Substrate specificity of recombinant prolinase from *Lactobacillus helveticus* CNRZ32, adapted from Shao *et al* (1997).

Substrate	Relative activity (%)[1]
Pro-Leu	100.0
Pro-Met	111.8
Pro-Phe	73.5
Thr-Leu	154.4
Leu-Ser	91.3
Met-Ala	92.3
Met-Gly	70.7
Met-Phe	54.0
Met-Leu	53.0
Leu-Arg	41.8
Ser-Phe	34.8
Gly-Leu	20.6
Met-Glu	12.9
Leu-Leu	10.9
Phe-Met	10.5
Phe-Leu	5.4
Gly-Tyr	3.8
Gly-Phe	3.5
Phe-Gly	3.1
Leu-Leu-Leu	1.2
Arg-Leu, Asp-Phe, Glu-Leu, Glu-Phe, Glu-Trp, His-Phe, Leu-Pro, Lys-Phe, Trp-Glu, Tyr-Glu, Tyr-Gly	BQL[2]
Gly-Phe-Leu, Leu-Gly-Gly, Leu-Leu-Leu, Leu-Ser-Phe, Met-Ala-Ser, Phe-Phe-Phe	BQL

[1] The activity of prolinase toward Pro-Leu is normalized to 100%.
[2] BQL, below quantifiable limit.

2.2.3 Proteolysis modes of prolinases

Amino acid sequences of prolinases (PepR) from *Lactobacillus helveticus and Lactobacillus rhamnosus* contain the same motif GQSWGG (Dudley and Steele, 1994; Varmanen *et al.*, 1996; Varmanen *et al.*, 1998). The identical serine catalytic site GQSWGG is also found in *Lactobacillus delbrueckii* iminopeptidase (PepI) (Klein *et al.*, 1994; Atlan *et al.*, 1994). This active site is a consensus sequence of prolyl oligopeptidase family (G×S×GG) (Rawlings *et al.*, 1991). Gene mutation of consensus region serine residue (Ser_{111}) results in the loss of detectable prolinase activity (Shao *et al.*, 1997). The result indicates that residue Ser_{111} is essential for prolinase catalysis.

In enzyme active site inhibition tests, *L. helveticus* PepR is inhibited by the serine protease inhibitor PMSF (phenylmethanesulfonylfluoride) with 33% reduced activity. The PepR activity is strongly constrained with pHMB (*p*-hydroxymercuribenzoate) (72% inhibition). It indicates that a thiol residue is either at or near the active site of PepR. The PepR is also inhibited by metallo-protease inhibitors (34% inhibition with EDTA and 45% inhibition with 1,10-phenanthroline) (Varmanen *et al.*, 1996). However, there is no significant inhibition observed on PepR activity by serine, thiol, aspartic, or metallo-protease inhibitors by Shao *et al* (1996).

2.2.4 Two forms of human prolinases

Prolinases from the human prostate has been characterized and found to have two forms (Masuda *et al.*, 1994). The two forms of prolinases I and II have similar substrate specificities (Table 2-9), which agree with the observation from previous studies (Kodama *et al.*, 1988; Butterworth and Priestman, 1982). Prolinases I and II have similar substrate specificity against six tested iminodipeptides in the following preference order: Pro-Ile > Pro-Val > Pro-Met > Pro-Gly > Pro-Ala > Pro-Pro. The other similarity of prolinases I and II is no significant change on their activities with and without Mn^{2+} preincubation. However, they differ in molecular weights, optimal pH and thermal stability. Prolinases I and II are separated into two peaks by ion exchange chromatography followed by gel filtration chromatography. The molecular weights of prolinases I and II have been confirmed to be about 85 kDa and 63 kDa, respectively. In terms of the optimal pH, prolinase I inclines to more alkali condition at pH 7.75-8.25 than prolinase II at pH 7.50-8.00. Prolinase I is highly thermal stable while prolinase II is instable. At present, no patient with prolinase deficiency has yet been found, and this might indicate the presence of two

forms of prolinase in human tissues (Masuda *et al.*, 1994).

Table 2-9 Substrate specificity of prolinases I and II separated from human prostate, adapted from (Masuda *et al.*, 1994).

	Prolinase I		Prolinase II	
	Activity[1]	Normalized activity (%)[2]	Activity	Normalized activity (%)
Pro-Ile	33.865	100.0	10.716	100.0
Pro-Gly	9.090	26.8	3.012	28.1
Pro-Ala	6.017	17.8	2.975	27.8
Pro-Val	24.573	72.6	8.790	82.0
Pro-Met	14.551	43.0	5.259	49.1
Pro-Pro	0.056	0.2	0.049	0.5

[1] The activities of prolinases are given as μmol/min/mg protein.
[2] Activities of prolinases I and II have been respectively normalized into 100% using Pro-Ile as substrate.

2.2.5 Assays of prolinase

The prolinase activity can be measured by quantifying the mount of the liberated Pro from dipeptide Pro-Xaa. The liberated Pro reacts with ninhydrin in glacial acetic acid under nearly anhydrous conditions and forms a red color. Investigations have been done on the ninhydrin-Pro interference (Van Slyke *et al.*, 1941; Chinard, 1952). These studies show that no significant amount of color is formed with most other amino acids at the pH near 1.0. The red color is a chromogenic formation of proline-ninhydrin interaction. A linear relationship exists between amount of free proline and optical density, which obeys the Bouguer-Beer-Law (Strong, 1952). In Chinard's study (1952), absorption of proline-ninhydrin has been scanned from wavelength of $OD_{400\ nm}$ to $OD_{600\ nm}$. The peak of the red product proline-ninhydrin has been found to be at $OD_{515\ nm}$. Mechanism of proline-ninhydrin reaction is illustrated in Reaction A, B and C in Fig. 2-4. Ninhydrin dehydrates and becomes indane-1,2,3-trione. Indane-1,2,3-trione reacts with proline and forms enol-betaine (I), which is an intermediate from the reaction of ninhydrin and pyrrolidine (imino ring). However, under neutral pH conditions, the reaction between proline and ninhydrin only proceeds as far as the unstable enol-betaine (I), and does not yield the final

product (II). Under acid and anhydrous conditions with heating at 95°C, the final product (II) forms through a reaction between 2-keto-group of second ninhydrin molecule and proline in compound (I). This proline-ninhydrin chromophore (II) is a resonance contributor to express red pigment (Hudson and Robertson, 1966). (Unlike proline-ninhydrin interaction, α-amino acid reacts with ninhydrin and generates a purple colored product (diketohydrin) termed as Ruhemann's purple, which consists of two dehydrated ninhydrin molecules bonding together by a central nitrogen.)

2.3 Potential therapies and treatment of a disease using prolinase

2.3.1 Prolidase deficiency disease

2.3.1.1 Clinical symptom

Prolidase deficiency is a rare inherited metabolic disorder (NCBI Online Mendelian Inheritance in Man code #26413), which is an autosomal recessive trait (Phang and Scriver, 1989). Prolidase deficiency is characterized by mental retardation, dermatological lesions, recurrent infections (otitis media, sinusitis), and disturbances of collagenous tissues (Myara *et al.*, 1984; Zanaboni *et al.*, 1994). Dermatological lesions (erythematous popular eruptions) may occur all over the body, on the lower extremities in particular. The main feature of prolidase deficiency is the chronic and periodic skin ulceration (usually on the lower limbs) ranging from mild to severe. In some cases, patients with severe ulcers are unable to walk, and even amputation is required (Zanaboni *et al.*, 1994). The age of prolidase deficient symptoms varies, but it occurs mostly from birth to 22 years of age (Royce and Steinmann, 1993). In some families, siblings of infected individuals have been found to possess deficient prolidase activity, though they were without symptom at the time of testing (Arata *et al.*, 1979; Isemura *et al.*, 1979; Dyne *et al.*, 1988). In Massachusetts, data from neonatal screening programs for aminoacidurias has suggested that prolidase deficiency has an incidence of 1 to 2 per million live births (Lemieux *et al.*, 1984).

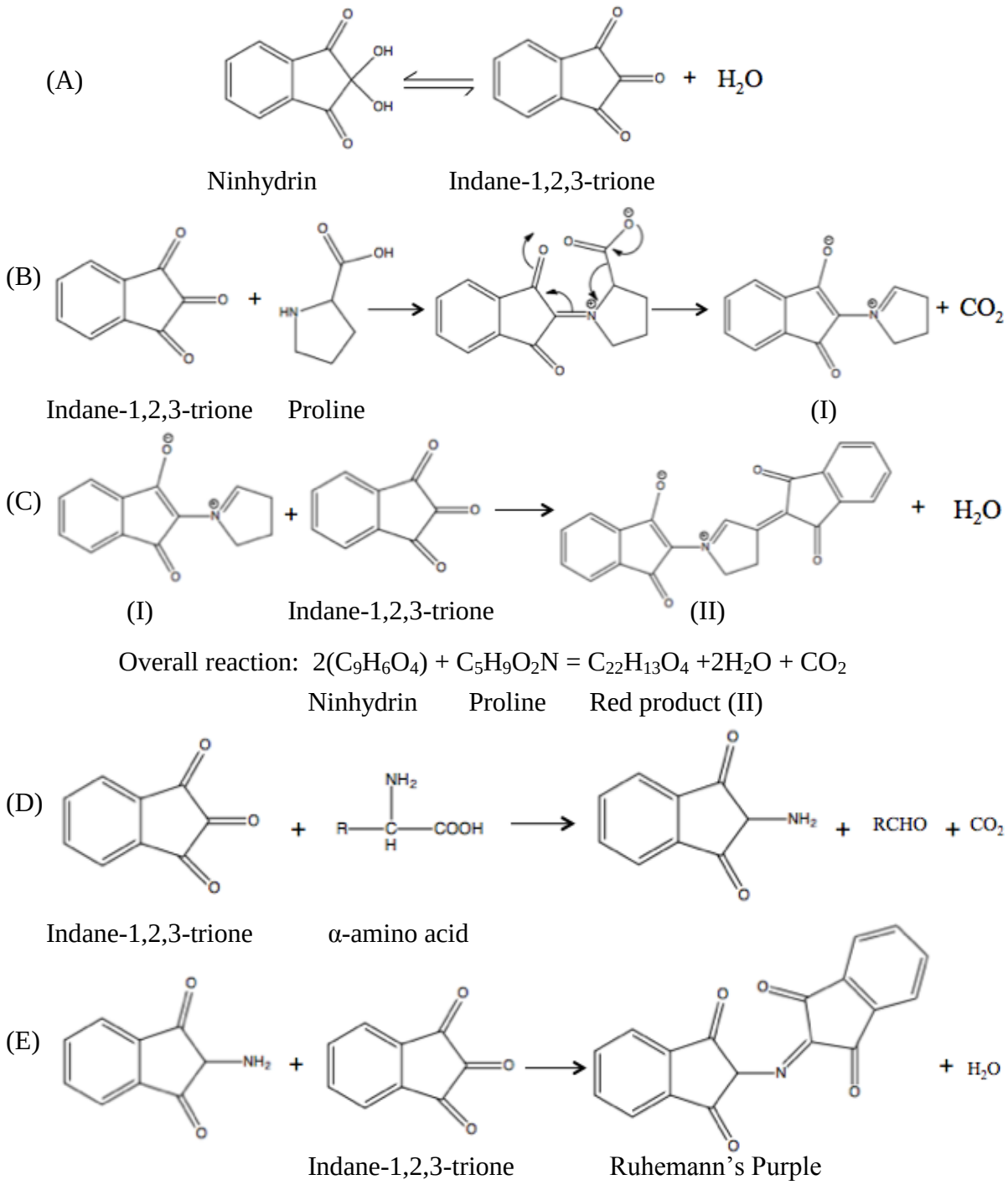

Fig. 2-4 Schematic demonstration of proline-ninhydrin interaction (A)(B)(C) and α-amino-acid-ninhydrin interaction (A)(D)(E), adapted from Johnson and McCaldin, 1958; McCaldin, 1960; Van Slyke *et al.*, 1941.

2.3.1.2 Pathogenesis

Prolidase is involved in the final stages of collagen degradation. Prolidase is responsible in wound healing and extracellular matrix remodeling; further supporting the role that prolidase plays in collagen synthesis and catabolism. For prolidase deficiency, there are two general biochemical mechanisms that could explain the pathophysiology of this disorder. The first mechanism postulates that prolidase deficiency results in a reduced amount of amino acid in the tissues and leads to the observed symptoms. The second mechanism suggests that a deficiency in prolidase activity can raise dipeptide levels to toxic levels, also leading to the observed symptoms.

As mentioned in the first mechanism, deficient prolidase could not hydrolyze imidopeptides (Xaa-Pro and Xaa-Hyp) into urinary excretion, and leads to a dramatic reduction of amino acid levels, especially proline. Proline is trapped in iminodipeptides and cannot be reused for the synthesis of new procollagen molecules (Myara *et al.*, 1983). The reduction in the supply of proline affects protein synthesis, particularly the synthesis of collagen. Generally, collagen contains up to 20-25% proline residues (Myara *et al.*, 1983; Isemura *et al.*, 1981). The reduced quantity of proline residues in collagen and the presence of skin alterations speculate that prolidase deficiency results in altered collagen metabolism. The second mechanism postulates that accumulations of one or more iminodipeptides to toxic levels in the tissues leading to the disorder. However, there is no evidence yet supporting the second mechanism (Senboshi *et al.*, 1996).

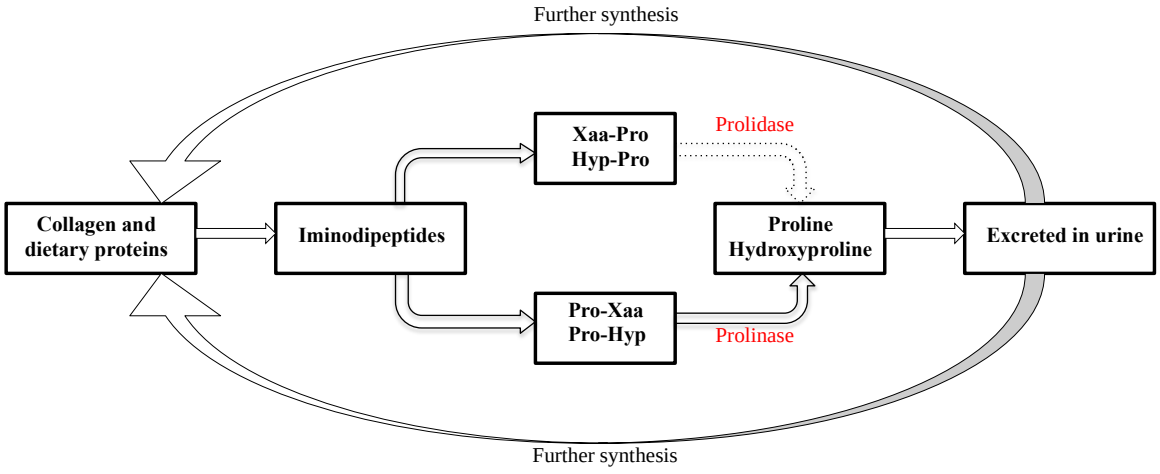

Fig. 2-5 Collagen metabolism pathways showing prolidase and prolinase activities. Deficient activity of prolidase is represented by the arrow of dash line. Xaa, amino acid; Pro, proline; Hyp, hydroxyproline. (adapted from Milligan *et al.*, 1989)

2.3.2 Potential therapies

In the process of collagen degradation, collagen is hydrolyzed by prolidase (cleaving dipeptides of Xaa-Pro and Xaa-Hyp) and prolinase (cleaving dipeptides of Pro-Xaa and Hyp-Xaa). The released proline is therefore recycled and used for further protein synthesis. By collagen metabolic pathways catalyzed by prolidase and prolinase, 90-95% of proline is conserved and reprocessed in protein synthesis (Jackson *et al.* 1975). Prolinase is a complementary enzyme to prolidase, which has an ability to maintain similar level of proline in prolidase-deficient fibroblast as in normal cells. Involvement of prolinase in collagen metabolism pathway in a prolidase-deficient patient is displayed in Fig. 2-5, demonstrating how prolinase compensates prolidase activity and maintains the quantity of proline and hydroxyproline. The released proline that is cleaved by prolinase can also be reutilized for the synthesis of collagen and dietary proteins, whereas the released hydroxyproline is excreted in the urine.

Investigations have been done to estimate deficient activity of prolidase and activity of prolinase. Prolinase activity is reported to increase in the plasma of prolidase-deficient patients (Myara and Stalder, 1986; Myara *et al.,* 1984), in the serum of patients (Kazunori *et al.*, 1993), and in prolidase-deficient fibroblasts (Miech *et al.,* 1988). In the research by Myara *et al.* (1984 and 1986) (Table 2-10), prolidase activity in healthy control plasma has a mean value of 900 U/L (median value 800 U/L and standard deviation 260 U/L). Prolidase activity is significantly reduced in the prolidase deficient plasma which is under detectable level. On the contrast, prolinase activity significantly increases from 16 ±14 U/L in healthy control plasma to 87 and 126 U/L in two prolidase deficient plasmas. Similarly in the study by Miech *et al.* (1988) (Table 2-11), the activity of prolidase is markedly reduced in a prolidase deficient patient than a normal control; whereas prolinase activity is higher in prolidase deficient cells than in normal control cells. The rise in prolinase activity indicates that prolinase compensates for the prolidase deficiency by raising the quantity of free proline necessary for collagen synthesis. And indeed no abnormality of prolinase has ever been reported (Milligan *et al.*, 1989).

Prolinase as a complementary supply in prolidase deficient patients may be the most suitable therapy. A variety of therapeutic attempts have been tried to compensate for the metabolic abnormality, such as blood transfusion, proline dietary supplement. However, blood transfusion to correct anaemia increases prolidase in red cells only last for several weeks with a temporary effect on the skin (Leoni *et al.*, 1987). Proline as a dietary supplement does not show improvement of leg ulcers (Ogata *et al.*, 1981; Isemura *et al.*, 1979).

Table 2-10 Prolidase and prolinase activity in control and prolidase-deficient plasmas. (adapted from Myara and Stalder, 1986)

	Prolinase activity[1] (U/L)	**Prolidase activity[2] (U/L)**
Control plasma	16 ±14 (n=338)[3]	900 ± 260 (n=106)
Case 1: 35-year-old woman	87	Not detectable
Case 2: 30-year-old man	126	Not detectable

[1] The activities of prolinase were tested using Pro-Val as substrate.
[2] The activities of prolidase were tested using Gly-Pro as substrate.
[3] n was samples size.

Table 2-11 Prolidase and prolinase activity in control and prolidase-deficient fibroblasts. (adapted from Miech *et al.*, 1988)

	Prolinase activity[1] (nmol/min·mg)	**Prolidase activity[2] (nmol/min·mg)**
Control fibroblasts (n=11)[3]	294 ± 50	106 ± 18
Prolidase deficient patients (n=3)	917 ± 67[4]	Not detectable

[1] The activities of prolinase were tested using Pro-Val as substrate.
[2] The activities of prolidase were tested using Gly-Pro as substrate.
[3] n is samples size.
[4] The activities of prolinase from prolidase deficient patients are significantly different from the control value (p<0.001).

3 HYPOTHESES AND OBJECTIVES

Prolinase (EC 3.4.13.8) is an enzyme applied in fermented foods debittering for the final hydrolysis of proline-containing dipeptides (cleaving iminodipeptides with N-terminal proline, i.e. Pro-Xaa). Two putative prolinases PepR1 and PepR2 in *Lactobacillus plantarum* WCFS1 may shed the light in the understanding in these proline-specific peptidases and their applications in fermented food debittering process and clinical treatments.

Objectives of this research is: 1) to clone and construct recombinant pET-32b(+)-prolinase (coded by genes of either *pep*R1 or *pep*R2) from *Lactobacillus plantarum*; 2) to optimize expression conditions, to purify the overexpressed of recombinant prolinases for comparison (r-PepR1 and r-PepR2), and to confirm the prolinase activities of two putative prolinases gene products; 3) to examine their characteristics through analyses on substrate specificity, pH dependence, temperature dependence, enzyme kinetics, proteolysis mode, thermal denaturation, protein secondary structure, native molecular mass and computer modeling.

4 RESEARCH STUDIES

4.1 Study 1: Construction of recombinant prolinase genes

4.1.1 Experimental approach

4.1.1.1 Materials

Enzymes for genetic engineering were purchased from Fermentas (Burlington, Canada) and Invitrogen (Burlington, Canada). All chemicals used in this study were commercially available ACS grade, and were purchased from VWR International (Edmonton, Canada) and Fisher Scientific (Ottawa, Canada). The *pep*R1 and *pep*R2 genes were obtained from pUC18-*pep*R1 and pUC18-*pep*R2 previously constructed in Dr. Takuji Tanaka's lab group (unpublished). *E. coli* were obtained from Invitrogen, including TOP10F' (F'[*lacI*^{q} Tn1*0*(tet^{R})] *mcrA Δ*(*mrr-hsdRMS-mcrBC*) φ80*lacZΔM15 ΔlacX74 deoR nupG recA1 araD139 Δ*(*ara-leu*)*7697 galU galK rpsL*(Str^{R}) *endA1* λ^{-}), BL21 (DE3) pLysS (F^{-} *ompT gal dcm lon hsdS*$_{B}$(r$_{B}^{-}$ m$_{B}^{-}$) λ(*DE3*) pLysS(cm^{R}), pLysS, Rosetta (DE3) (*Δ*(*ara-leu*)*7697 ΔlacX74 ΔphoA PvuII phoR araD139 ahpC galE galK rpsL* (*DE3*) F'[*lac*$^{+}$ *lacI*^{q} *pro*] *gor522*::Tn*10 trxB* pLysSRARE (Cam^{R}, Str^{R}, Tet^{R}).

4.1.1.2 Polymerase chain reaction (PCR) amplification

Two pairs of primers for PCR were designed, based on the genomic DNA sequences of prolinase in GenBank (*pep*R1, accession: AL935263, region: 792560−793468; *pep*R2, accession: AL935263, region: 2597065−2597961), and then custom-synthesized (Integrated DNA Technologies Inc, Coravile, IL, USA). The primers for *L. plantarum pep*R1 were designed with a *Hind*III restriction enzyme site in the forward primer and an *Nco*I restriction enzyme site in the reverse primer (Table 4-1). The primers for *L. plantarum pep*R2 possessed *EcoR*I and *BamH*I restriction enzyme sites on the flanking ends of the open reading frame (Table 4-1). The PCR reaction mixtures (total volume of 50 µL) consisted of 20 pmol of each primer, 20 ng of recombinant pUC18-*pep*R1 or pUC18-*pep*R2 DNA template, 0.04 mM of each 2'-deoxynucleotide 5'-triphosphate (dNTP), and 0.5 U of *Pfu* polymerase (Fermentus International). The PCR program was set to 25 cycles of 30 sec at 95°C for denaturation, 30 sec

at 55°C for annealing, and 2 min at 72°C for extension. After PCR amplification, the mixtures was purified by EZ-10 Spin Column PCR Purification Kit (VWR International).

Table 4-1 Forward and reverse PCR primers utilized for prolinase-coding gene amplification.

Gene	Name	Primer[1]
*pep*R1	Forward primer	CCGCCATGGAG**TTG**AAACAAGGAAC *
	Reverse primer	TTAAAAGCTTTTTTTGATTAA AGCTGCCA **
*pep*R2	Forward primer	CCGGGGATCCC**ATG**AAAAACGTGACACGAAT +
	Reverse primer	GAAGGAATTCTTGCGGCCCAATTGATCAGA ++

[1] Restriction enzyme sites were underlined. Initiation codons were indicated in bold.
* *Nco*I restriction enzyme site
****Hind*III restriction enzyme site
+*BamH*I restriction enzyme site
++*EcoR*I restriction enzyme site

4.1.1.3 Recombinant plasmid construction using His-tagged vector

The purified gene fragments of *L. plantarum pep*R1 and His-tagged vector (pET-32b(+)) were digested with *Nco*I and *Hind*III, which created adhesive ends for ligation. The purified PCR fragments of *L. plantarum pep*R2 and His-tagged vector were digested with *BamH*I and *EcoR*I restriction enzymes. The enzyme digestions were performed according to protocols from the manufacturers. The digested His-tagged vector preparations were dephosphorylated with shrimp alkaline phosphatase (SAP) to avoid self-ligation (Ausubel *et al*., 1990). The digested gene and plasmid preparations were purified using a PCR product purification kit to remove the enzymes and salts in the mixtures. Purified gene fragments and corresponding digested plasmids were ligated overnight at 16°C with T4 DNA ligase under the conditions recommended by the manufacturer. The constructed recombinant plasmids (Fig. 4-1 and Fig. 4-2) were kept at -20°C until necessitated

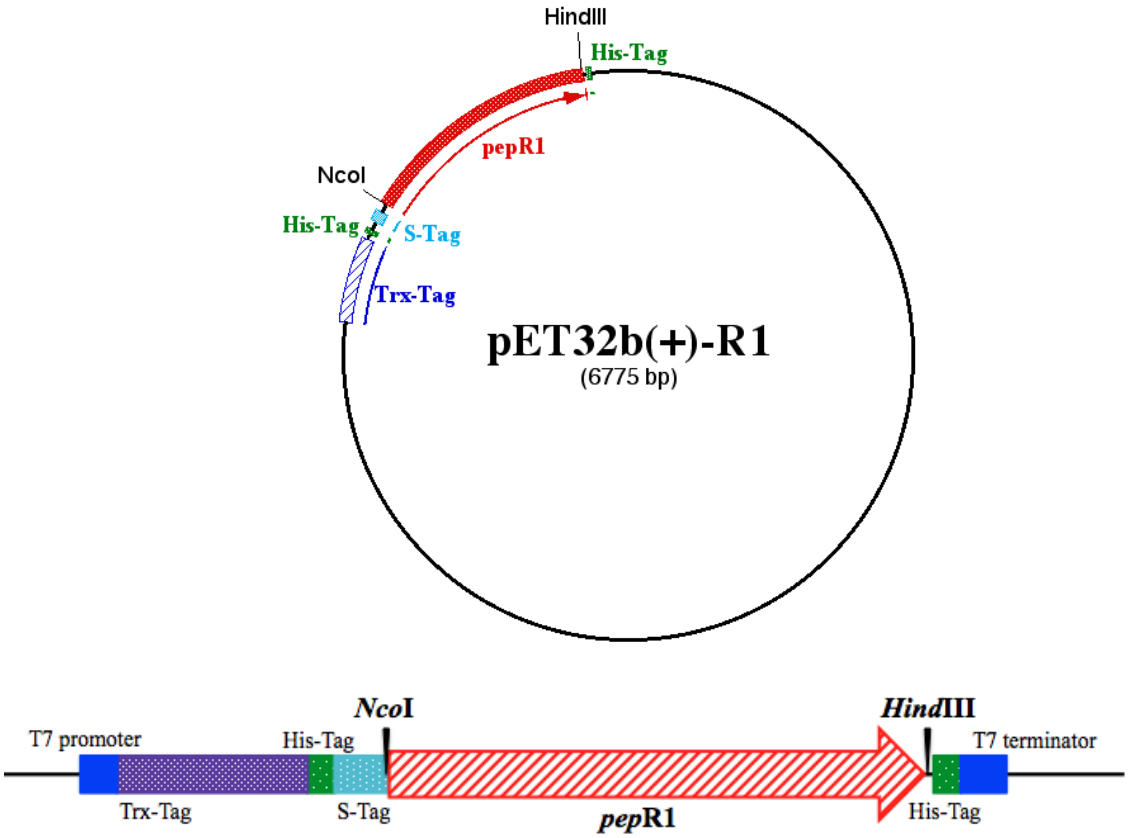

Fig. 4-1 Recombinant prolinase rH-PepR1. *L. plantarum* prolinase gene *pep*R1 was inserted into His-tagged vector (pET-32b(+)) between the *Nco*I and *Hind*III restriction enzyme sites.

Fig. 4-2 Recombinant prolinase rH-PepR2. *L. plantarum* prolinase gene *pep*R2 was inserted into His-tagged vector (pET-32b(+)) between the *BamH*I and *Eco*RI restriction enzyme sites.

4.1.1.4 Preparation of competent cells

Escherichia coli TOP10F', BL21 and Rosetta strains were separately cultivated in LB medium (1% tryptone, 0.5% yeast extract, 0.5% NaCl, with addition 34 µg/mL chloramphenicol only for Rosetta culture) overnight as starter cultures. One milliliter from the overnight starter culture was added into 100 mL of LB medium (with chloramphenicol 34 µg/mL addition to Rosetta culture), and was incubated at 37°C with vigorous agitation till $OD_{600\ nm}$ reached 0.4-0.6. The cultures were transferred to autoclaved centrifuge tubes and the cells were harvested by centrifugation (6000 rpm, 15 sec, and 4°C, Sorval GSA-3 rotor). The bacterial pellet was gently resuspended in 50 mL of autoclaved ice-cold 10% (w/v) glycerol. The suspension was chilled on ice for 30 min, and was then centrifuged at 6000 rpm for 15 sec at 4°C in a Sorval ss-34 rotor. Supernatant was discarded and the bacterial pellet was gently resuspended in approximately 2 mL of the remaining glycerol solution. The suspension of *E. coli* TOP10F', BL21 and Rosetta eletrocompetent cells were aliquoted into 50 µL each in microtubes and kept at -80°C.

4.1.1.5 Transformation and positives screening

The constructed His-tagged clones can be expressed in either *E. coli* BL21 or Rosetta but not in *E. coli* TOP10F' while generally *E.* coli TOP10F' shows higher transformation efficiency. To obtain higher transformation efficiency, the constructed His-tagged clones were firstly transformed into *E. coli* TOP10F' for screening purpose, and the plasmids of positive clones were then transformed to *E.* coli Rosetta and BL21 individually. Procedures of transformation were as follows. Electroporation cuvettes (1 mm gap cuvettes) were stored in 70% (v/v) ethanol overnight for disinfection. Electroporation cuvettes were rinsed with autoclaved water, and chilled on ice and allowed to air dry. Electrocompetent cells (50 µL) were thawed on ice and gently mixed with the ligation reaction mixture of the constructed recombinant plasmids (2 µL), and then the mixture was transferred to an electroporation cuvette. The cuvette was wiped off excess moisture from outside and placed in an electorporator with a voltage setting at 1800 volts (*E.* coli mode). After electroporation, the shocked cells were immediately added with 1 mL LB broth and transferred to a microtube and incubated at 37 °C for 1 hour to permit revitalization of cells. The cells were centrifuged at 12,000 rpm for 2 min in a microcentrifuge and the cell pellet was resuspended in 200 µL of LB broth. The suspension was spread on a LB-agar plate (1% tryptone, 0.5% yeast extract, 0.5% NaCl, 1.5% agar, 100 µg/mL of ampicillin, with addition 34

μg/mL chloramphenicol only for Rosetta) and was incubated at 37°C overnight. After the incubation, propagated colonies were checked using colony PCR. For colony PCR, the propagated colonies were picked with autoclaved tooth picks, and mixed with PCR reaction mixtures (total volume of 50 μL) including 10× PCR buffer (500 mM KCl, 100 mM Tris-HCl (pH 9.0), 1.0% Triton X 100), 3 μL of 25 mM $MgSO_4$, 1 μL of 20 μM forward primer and reverse primer (Table 4-1), 0.04 mM of each dNTP, and 0.5 U of *HP Taq* polymerase (United Bioinformatica Inc., Calgary, AB)). The PCR program was set to 25 cycles of 30 sec at 95°C for denaturation, 30 sec at 55°C for annealing, and 2 min at 72°C for extension. PCR products were examined on agarose gel electrophoresis. The positive clones were identified by the size of either *pep*R1 or *pep*R2 bands on the agarose gel. Positive clones were further confirmed using DNA sequencing at PBI (Plant Biotechnology Institute, National Research Council of Canada, Saskatoon, SK). After confirmation, recombinant plasmids of the positive His-tagged clones were transformed to *E.* coli BL21 and *E.* coli Rosetta cells in the same protocol and stored as a 20%(v/v) glycerol solution at -80°C for further overexpression and characterization of the prolinases.

4.1.2 Connection to next study

In this section, *pep*R1 and *pep*R2 were constructed into a His-tagged pET32b(+) expression system. These recombinant plasmids were transformed into *E. coli* BL21 and Rosetta. The overexpression of recombinant rH-PepR1 and rH-PepR2 will be optimized under different culturing conditions to obtain high productivity. The overexpressed rH-PepR1 and rH-PepR2 will be purified and the N-terminal His-tag will be removed. Pure r-PepR1 and r-PepR2 (His-tag removed) are expected to show a single protein band on SDS-PAGE being homology.

4.2 Study 2: Optimization of expression conditions and protein purification

4.2.1 Experimental approach

4.2.1.1 Materials

Columns for chromatography were purchased from GE Healthcare Bio-sciences (Mississauga, Canada). Standard proteins were bought from Bio-Rad Laboratories (Mississauga, Canada). Recombinant plasmid pKK223-3-*pep*R2 was constructed in Dr. Takuji Tanaka's lab group (unpublished data).

4.2.1.2 Optimization of expressed prolinases

Escherichia coli BL21 and Rosetta with either plasmid pH-pepR1 or pH-pepR2 were individually cultivated in 50 mL of LB broth at 16°C until $OD_{600\ nm}$ reached 0.5. The protein expression was induced with 1 mM IPTG and cultured at 16 °C for three more days. Cells were harvested using 6,000 rpm centrifugation (Sorval GSA3) at 20 min, 4°C, and were resuspended in 5 volumes of ice-cold buffer (20 mM Tris-HCl pH7.5) per weight of wet cell pellet. Resuspended cells were disrupted with ultrasonication (model 450, Sonifier, Branson Ultrasonics Co., CT, USA; 25 sec burst and 35 sec pause operations for 15 min in an ice bath). The disrupted cells were centrifuged at 12,000 rpm, 30 min, 4°C, in a Sorval ss-34 rotor for separating the crude extract in supernatant from cell debris in sediment. Crude extract, cell debris and whole cell samples were analyzed on 10% SDS-PAGE to examine the expression of recombinant prolinases in different hosts.

Improvements in prolinase expression can be obtained by using different hosts as well as by modification of the bacteria growth conditions. Recombinant prolinases were cultivated under different temperature (16°C, 25°C and 37°C), different pH (pH 5.5, 6.5, 7.0, 7.5, 8.5), using different media (LB and M9), with different inducers when $OD_{600\ nm}$ reached 0.5 (1 mM IPTG, 0.5 mM IPTG, 0.01 mg/mL lactose). The expression level of prolinase was checked by comparing whole cell, cell debris and crude extract from different culturing conditions on 10% SDS-PAGE.

Non-tagged PepR2 expression was conducted using a pKK223-3-*pep*R2 clone (Dr. Tanaka's lab stock). *Escherichia coli* TOP10F' carrying this plasmid was cultured in 30 mL LB media at 37 °C over night. This preculture inoculated in 3 L of LB broth and incubated with vigorous aeration at 16 °C. When the absorption at 600 nm reached 0.5, 1 mM IPTG was added. After another 72-hour incubation under the same conditions, the cells were harvested. The crude extracts of proteins were recovered using the same method described for His-tagged expression above.

4.2.1.3 Purification of recombinant prolinases

4.2.1.3.1 Purification of His-tagged prolinases

His-tagged protein purification

Crude extract of His-tagged recombinant prolinases (600 μL of 8.5 mg/mL rH-PepR1 or rH-PepR2) were applied to a pre-equilibrated Ni-NTA spin column (equilibrate buffer: 50 mM NaH_2PO_4, 300 mM NaCl, 10 mM imidazole pH8.0) respectively (QIAGEN CAT. No. 31014). After applying sample, the column was centrifuged at 1600 rpm, 4°C, 5min, and flow-through was collected. The column was then washed twice with wash buffer using 2900 rpm centrifugation (Hettich Zentrifugen, GmbH, Tuttlingen, Germany), at 4°C, 2 min. Wash buffer was optimized for higher purity of rH-PepR1 and rH-PepR2 having a variety of imidazole concentrations from 20 to 100 mM in a buffer solution (50 mM NaH_2PO_4 and 300 mM NaCl, pH8.0). Wash flow-through was saved for analysis on SDS-PAGE. After washing, His-tagged protein was eluted from the column with an elution buffer (50 mM NaH_2PO_4, 300 mM NaCl, 500 mM imidazole pH8.0) using 2900 rpm centrifugation, 4°C, 2 min. This step of purification was repeated for 7 times and using 10 Ni-NTA spin column at the same time. Elution, crude extract flow-through and wash flow-through were checked on SDS-PAGE to examine the effectiveness of the washing buffers.

Cleavage of protein tags

Pure rH-PepR1 or rH-PepR2 (about 35 mL of 3 mg/mL) was dialyzed against 2-L buffer (50 mM sodium phosphate buffer pH8.0) at 4°C for 1 hour, and followed by dialysis against 3 L of the same buffer over night. The dialyzed His-tagged prolinases were treated with thrombin (thrombin 5 μL of 0.2 U/μL for every 1 mL 1 mg/mL His-tagged prolinase) (New England Biolabs Inc. Cat. 94547) at 16°C overnight for N-terminal His-tag removal.

Gel filtration chromatography

The cleaved rH-PepR1 (or rH-PepR2) sample was applied on a gel filtration column (Superdex 200 HR 10/300: 1 cm diameter × 30 cm lengths, 24 mL volume, General Electrics Healthcare Bio-sciences Co., Mississauga, ON) equilibrated with 50 mM sodium phosphate pH8.0 buffer. The cleaved prolinase was eluted using 50 mM sodium phosphate pH8.0 buffer at a flow rate 0.2 mL/min. The eluent was collected and examined on 10% SDS-PAGE gel to

identify the fraction with prolinase. The pure cleaved prolinase (N-terminal His-tag removed r-PepR1) was added with 50% (v/v) glycerol for storage in a -20°C freezer.

4.2.1.3.2 Purification of non-tagged prolinase

Ammonium sulfate precipitation

The recombinant prolinase expressed with pKK223-3 (r-PepR2) crude extract was adjusted to protein concentration 10 mg/mL. The adjusted crude extract was transferred to a beaker containing a stir bar and placed in ice while it was being stirring on a magnetic stirrer. The crude extract of r-PepR2 was slowly added with ammonium sulfate to a final concentration of 20% saturation and kept at 4°C for 3 hours. Precipitated protein was removed by centrifugation at 12,000 rpm, 20 min, 4°C (Sorval SS-34 rotor). Supernatant was collected after the previous step of ammonium sulfate saturation (20%, 40%) and brought to the next step of ammonium sulfate saturation (40%, 60%). Precipitated proteins from 20%, 40% and 60% ammonium sulfate saturation were transferred to dialysis tubing and dialyzed against 2-L buffer (20 mM Tris-HCl pH7.5) at 4°C for 1 hour, and followed by dialysis against another 3-L buffer (20 mM Tris-HCl pH7.5) overnight at 4°C. The fractions were checked on SDS-PAGE to identify prolinase.

Ion-exchange column chromatography

After dialysis, the sample obtained from 60% ammonium sulfate saturation was applied to an ion-exchange column (DEAE-Sephacel anion exchange column: 3 cm diameter × 15 cm lengths, General Electrics Healthcare Bio-sciences Co., Mississauga, ON, Canada) equilibrated with 20 mM Tris-HCl (pH 7.5). r-PepR2 was eluted using a linear gradient of NaCl from 0 to 1 M. The eluent was fractionated and fractions were examined on 10% SDS-PAGE gel to identify the fractions of prolinase.

Hydrophobic interaction chromatography

A hydrophobic interaction column (PhenylSephorose, 0.5 cm diameter × 15 cm lengths, General Electrics Healthcare Bio-sciences Co., Mississauga, ON, Canada) was equilibrated with ten-column volumes of equilibrate buffer (20 mM Tris-HCl 1 M ammonium sulfate pH 7.5). The fractions from the ion-exchange column chromatography of r-PepR2 were combined and prepared in 0.8 M ammonium sulfate saturation for the hydrophobic interaction chromatography.

The hydrophobic interaction column was washed in step-wise gradient with three-column volumes of wash buffer at different ammonium sulfate concentrations (1, 0.75, 0.5, 0.25 and 0 M). The eluent from the column was fractionated and the fractions were examined on a 10% SDS-PAGE gel to identify the pure prolinase fractions.

4.2.2 Connection to next study

Characterization of prolinases requires a lot of enzymes that go far beyond their abundance in the cell. The study described here provides overexpression of recombinant prolinases and efficient purification. Sufficient amount of proteins are obtained for characterization in the following study.

4.3 Study 3: Characterization of recombinant prolinases

4.3.1 Experimental approach

4.3.1.1 Materials

All chemicals used in this study were commercially available ACS grade, and were purchased from VWR International (Edmonton, Canada) and Fisher Scientific (Ottawa, Canada). Protein size marker was obtained from Bio-Rad Laboratories Ltd, Mississauga, ON, Canada.

4.3.1.2 Quantification of proline

Proline released from substrate Pro-Xaa was assessed by a colorimetric assay that detects proline as a colored proline-ninhydrin complex using light absorption at 500 nm. To establish the standard curve of proline at different concentrations, 20 µL of proline solutions were transferred into 200 µL of ninhydrin solution (15 mg/mL (w/v) ninhydrin and 0.03 mL/mL (v/v) glacial acetic acid in 1 mL of n-butanol, pH1 adjusted with HCl). The mixture was heated at 95°C for 5 min, and was then chilled on ice. The mixtures were measured at $ABS_{500\ nm}$ using a spectrophotometer.

4.3.1.3 Enzyme activity quantification

Mixture of 60 µL of water, 10 µL of 10× buffer (described in the following sections) and 10 µL of 20 mM Pro-Xaa was incubated in 37°C water bath for 5 min. Twenty microliters of

prolinase were mixed with the pre-incubated mixture to initiate reaction, and 20 μL was transferred from the reaction mixture to 200 μL of ninhydrin solution at every one minute for four times (or with longer time interval if the enzyme activities were low). After heated at 95°C for 5 min and chilled on ice, the absorption of mixtures was measured at 500 nm. Observed absorption was converted into the amount of liberated proline in accordance with the standard curve of proline determined in section 4.3.1.2. The rate of liberated proline implied the hydrolysis activity of recombinant prolinase. Enzyme reaction velocity was then calculated from the slope (μmol/mg·min) of the linear regression between the amount of liberated proline and reaction time. All of the experiment was conducted in triplicate. The following activity determination was conducted based on the method described here with specific variations given in each section.

4.3.1.4 Substrate specificity of recombinant prolinases

A variety of Pro-Xaa dipeptides were examined as the substrates, including Pro-Pro, Pro-Glu, Pro-Met, Pro-Ser, Pro-Arg, Pro-Phe, Pro-Leu and Pro-Gly. The substrates at 2 mM were hydrolyzed at 37°C in a 50 mM Tris-HCl (pH7.5) buffer solution to determine activities of recombinant prolinases against different substrates. Experiments were done in triplicate.

4.3.1.5 pH dependence on enzymatic activity

The pH optima of recombinant prolinases activities were identified through measurements of activities in the range of pH 3.0 to 10.0 using different buffers with various pH (Table 4-2). Hydrolysis reactions of recombinant prolinases were conducted at 37°C and with the most preferred substrate (Pro-Gly). Experiments were conducted in triplicate.

Table 4-2 A variety of buffers used for pH dependence test

Buffer	pH
50 mM sodium acetate	3.0 3.5 4.0 4.5
50 mM sodium citrate	4.5 5.0 5.5 6.0
50 mM MES	5.5 6.0 6.5
50 mM sodium phosphate	6.0 6.5 7.0 7.5
50 mM MOPS	6.5 7.0 7.5
50 mM HEPES	7.0 7.5 8.0
50 mM Tris-HCl	7.5 8.0 8.5 9.0
50 mM sodium carbonate	9.0 9.5 10.0

4.3.1.6 Temperature dependence on enzymatic activity

Enzyme velocities at different temperatures were determined to identify the optimal temperature. Similar to the method in section 4.3.1.3, a reaction mixture without prolinase was pre-incubated at the pH optima with 2 mM of the most preferred substrate (Pro-Gly) at a variety of temperatures (5, 15, 20, 25, 30, 37, 40, 45, and 55°C). After 5-min pre-incubation at the designated temperature, 20 µL of prolinase was added to initiate the hydrolysis reaction. The time interval of sampling of the reaction mixture varied among temperature to have the liberated proline concentration within the concentration range used in the calibration of standard. Experiments were conducted in triplicate.

4.3.1.7 Secondary structure and thermal denaturation temperature

To analyze secondary structure and thermal denaturation temperature, far UV circular dichroism (CD) spectroscopy was measured on a PiStar-180 CD spectrophotometer (Applied Phytophysics Ltd, Leatherhead, Surrey, UK) at SSSC (Saskatchewan Structural Sciences Centre, University of Saskatchewan). Pure recombinant prolinase solutions (10 mg/mL) were desalted by dialysis against the optimal HEPES buffer (50 mM HEPES pH7.5 for r-PepR1 and 50 mM HEPES pH8.0 for r-PepR2). Secondary structure analyses and thermal denaturation tests used 300 and 700 µL of desalted recombinant prolinase solutions, respectively. The CD spectra were measured between 190 nm and 250 nm for secondary structure test. Collected data was analyzed using CDNN software (Bohm *et al.*, 1992) to deduce five different secondary structure fractions (α-helix, parallel and antiparallel β-sheet, β-turn and random coil). Thermal denaturation temperature was deduced from the change of CD spectra over the temperature range from 20°C

to 85°C. Sample was measured at spectra of 222 nm with the increment in the temperature, and signal strength was recorded. Correlation between the rates of CD spectra change over different temperature was calculated to measure the temperature of denaturation.

4.3.1.8 Enzyme kinetics

Reaction rates of recombinant prolinases were measured at a series of substrate concentrations (0.5, 1, 2, 4 and 8 mM) under the optimal conditions (in 50 mM HEPES buffer pH7.5, at 25°C for r-PepR1; and in 50 mM HEPES buffer pH8.0, at 30°C for r-PepR2) using the method described in section 4.3.1.3. Enzyme kinetic values K_m and k_{cat} were obtained by plotting the double-reciprocal reactions rates against different concentrations of substrate (as shown in Equation (1) and Fig. 4-3). K_m is defined as Michaelis-Menten constant at which the velocity of the product generation reaches half of the maximum rate V_{max}.

$$\frac{1}{V} = \frac{K_m + [S]}{V_{\max}[S]} = \frac{K_m}{V_{\max}}\frac{1}{[S]} + \frac{1}{V_{\max}} \qquad \text{Equation (1)}$$

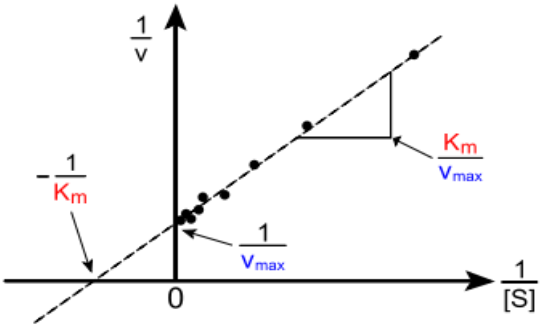

Fig. 4-3 Linear regression of 1/*V* vs. 1/[*S*]. *V* is the initial velocity, [*S*] is the initial concentration of substrate, K_m and V_{max} are enzyme kinetic values.

4.3.1.9 Identification of proteolysis mode

The effects of several chemical inhibitors on protease activities were investigated through addition of the agent to the reaction mixture. The reaction mixture was pre-incubated with an inhibitor and the reaction was initiated by addition of enzyme. A control reaction for assay

interference was conducted for each inhibitor by adding the agent after the enzymatic reaction quenched by addition of the ninhydrin solution. The inhibited activity was measured using the same method in section 4.3.1.3. All reactions were under the optimized condition (in 50 mM HEPES buffer pH7.5, at 25°C for r-PepR1; and in 50 mM HEPES buffer pH8.0, at 30°C for r-PepR2) and all experiments were conducted in triplicate. PMSF, EDTA, DTT and maleimide (2,5-pyrroledione; MAL) were used to suggest the mode of proteolysis.

4.3.1.10 Determination of native molecular mass by gel filtration

A gel filtration column (Superdex 200 HR 10/300: 1 cm diameter × 30 cm lengths, 24 mL volume; GE Healthcare Bio-sciences Co., Mississauga, ON) was equilibrated with 20 mM sodium phosphate buffer, pH8.0. Two hundred microliters of either r-PepR1 or r-PepR2 sample or water as control with ten microliter of standard proteins were applied to the column. Standard proteins are listed in Table 4-3. The column was washed with the same buffer (20 mM sodium phosphate, pH8.0) at flow rate 0.20 mL/min. Column effluents were continuously measured by a UV detector at absorbance 280 nm.

Table 4-3 Gel filtration standard components.

Components	Molecular Weight[1]	Amount Used
Thyroglobulin (bovine)	670,000	100 μg
γ-globulin (bovine)	158,000	100 μg
Ovalbumin (chicken)	44,000	100 μg
Myoglobin (horse)	17,000	50 μg
Vitamin B_{12}	1,350	10 μg

[1] Estimates of molecular weights from (Sober *et al.*, 1968; Windholz *et al.*, 1976)

5 RESULTS AND DISCUSSION

5.1 Construction of recombinant prolinases

The amplified genes were successfully digested and ligated to His-tagged vector pET-32b(+). Constructed recombinant His-tag-prolinase genes (both *pep*R1 and *pep*R2) were transformed into *E. coli* Rosetta and BL21. Positive clones were confirmed by both colony PCR (Fig. 5-1) and DNA sequencing methods. This study focused on constructing of prolinase genes from *L. plantarum* into *E. coli* BL21 and Rosetta utilizing the high expression His-tagged vector pET-32b(+). There were two His-tagged sites on both N- and C-terminal of the insertion gene in the vector as shown in Fig. 4-1 and Fig. 4-2, which were useful in purification by recombinant prolinase with His-tag efficiently binding to Ni-NTA column (nickel chelating ligand). The vector pET-32b(+) (about 5.9 kb) with the 1-kb insert (*pep*R1 or *pep*R2) as recombinant plasmids were designated as pH-pepR1 and pH-pepR2, respectively. pH-pepR1 and pH-pepR2 were successfully constructed as designed by sequence confirmation.

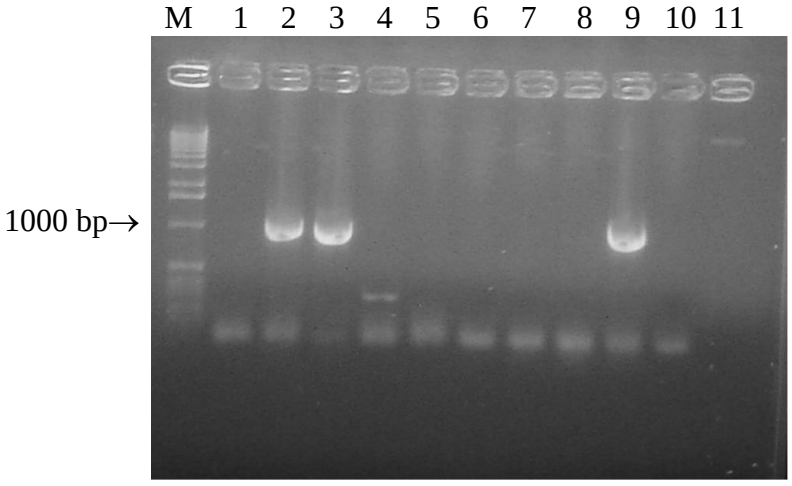

Fig. 5-1 Ethidium bromide-stained agarose gel showing PCR amplified *pep*R1 and *pep*R2 genes (*pep*R1 909 bp and *pep*R2 897 bp). M: DNA marker. Lane 2 and 3 are positive *pep*R1, and Lane 9 is positive *pep*R2; whereas the rest lanes are negative.)

5.2 Optimization of protein expression

The two recombinant His-tagged prolinases rH-PepR1 and rH-PepR2 were overexpressed with higher production using *E. coli* Rosetta as host rather than *E. coli* BL21. They were overexpressed as soluble proteins at 16°C but as inclusive aggregation at 25°C and 37°C. They were overexpressed at a higher rate using 1 mM IPTG as the inducer rather than 0.5 mM IPTG or 0.01 mg/mL lactose. But there was no significant difference between using LB or M9 as growth media. Higher production of prolinase was obtained in growth media at pH 7.0 to 7.5. Briefly, rH-PepR1 and rH-PepR2 showed their optimum production using *E. coli* Rosetta as host, grown in LB media pH 7.0-7.5 at 16°C for three days with 1 mM of IPTG induction at $OD_{600\ nm}$ 0.5 (data not shown).

5.3 Purification

5.3.1 Purification of His-tagged prolinase

The His-tagged rH-PepR1 (53.4 kDa) and rH-PepR2 (54.6 kDa) was purified using Ni-NTA spin column with wash buffer of different imidazole concentrations (20, 40, 60, 80 and 100 mM) to obtain higher purity. It was shown that rH-PepR1 was with high purity using 80 or 100 mM imidazole in wash buffer (50 mM sodium phosphate, 300 mM NaCl, pH8.0). However, 100 mM imidazole resulted in a slight decrease in the recovery of rH-PepR1 (Fig. 5-2) and rH-PepR2 (Fig. 5-3). Thus, the 80 mM imidazole in wash buffer was chosen for purification of rH-PepR1 and rH-PepR2. Purification results are summarized in Table 5-1.

Pure rH-PepR1 was cleaved with thrombin to remove N-terminal His-tag and Trx-tag. The cleaved rH-PepR1 (named as r-PepR1) was theoretically 39.2 kDa, and the removed N-terminal His-tag and Trx-tag was 14.2 kDa (Fig. 5-4). r-PepR1 was purified from the cleaved tag fragment with the gel filtration chromatography (Fig. 5-5). Cleavage of rH-PepR2 was also examined to obtain tag cleaved PepR2 (r-PepR2); however, the conditions used in this experiments led to undesired and non-specific cleavage of the protein, and we could not find the conditions to recover tag-cleaved r-PepR2 from rH-PepR2. Hence, the r-PepR2 expressed from conventional non-tagged vector pKK223-3 was purified and used for characterization. The purification steps are summarized in Table 5-2.

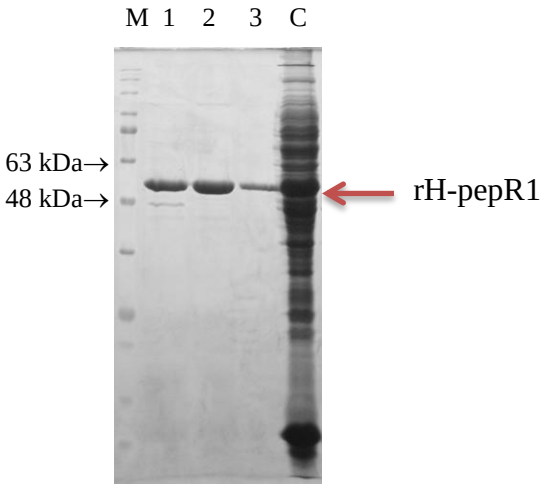

Fig. 5-2 Coomassie Brilliant Blue G250-stained 10% SDS-PAGE gel showing His-tag-R1 purified with Ni-NTA spin column with wash buffer of different concentration imidazole. M: protein marker. Lane 1 to 3: rH-pepR1 elution washed with different concentration of imidazole wash buffer (1: 20 mM, 2: 80 mM, 3: 100 mM). C: crude extract of rH-pepR1 after cell disruption.

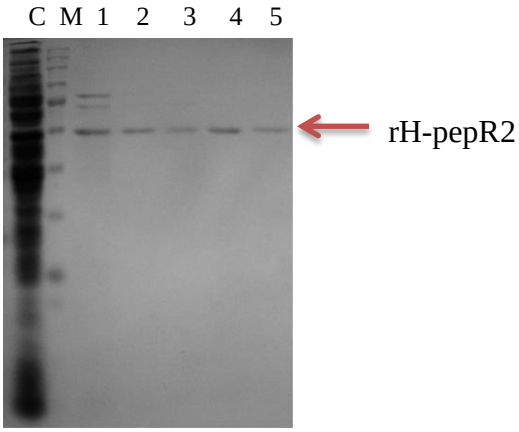

Fig. 5-3 Coomassie Brilliant Blue G250-stained 10% SDS-PAGE gel showing His-tag-R2 purified with Ni-NTA spin column with wash buffer of different concentration imidazole. C: crude extract of rH-pepR2 after cell disruption. M: protein maker. Lane 1 to 5: rH-pepR2 elution washed with different concentration of imidazole wash buffer (1: 20 mM, 2: 40 mM, 3: 60 mM, 4: 80 mM, 5: 100 mM).

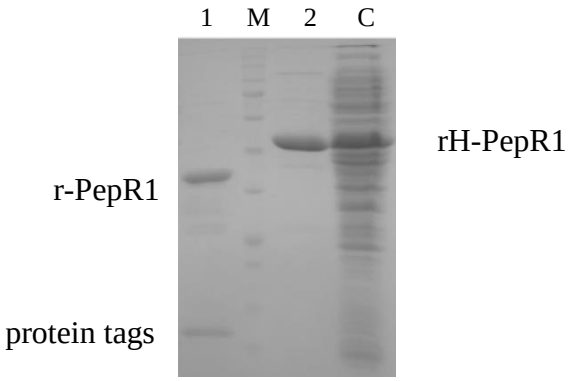

Fig. 5-4 Coomassie Brilliant Blue G250-stained 10% SDS-PAGE gel showing pure r-PepR1 cleaved with thrombin. Lane 1: cleaved r-pepR1. M: protein marker. Lane 2: rH-PepR1. C: crude extract of rH-PepR1. Lane 1 sample was loaded onto gel filtration chromatography for separation.

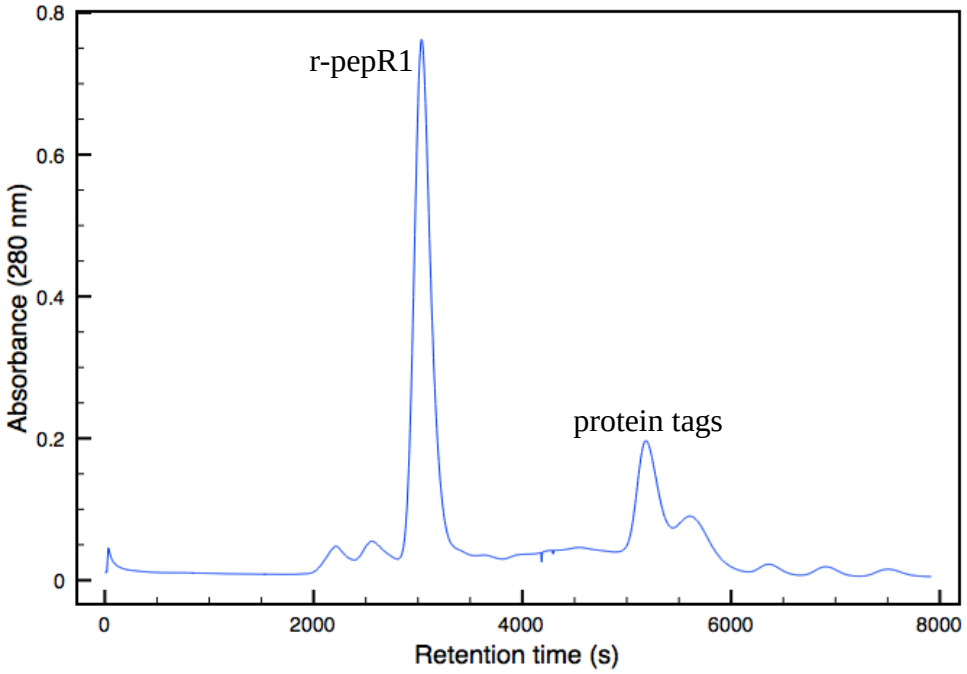

Fig. 5-5 Gel filtration chromatogram of r-PepR1. The separated protein peaks of r-pepR1 and protein tags (Trx-tag and N-terminal His-tag) were displayed in the chromatograph.

5.3.2 Purification of non-tagged prolinase

Since rH-PepR2 could not provide non-tagged r-PepR2 proteins, we used a conventional non-tag expression to obtain r-PepR2. Cell lysate of non-tagged recombinant prolinase pKK-223-3-*pep*R2 was firstly purified with the method of ammonium sulfate precipitation. Precipitated proteins from sequentially increased saturation were checked on SDS-PAGE (Fig. 5-6). During ion exchange chromatography (Fig.5-7), r-PepR2 was eluted in the peak pointed with a red arrow in Fig 5-7, where the salt concentration was approximately 0.35 M NaCl in buffer (20 mM Tris-HCl pH7.5). Fractionated r-PepR2 samples were checked on SDS-PAGE gel (Fig. 5-8). After hydrophobic interaction chromatography, r-PepR2 fractions were checked on SDS-PAGE to visualize the purity (Fig. 5-9). Results of each step purification are summarized in Table 5-2.

His-tagged r-PepR1 had a higher percentage of recovery than using non-tagged r-PepR2. The His-tagged expression simplified purification and increased yield of recombinant prolinase; whereas the non-tagged vector going through multi-step of purification and losing some of prolinase in each step.

In this study, purification of His-tagged prolinase was based on the use of chelated metal ion nickle and enabled the purification from the crude extract of the host cell in minimum steps. This minimum-step purification of recombinant His-tagged prolinases (rH-PepR1 and rH-PepR2) were found to be more efficient than purification via recombinant non-tagged prolinase (r-PepR2). His-tagged prolinase had Trx-tag, S-tag, N- and C-terminal His-tags. While the tags assisted the purification, these protein tags could directly and indirectly enhance protein yield by increasing protein solubility (Rajan *et al.*, 1998; Sun *et al.*, 2005; Chen *et al.*, 2005; Dyson *et al.*, 2004; Hammarstrom *et al.*, 2002; Nallamsetty *et al.*, 2005). Purification of His-tagged prolinase was a quick and cost-effective approach with advantages of higher protein yields, higher protein solubility over non-tagged prolinase. Additionally, the protein tags on His-tag-prolinase may have positive effects in the biochemical properties of prolinase. A literature survey revealed that protein tags prevented proteolysis, facilitated protein refolding, protected antigenicity of the fusion protein (Tang *et al.*, 1997; Shi *et al.*, 2005; Mayer *et al.*, 2004). However, one of the drawbacks to use affinity tags for purification is the uncertainty of cleavage events in the fusion protein. In some cases, cleavage occurs at secondary sites instead of at the specific cleavage site (Kenig *et al.*, 2005). The non-specific cleavage can lead to fusion protein degradation and lower

yields (Jenny *et al.*, 2003; Kwon *et al.*, 2005). Similar to these examples, the digestion of rH-PepR2 with thrombin resulted in degradation of prolinase rather than cleavage of the tags. Thus, we did not pursue the removal of tags but opted to use a conventional expression system to obtain non-tagged r-PepR2. Other negative impacts of adding affinity tags include a change in protein conformation, lower protein yields, inhibition of enzyme activity, alteration in biological activity, undesired flexibility in structure and toxicity (Chant *et al.*, 2005; Goel, *et al.*, 2000; Kim, *et al.*, 2001; Cadel, *et al.*, 2004; Fonda, *et al.*, 2002; Smyth, *et al.*, 2003; de Vries, *et al.*, 2003). Affinity tags may lead to different characteristics of tagged and non-tagged prolinases. Therefore, in the following characterization, both tagged and non-tagged prolinases were examined.

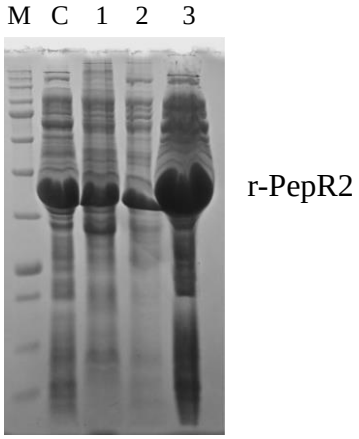

Fig. 5-6 Coomassie Brilliant Blue G250-stained 10% SDS-PAGE gel showing r-PepR2 cell lysate treated step-wisely with increasing ammonium sulfate concentrations. (M: molecular marker, C: r-PepR2 cell lysate as control. Lane 1: r-PepR2 precipitant with 20% ammonium sulfate saturation. Lane 2: r-PepR2 precipitant with 40% ammonium sulfate saturation. Lane 3: r-PepR2 precipitant with 60% ammonium sulfate saturation.

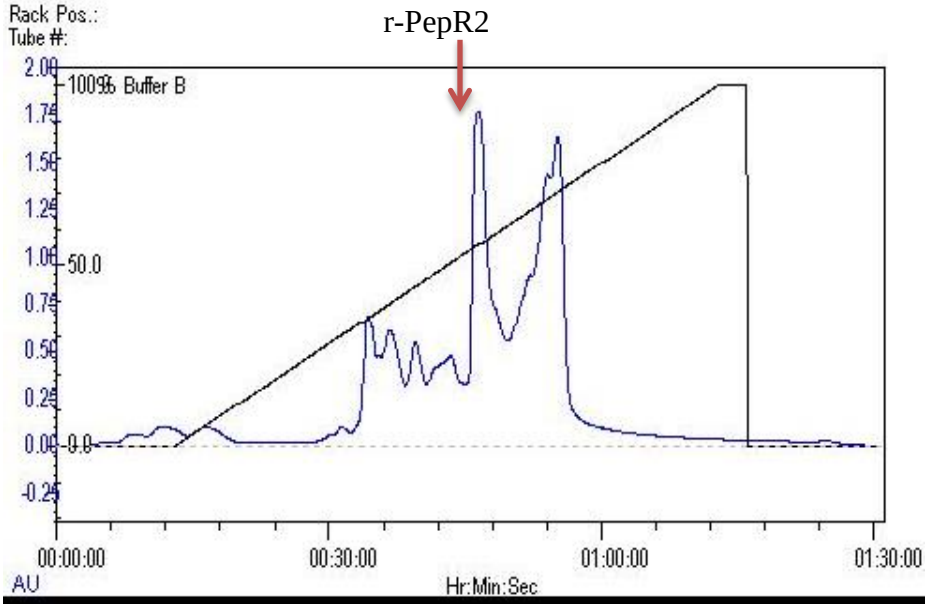

Fig. 5-7 Ion exchange chromatograph showing that r-PepR2 was separated over 20 mM Tris-HCl pH7.5 buffer with a linear NaCl gradient (0 M to 1 M). The peak containing r-PepR2 is pointed at with a red arrow at approximate 0.35 M NaCl.

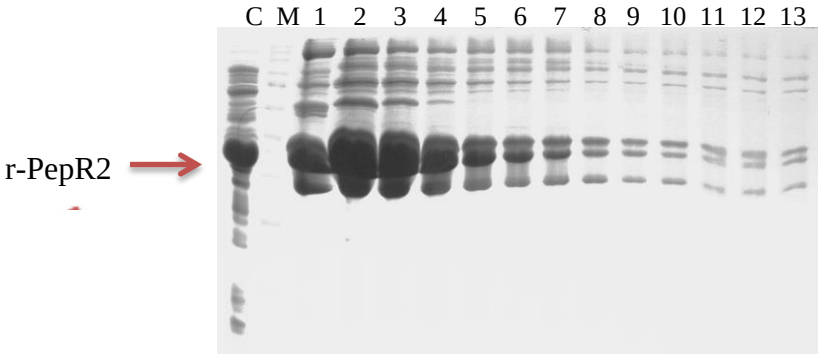

Fig. 5-8 Coomassie Brilliant Blue G250-stained 10% SDS-PAGE gel showing fractionated r-PepR2 separation of ion exchange chromatography. C: r-PepR2 precipitant with 60% ammonium sulfate saturation as control. M: protein marker. Lane 1 to 13: r-PepR2 fractions eluted in the buffer with approximate 0.35 M NaCl. Fraction #1 to 4 were used for the further purification.

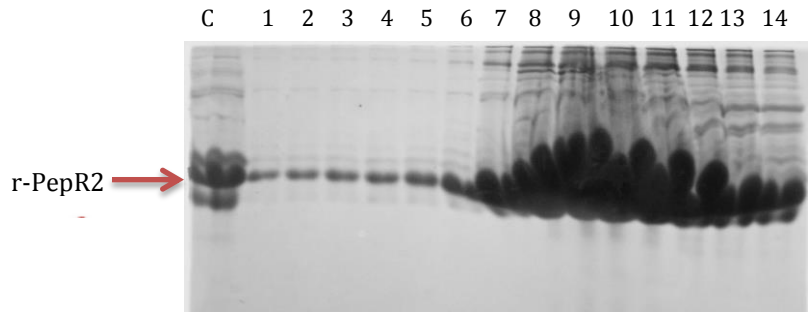

Fig. 5-9 Coomassie Brilliant Blue G250-stained 10% SDS-PAGE gel showing fractionated r-PepR2 separation of hydrophobic interaction chromatography. C: r-PepR2 after ion exchange chromatography as control. Lane 1 to 14: fractionated r-PepR2 of hydrophobic interaction chromatography. Noisy background of some fractions is due to ammonium sulfate in the sample.

Table 5-1 Summary of the purification of His-tagged prolinase r-PepR1

Purification step	Total protein (mg)	Specific activity (μmol/mg·min)	% Yield	Purification (fold)
1. Crude extract[1]	336.0	----[2]	100	----
2. Ni-NTA	98.8	0.309 ± 0.002	29.4	1
3. Gel filtration	87.6	0.359 ± 0.019	26.1	1.2

[1] Bacteria with r-PepR1 was cultured in 800-mL of LB media for three days, and 5.60 g of bacterial cell pellet was obtained.
[2] Specific activity of crude extract could not be accurately measured owing to substantial amount of proline and hydroxyproline in bacteria lysate.

Table 5-2 Summary of the purification of non-tagged prolinase r-PepR2

Purification step	Total protein (mg)	Specific activity (μmol/mg·min)	% Yield	Purification (fold)
1. Crude extract[1]	2156.4	----[2]	100	----
2. Ammonium sulfate precipitation	1617.0	0.015 ± 0.000	75.0	1
3. Ion exchange	751.3	0.031 ± 0.001	34.8	2.1
4. Hydrophobic interaction	304.8	0.618 ± 0.009	14.1	41.2

[1] Bacteria with r-PepR2 was cultured in 2-L of LB media for three days, and 10.43 g of bacterial cell pellet was obtained.
[2] Specific activity of crude extract could not be accurately measured owing to substantial amount of proline and hydroxyproline in bacteria lysate.

5.4 Characterization of recombinant prolinases

Characteristics of recombinant *Lactobacillus plantarum* prolinase r-PepR1 and r-PepR2 were examined for pH dependence, temperature dependence, substrate specificity, secondary structure, thermal denaturation temperature, molecular modeling, enzyme kinetics, and proteolysis mode.

5.4.1 Examination on ninhydrin reaction with various proline dipeptides

The ninhydrin method can be specific for proline when the conditions are optimized for it as discussed in the literature review. At the beginning of this study, we measured the blanks for each substrates and products of prolinase reactions. Results of anhydrous and acidic ninhydrin reactions with free amino acids (proline, glutamic acid, phenylalanine, glycine, methionine, leucine, serine, arginine) and dipeptides (Pro-Pro, Pro-Glu, Pro-Phe, Pro-Gly, Pro-Met, Pro-Leu, Pro-Leu, Pro-Arg) are summarized in Table 5-3. There was no color change with the tested α-amino acids; whereas slight color change was observed for the tested Pro-Xaa. The slight color change with Pro-Xaa may be due to 1) the exposed imino ring of Pro-Xaa reacting with ninhydrin and forming transient and unstable coloration; 2) impurity from the Pro-Xaa preparations (about 95% of purity) possibly containing free proline; 3) chemical hydrolysis (instead of enzymatic hydrolysis) of Pro-Xaa at high temperature (95°C), which was also the temperature for ninhydrin-proline color formation. However, the slight coloration between ninhydrin and Pro-Xaa was not a significant interference to the quantification of ninhydrin-proline. It had been claimed that strong acid conferred specificity for imino acids (Wren and Wiggall, 1964). In this study, the color yield of ninhydrin-proline was significantly higher than the α-amino acids and the Pro-Xaa dipeptides being tested. The results agreed with Wren and Wiggall's study (1964) that modified ninhydrin solution was sensitive to proline and gave highly precise values with an accuracy of about ± 5%. Thus we concluded this modified method could be utilized for proline quantification in this study.

Table 5-3 Interference test of ninhydrin reaction with Pro against other compounds

	$ABS_{500\ nm}$	Significant factor[2]
Pro[1]	1.241 ± 0.004	a
Glu	0.042 ± 0.001	b
Phe	0.045 ± 0.001	b
Gly	0.045 ± 0.001	b
Met	0.041 ± 0.001	b
Leu	0.042 ± 0.001	b
Ser	0.045 ± 0.000	b
Arg	0.046 ± 0.002	b
Pro-Pro	0.125 ± 0.021	b
Pro-Glu	0.085 ± 0.075	b
Pro-Phe	0.102 ± 0.009	b
Pro-Gly	0.091 ± 0.002	b
Pro-Met	0.087 ± 0.016	b
Pro-Leu	0.061 ± 0.010	b
Pro-Ser	0.117 ± 0.003	b
Pro-Arg	0.075 ± 0.001	b

[1] All of amino acids and Pro-Xaa were tested at concentration 12 mM, which was the maximum concentration used in enzymatic kinetic test.
[2] Data was analyzed using Excel add-in StatPlus for ANOVA F-test. The *p* value was less than 0.05, which indicated that color yield from Pro was significantly different from the others being tested. Significant factors a and b were obtained by comparing the pairwise comparison of the means and the Fisher's Least Significant Difference value (0.012). All experiments were done in triplicate.

5.4.2 Establish ninhydrin-proline standard curve

Linear standard curve of ninhydrin-proline was established using a series of proline concentrations ranging from 0 to 0.4 μmol. Proline solution (20 μL) was added to 200 μL of modified ninhydrin solution (15 mg/mL (w/v) ninhydrin and 0.03 mL/mL (v/v) glacial acetic acid in 1 mL of n-butanol, pH1 adjusted with HCl). The mixture was then incubated at 95°C for 5 min, and chilled on ice. As in Fig. 5-10, the linear regression was $y = 3.1163x + 0.0881$, where y was the measured absorption at 500 nm and variance x was the amount of proline. R square of the linear regression was 0.97, indicating that accuracy was high within ± 3%.

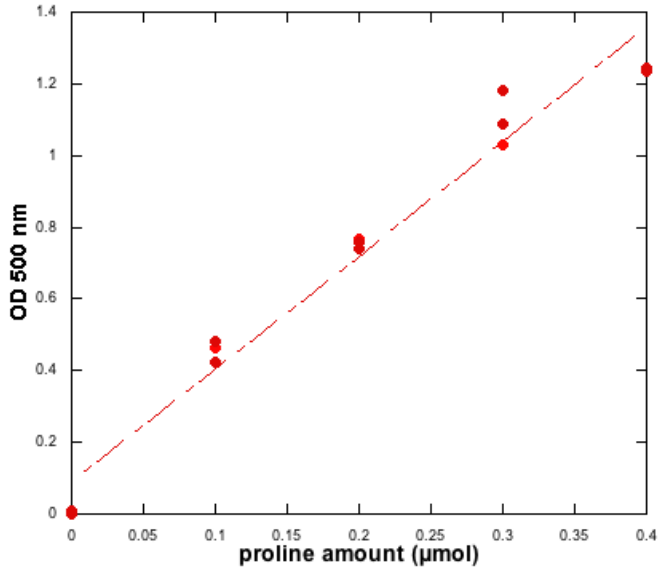

Fig. 5-10 Standard curve of ninhydrin-proline. The linear regression was y = 3.1163x + 0.0881 (R^2 = 0.97). All experiments were done in triplicate.

5.4.3 Summary of tagged, tag-removed and non-tagged recombinant prolinases used in characterization

Affinity tags (such as His-tag in the present study) were highly efficient tools for protein purification. However, the presence of affinity tags in recombinant proteins can pose unwanted and negative effects in prolinase activities, resulting in a change in protein conformation, inhibition of enzyme activity, alteration in biological activity, undesired flexibility in protein structure, and toxicity (Chant, *et al.*, 2005; Goel, *et al.*, 2000; Kim, *et al.*, 2001; Cadel, *et al.*, 2004; Fonda, *et al.*, 2002; Smyth, *et al.*, 2003; de Vries, *et al.*, 2003). In order to investigate unpredictable changes through the presence of affinity tags in prolinases, both tagged and non-tagged recombinant prolinases were examined in the following characteristic tests (Table 5-4).

Table 5-4 Summary of different recombinant prolinases used in the following tests

	rH-PepR1[1]	r-PepR1	rH-PepR2	r-PepR2
Substrate specificity	☑[2]			☑
Temperature dependence	☑	☑	☑	☑
pH dependence	☑	☑	☑	☑
Proteolysis mode	☑	☑	☑	☑
Secondary structure	☑	☑	☑	☑
Thermal denaturation	☑	☑	☑	☑
Native molecular mass	☑	☑		☑

[1] rH-PepR1 and rH-PepR2 were His-tagged recombinant prolinases constructed with pET32b(+) vector. r-PepR1 was tag-removed recombinant prolinase and free of N-terminal Trx-tag and N-terminal His-tag. r-PepR2 was non-tagged recombinant prolinase constructed with pKK223-3 vector.
[2] Symbol of ☑ represents the characterization was conducted, whereas blanks indicates that it was not examined.

5.4.4 Substrate specificity determination

Substrate specificity tests were conducted to determine the most active substrate for prolinase for the following characterizations. The most active substrate would be further confirmed by comparing the enzyme kinetic values under the optimal conditions for prolinase hydrolysis. Recombinant prolinases rH-PepR1 and r-PepR2 were tested with 2 mM different substrates at the same temperature (37°C) using the same buffer (20 mM Tris-HCl pH7.5). These preliminary substrate specificity tests are summarized in Table 5-5 and Table 5-6. The most active substrate to rH-PepR1 was Pro-Gly, followed by Pro-Ser, Pro-Met, Pro-Leu, Pro-Ser, Pro-Arg, Pro-Pro, Pro-Phe, Pro-Glu. Pro-Gly was also found to be the most preferred substrate for r-PepR2, followed by Pro-Ser, Pro-Arg, Pro-Leu, Pro-Pro, Pro-Met, Pro-Glu, Pro-Phe. Both rH-PepR1 and r-PepR2 had the highest activities against Pro-Gly, but their substrate specificities against other substrates were different.

Table 5-5 Substrate specificity tests of r-PepR1

Substrate[1]	Activity (μmol/mg·min)[2]	Relative activity (%)[3]
Pro-Gly	0.247 ± 0.016	100
Pro-Arg	0.068 ± 0.007	27
Pro-Ser	0.124 ± 0.002	50
Pro-Leu	0.138 ± 0.003	56
Pro-Pro	0.042 ± 0.007	17
Pro-Met	0.145 ± 0.005	59
Pro-Glu	0.026 ± 0.005	11
Pro-Phe	0.035 ± 0.006	14

[1] All of substrates were examined at concentration 2 mM under the same condition (37°C, 20 mM Tris-HCl pH7.5 buffer).
[2] Ninhydrin reactions with the released free proline from substrates were measured at $ABS_{500\ nm}$
[3] The activity against Pro-Gly was normalized to 100%, and the relative activities against other substrates were calculated accordingly.

Table 5-6 Substrate specificity tests of r-PepR2

Substrate[1]	Activity (μmol/mg·min)[2]	Relative activity (%)[3]
Pro-Gly	0.353 ± 0.044	100
Pro-Arg	0.234 ± 0.020	66
Pro-Ser	0.304 ± 0.018	86
Pro-Leu	0.154 ± 0.014	44
Pro-Pro	0.103 ± 0.003	29
Pro-Met	0.065 ± 0.003	18
Pro-Glu	0.046 ± 0.002	13
Pro-Phe	0.029 ± 0.000	8

[1] All of substrates were examined at concentration 2 mM under the same condition (37°C, 20 mM Tris-HCl pH7.5 buffer).
[2] Ninhydrin reactions with the released free proline from substrates were measured at $ABS_{500\ nm}$
[3] The activity against Pro-Gly was normalized to 100%, and the relative activities against other substrates were calculated accordingly.

5.4.5 Temperature dependence

Recombinant prolinase r-PepR1 and r-PepR2 were examined at different temperatures (5, 15, 20, 25, 30, 37, 40, 45, 50 and 55°C) using the same substrate (2 mM Pro-Gly) and the same buffer (50 mM HEPES pH7.5). r-PepR1 had the highest activity at 25°C; whereas r-PepR2 did so at 30°C (Fig. 5-11). The tagged recombinant prolinase rH-PepR1 compared with tag-removed (r-PepR1), and the tagged rH-PepR2 compared with non-tagged r-PepR2 were all tested on temperature dependence. Results showed that the presence of N-terminal Trx-tag and N-terminal His-tag did not influence the temperature dependence. Both tagged rH-PepR1 and tag-removed r-PepR1 had their optimal temperature at 25°C (Fig. 5-12). Likewise, both tagged rH-PepR2 and non-tagged r-PepR2 were most active at 30°C (Fig. 5-13).

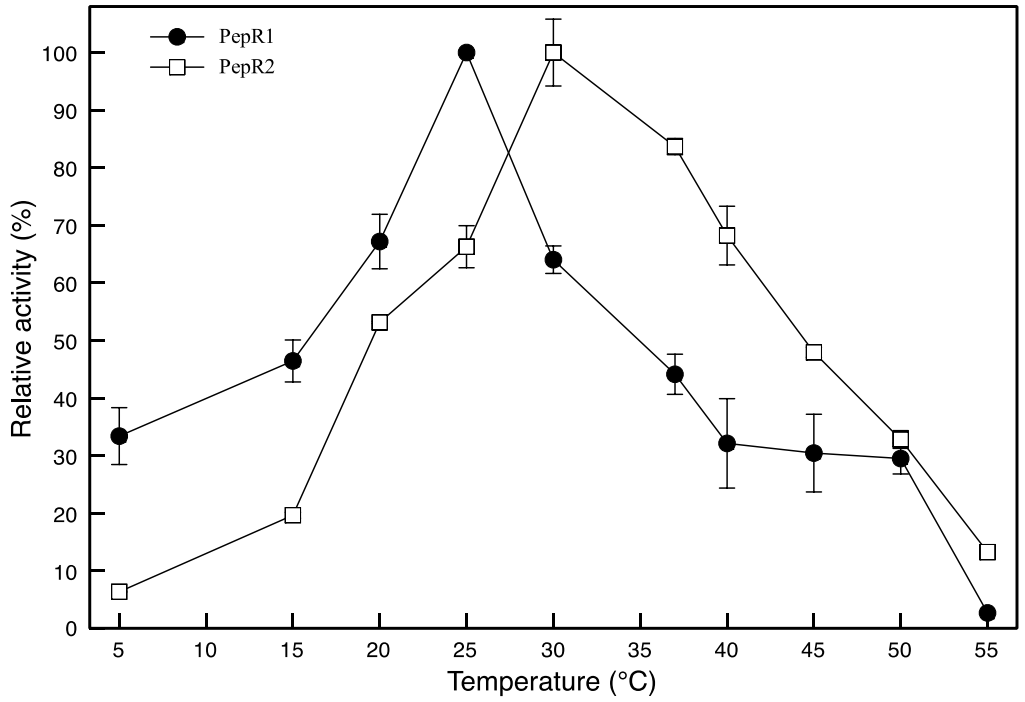

Fig. 5-11 Effects of temperature on recombinant prolinases r-PepR1 and r-PepR2 activity. Both r-PepR1 and r-PepR2 were tested on temperature (5, 15, 20, 25, 30, 37, 40, 45, 50 and 55°C). The highest activity of r-PepR1 (0.1771 μmol/mg·min) and r-PepR2 (0.6455 μmol/mg·min) were normalized to 100%, respectively. Results were expressed as standard deviations with error bars. Invisible error bars were within the symbol.

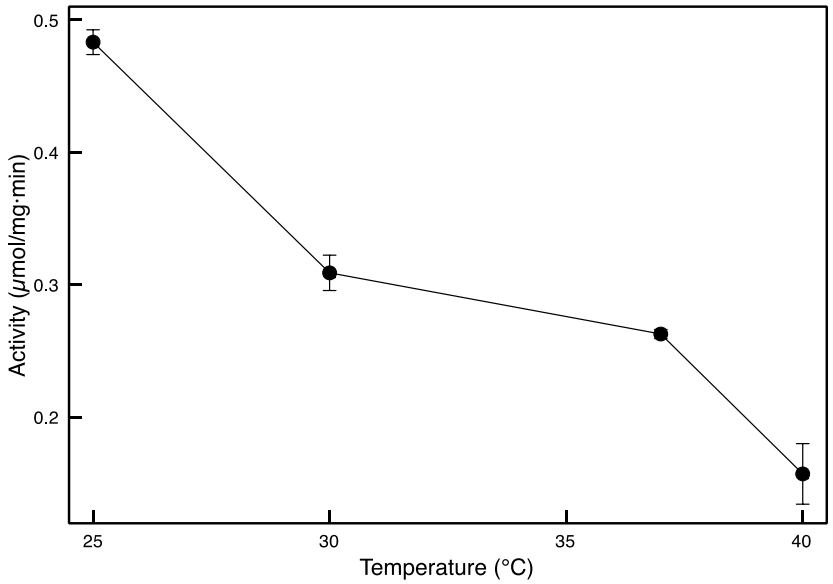

Fig. 5-12 Temperature effect on rH-PepR1. Results were expressed as standard deviations with error bars. Invisible error bars were within the symbol. All experiments were done in triplicate.

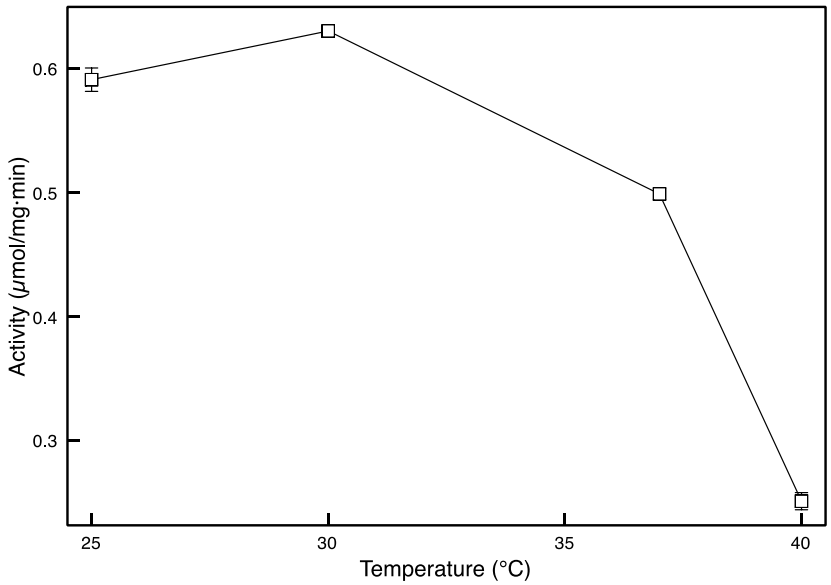

Fig. 5-13 Temperature effect on rH-PepR2. Results were expressed as standard deviations with error bars. Invisible error bars were within the symbol. All experiments were done in triplicate.

5.4.6 pH dependence

Recombinant prolinases r-PepR1 and r-PepR2 were examined in the pH range from 3.0 to 10.0 using different buffers. The highest r-PepR1 activity was observed at pH7.5 using 50 mM HEPES buffer (Fig. 5-14). The highest r-PepR2 activity was obtained at pH8.0 using 50 mM HEPES buffer (Fig. 5-15). Both tagged rH-PepR1 and tag-removed r-PepR1 had their optimal pH at 7.5 (Fig. 5-16). Similarly, both tagged rH-PepR2 and non-tagged r-PepR2 were most active at pH8.0 (Fig. 5-17). It indicated that N-terminal Trx-tag and N-terminal His-tag did not affect the pH dependence.

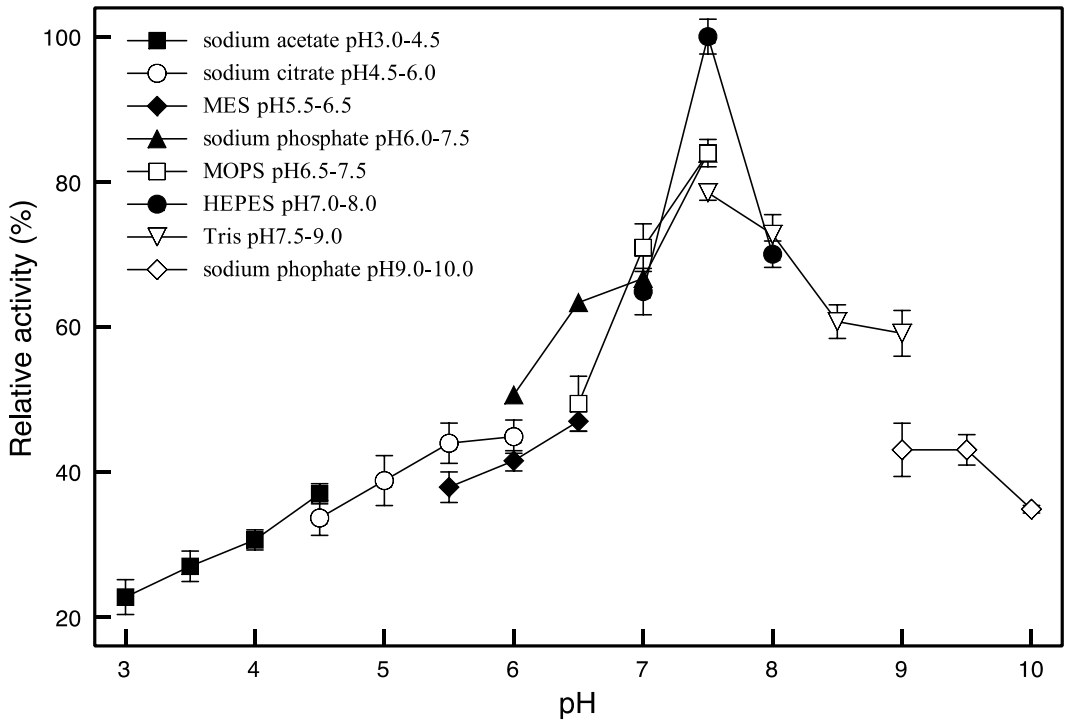

Fig. 5-14 Effect of pH on recombinant prolinase r-PepR1 activity. Different pH buffers (50 mM) were utilized: sodium acetate buffer (pH3.0 to 4.5), sodium citrate buffer (pH4.5 to 6.0), MES buffer (pH5.5 to 6.5), sodium phosphate buffer (pH6.0 to 7.5), MOS buffer (pH6.5 to 7.5), HEPES buffer (pH7.0 to 8.0), Tris buffer (pH7.5 to 9.0), sodium carbonate buffer (pH9.0 to 10.0). Hydrolysis of Pro-Gly (2 mM) was quantified by modified ninhydrin method at Abs 500 nm. The highest r-PepR1 activity (0.2479 μmol/mg·min) was normalized to 100%. Results were expressed as standard deviations with error bars. All experiments were done in triplicate.

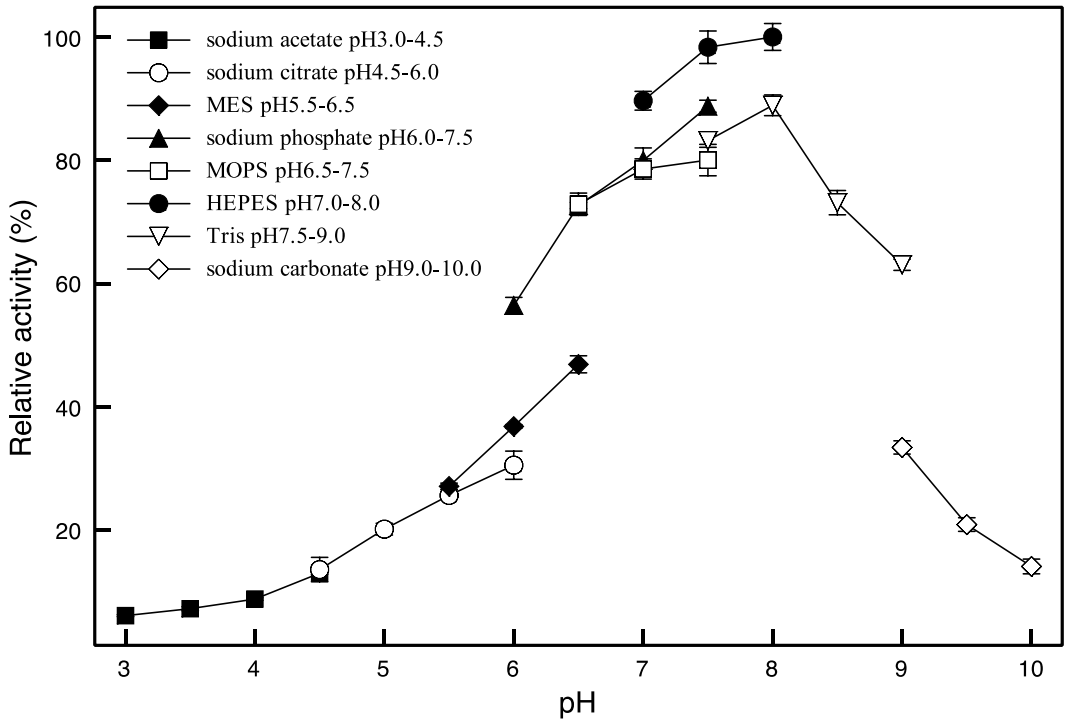

Fig. 5-15 Effect of pH on recombinant prolinase r-PepR2 activity. Different pH buffers (50 mM) were utilized: sodium acetate buffer (pH3.0 to 4.5), sodium citrate buffer (pH4.5 to 6.0), MES buffer (pH5.5 to 6.5), sodium phosphate buffer (pH6.0 to 7.5), MOS buffer (pH6.5 to 7.5), HEPES buffer (pH7.0 to 8.0), Tris buffer (pH7.5 to 9.0), sodium carbonate buffer (pH9.0 to 10.0). Hydrolysis of Pro-Gly (2 mM) was quantified by modified ninhydrin method at Abs 500 nm. The highest r-pepR2 activity (0.3101 μmol/mg·min) was normalized to 100%. Results are expressed as standard deviations with error bars. All experiments were done in triplicate.

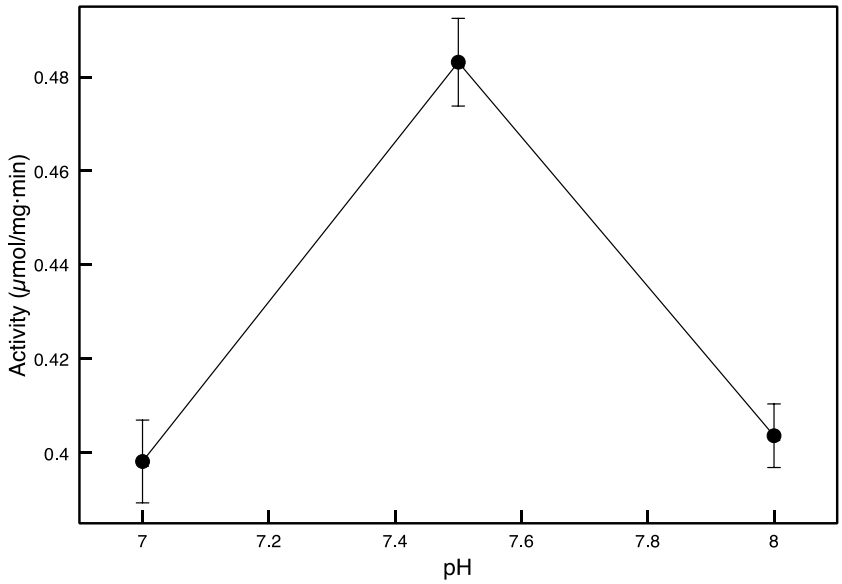

Fig. 5-16 pH effect on rH-PepR1. Results were expressed as standard deviations with error bars. All experiments were done in triplicate.

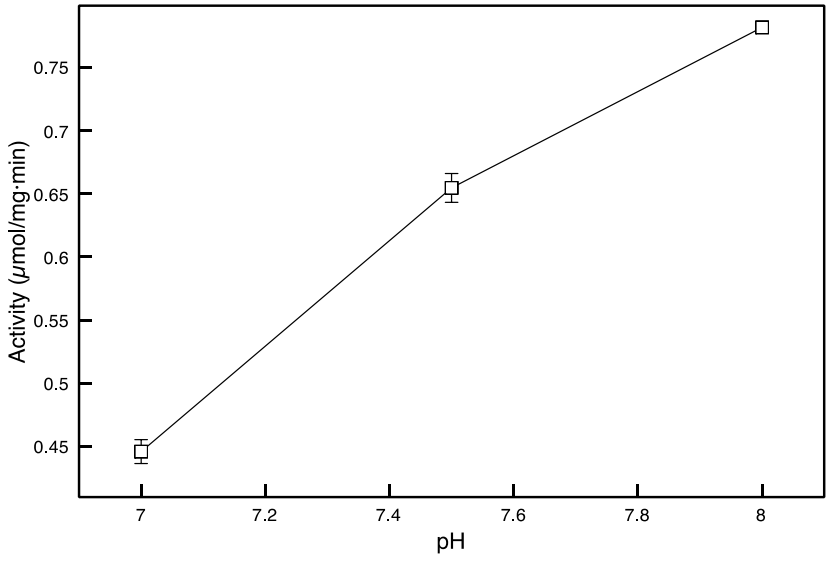

Fig. 5-17 pH effect on rH-PepR2. Results were expressed as standard deviations with error bars. Some invisible error bars were within the symbol. All experiments were done in triplicate.

5.4.7 Enzyme kinetic

The enzyme kinetic constants were determined from the initial velocities at various substrate concentrations based on the Michaelis-Menten equation. The reported data was the average of at least three independent experiments (r-PepR1 shown in Fig. 5-18, and r-PepR2 displayed in Fig. 5-19). K_m is the substrate concentration (defined as Michaelis-Menten constant) at which the velocity of the product generation reaches a half of the maximum rate V_{max}. Lineweaver Burk plot was obtained by double reciprocal of velocity and the concentration of substrate [S]. At a very low substrate concentration, when [S] is much less than K_m, the velocity is directly proportional to the substrate concentration. At high substrate concentration, when [S] is much greater than K_m, the velocity is maximal and it is independent of substrate concentration. k_{cat} is the turnover number indicating how much substrate is converted to product in per unit time. k_{cat}/K_m is catalytic efficiency showing how fast an enzyme reacts with the substrate once it encounters the substrate.

In this study (Table 5-7), the highest catalytic efficiency k_{cat}/K_m of r-PepR1 was against Pro-Met (19.6 ± 0.3 $min^{-1} \cdot mM^{-1}$), followed by Pro-Gly, Pro-Ser, Pro-Leu, Pro-Arg, Pro-Pro, Pro-Phe, Pro-Glu. But r-PepR1 had larger k_{cat} against Pro-Gly (68.6 ± 0.2 min^{-1}) than Pro-Met (31.4 ± 0.3 min^{-1}). The K_m of r-PepR1 towards Pro-Met (1.6 ± 0.3 mM) was smaller than Pro-Gly (3.7 ± 0.2 mM) and contributed to the larger value k_{cat}/K_m of Pro-Met (19.6 ± 1.0 $min^{-1} \cdot mM^{-1}$) than Pro-Gly (18.5 ± 0.2 $min^{-1} \cdot mM^{-1}$). The results indicated that Pro-Met was the optimal substrate for r-PepR1 in terms of catalytic effectiveness. For r-PepR2 (Table 5-8), the highest catalytic efficiency k_{cat}/K_m was against Pro-Gly (34.0 ± 0.3 $min^{-1} \cdot mM^{-1}$), followed by Pro-Ser, Pro-Arg, Pro-Leu, Pro-Pro, Pro-Met, Pro-Phe, Pro-Glu. The value of k_{cat} was also the highest to Pro-Gly (161.0 ± 0.3 min^{-1}). Apparently, Pro-Gly was the optimal substrate to r-PepR2.

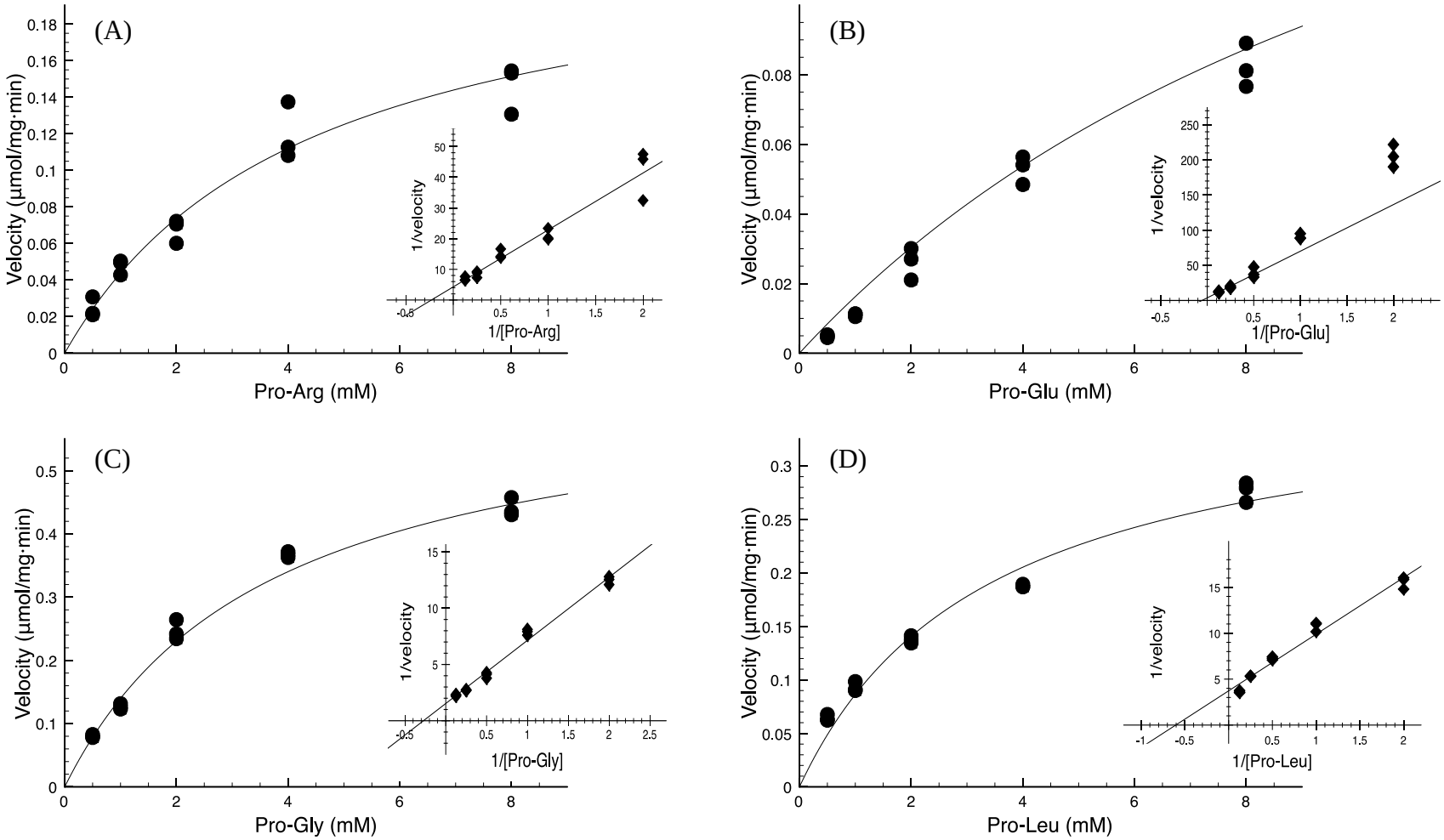

Fig. 5-18 Michaelis-Menten and Lineweaver-Burk plots of r-PepR1 (A)(B)(C)(D). The Michaelis-Menten plot shows the relationship between the concentration of substrate and the velocity of enzyme. The Lineweaver-Burk plot (or known as double-reciprocal plot of Michaelis-Menten plot) is displayed for calculating enzyme kinetic values. The substrates used in the test are (A) Pro-Arg, (B) Pro-Glu, (C) Pro-Gly, (D) Pro-Leu (E) Pro-Met, (F) Pro-Phe, (G) Pro-Pro, (H) Pro-Ser.

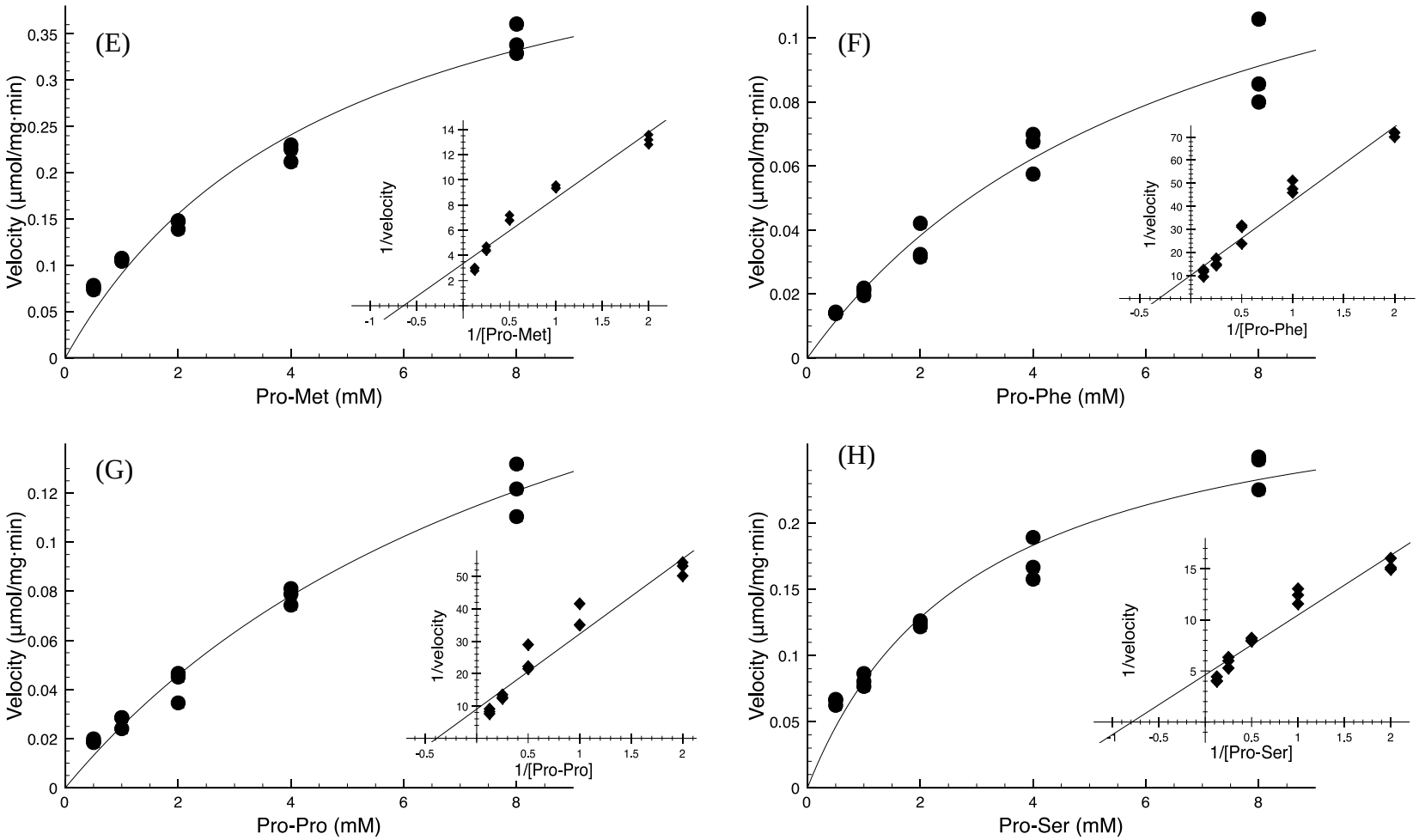

Fig. 5-18 Michaelis-Menten and Lineweaver-Burk plots of r-PepR1 (E)(F)(G)(H). The Michaelis-Menten plot shows the relationship between the concentration of substrate and the velocity of enzyme. The Lineweaver-Burk plot (or known as double-reciprocal plot of Michaelis-Menten plot) is displayed for calculating enzyme kinetic values. The substrates used in the test are (A) Pro-Arg, (B) Pro-Glu, (C) Pro-Gly, (D) Pro-Leu (E) Pro-Met, (F) Pro-Phe, (G) Pro-Pro, (H) Pro-Ser.

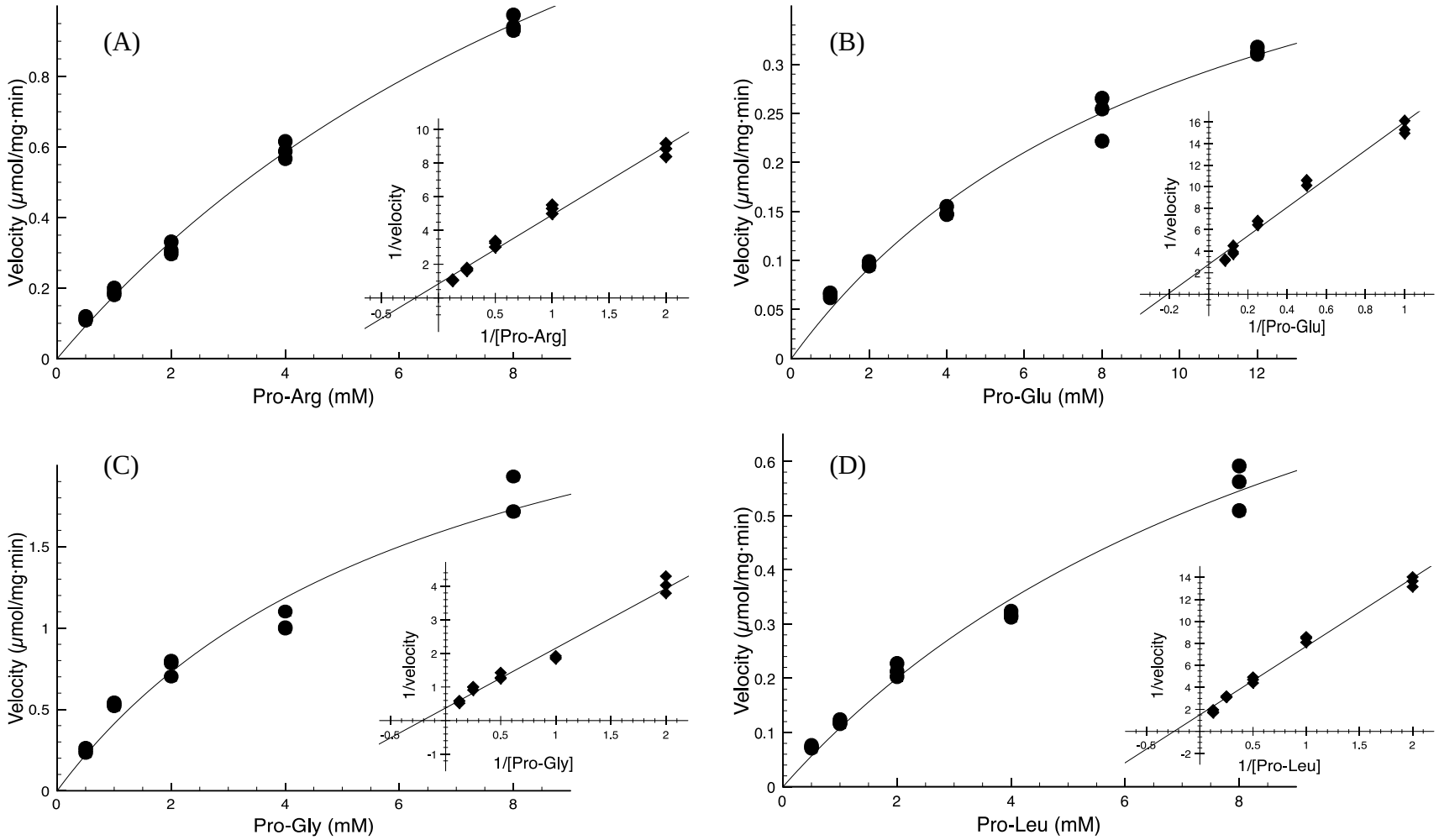

Fig. 5-19 Michaelis-Menten and Lineweaver-Burk plots of r-PepR2 (A)(B)(C)(D). The Michaelis-Menten plot shows the relationship between the concentration of substrate and the velocity of enzyme. The Lineweaver-Burk plot (or known as double-reciprocal plot of Michaelis-Menten plot) is displayed for calculating enzyme kinetic values. The substrates used in the test are (A) Pro-Arg, (B) Pro-Glu, (C) Pro-Gly, (D) Pro-Leu (E) Pro-Met, (F) Pro-Phe, (G) Pro-Pro, (H) Pro-Ser.

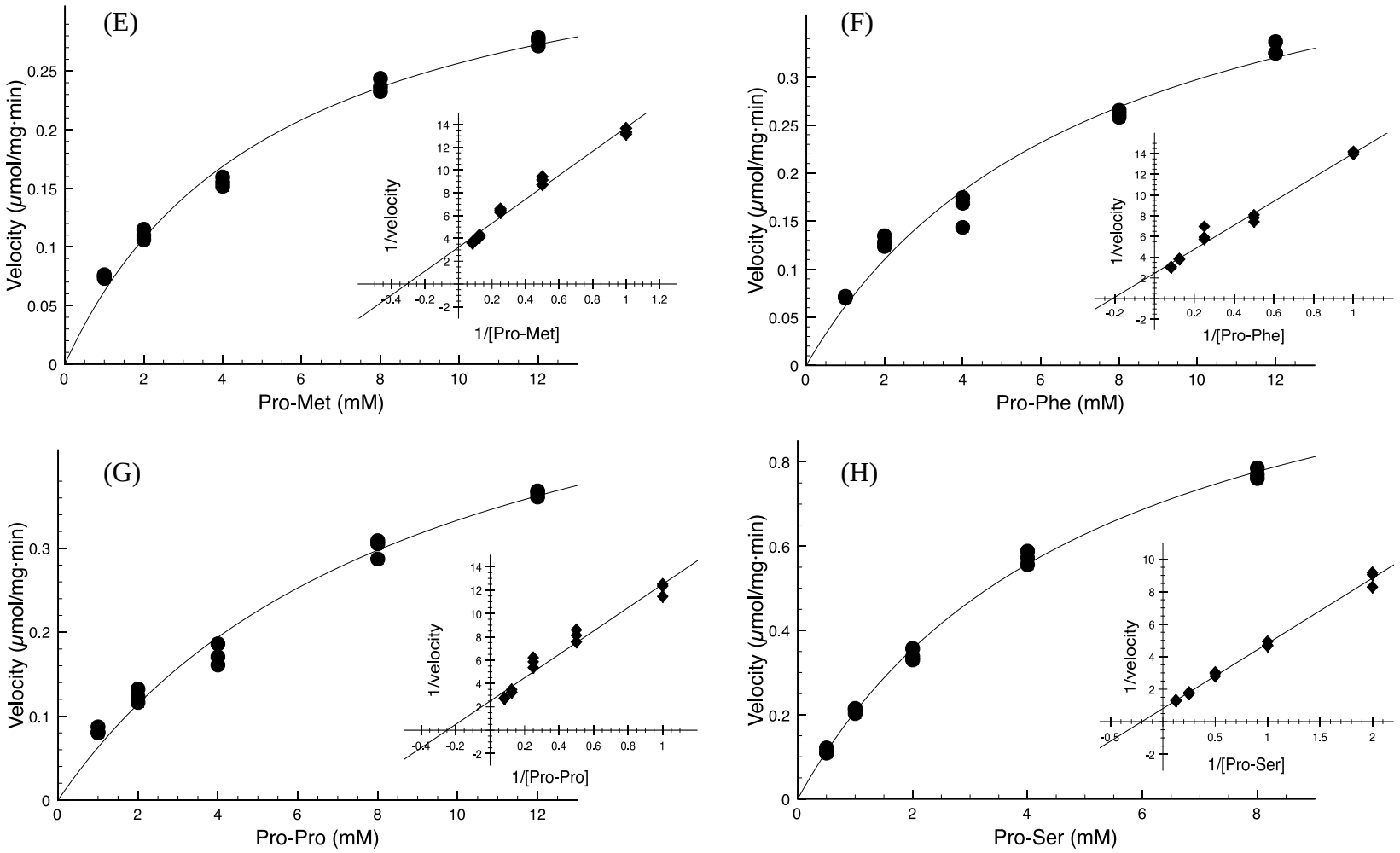

Fig. 5-19 Michaelis-Menten and Lineweaver-Burk plots of r-PepR2 (E)(F)(G)(H). The Michaelis-Menten plot shows the relationship between the concentration of substrate and the velocity of enzyme. The Lineweaver-Burk plot (or known as double-reciprocal plot of Michaelis-Menten plot) is displayed for calculating enzyme kinetic values. The substrates used in the test are (A) Pro-Arg, (B) Pro-Glu, (C) Pro-Gly, (D) Pro-Leu (E) Pro-Met, (F) Pro-Phe, (G) Pro-Pro, (H) Pro-Ser.

Table 5-7 Kinetic parameters of r-PepR1

Substrate	k_{cat} (min^{-1})	K_m (mM)	k_{cat}/K_m ($min^{-1}\cdot mM^{-1}$)
Pro-Arg	24.6 ± 1.4	4.3 ± 0.4	5.7 ± 1.4
Pro-Glu	24.6 ± 1.8	13.4 ± 0.3	1.8 ± 1.4
Pro-Gly	68.6 ± 0.2	3.7 ± 1.4	18.5 ± 0.2
Pro-Leu	28.3 ± 0.3	1.7 ± 0.8	16.6 ± 0.3
Pro-Met	31.4 ± 0.3	1.6 ± 0.9	19.6 ± 0.3
Pro-Phe	10.5 ± 1.8	3.2 ± 1.8	3.2 ± 1.8
Pro-Pro	11.7 ± 1.8	2.6 ± 1.9	4.5 ± 1.7
Pro-Ser	22.8 ± 0.5	1.3 ± 0.3	17.5 ± 0.5

[1] Hydrolysis was conducted under the optimal condition of r-PepR1 in 50 mM HEPES buffer pH7.5, at 25°C.

Table 5-8 Kinetic parameters of r-PepR2

Substrate	k_{cat} (min^{-1})	K_m (mM)	k_{cat}/K_m ($min^{-1}\cdot mM^{-1}$)
Pro-Arg	72.0 ± 0.4	4.9 ± 0.3	14.7 ± 0.4
Pro-Glu	21.7 ± 0.6	4.8 ± 0.2	4.5 ± 1.1
Pro-Gly	161.0 ± 0.3	4.7 ± 0.5	34.0 ± 0.3
Pro-Leu	40.0 ± 0.6	4.1 ± 0.2	9.8 ± 0.6
Pro-Met	18.7 ± 0.5	3.2 ± 0.2	5.8 ± 0.9
Pro-Phe	24.7 ± 0.3	4.7 ± 0.1	5.3 ± 0.6
Pro-Pro	24.2 ± 0.2	4.0 ± 0.1	6.1 ± 0.4
Pro-Ser	75.0 ± 0.2	5.0 ± 0.1	15.0 ± 0.2

[1] Hydrolysis was conducted under the optimal condition of r-PepR2 in 50 mM HEPES buffer pH8.0, at 30°C.

5.4.8 Proteolysis mode

The effect of inhibitors on r-PepR1 and r-PepR2 were shown in Fig. 5-20 and Fig. 5-21, and were summarized in Table 5-9 and Table 5-10, respectively. The strongest inhibition was observed using EDTA for the r-PepR1 activity where its k_{cat}/K_m value was reduced by 38%, and followed by 27% decreased activity with PMSF, 21% with DTT and a slight reduction (12%) with MAL. The effect of inhibitors on r-PepR2 was different from r-PepR1. PMSF caused 47% reduction on r-PepR2 activity, followed by 24% inhibition with DTT, 23% inhibition with EDTA, and 7% inhibition with MAL. The results showed that r-PepR1 was most strongly inhibited with EDTA among tested inhibitors, whereas r-PepR2 was most strongly inhibited with PMSF among tested inhibitors.

EDTA is a metal-chelating agent and significantly inhibited r-PepR1, suggesting that r-PepR1 was a metallo-protease. This result corresponded to previous observation in human prolinases. Butterworth and Priestman (1982) found that Mn^{2+} activated prolinase form human kidney. Wang *et al* (2004) also stated that a concentration of 0.1 mM $MnCl_2$ enhanced prolinase activity in normal erythrocytes. Cd^{2+} were also observed to activate prolinase activity (Neuman and Smith, 1951, Sarid *et al.*, 1962). Interestingly, r-PepR2 was not significantly inhibited with EDTA, implicating that it was independent on metal. r-PepR2 was inhibited by PMSF which was a serine protease inhibitor. Previously, it had been found that bacterial prolinase had a conserved catalytic site (GQSWGG) (Dudley and Steele, 1994; Varmanen *et al.*, 1996 and 1998). Among the motif, residue Ser_{111} was a conserved catalytic residue to bacterial prolinase. Neither the cysteine protease inhibitors DTT or MAL significantly reduced the activity of r-PepR1 and r-PepR2. The results suggested r-PepR1 and r-PepR2 were unlikely to be cysteine proteases. And there was no cysteine residue in the vicinity of active site in the molecular model discussed in the following section. The present results agreed with Shao *et al.* study (1997) that *Lactobacillus helveticus* CNRZ32 prolinase and its prolinase mutant with replacement of the cysteine residue (Cys_{166}) by an alanine residue using site-directed mutagenesis method exhibited indistinguishable activity.

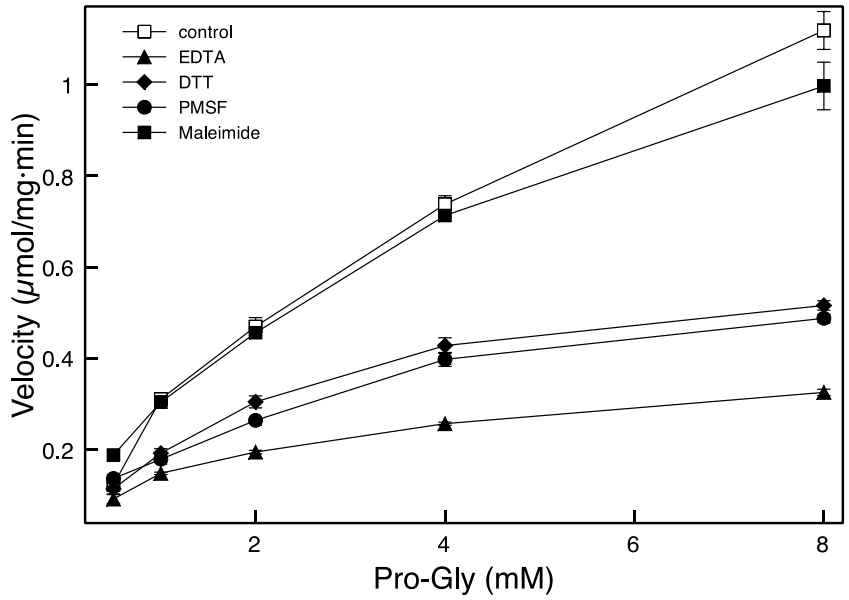

Fig. 5-20 Inhibition of r-PepR1. Inhibitors of EDTA (5 mM), DTT (1 mM), PMSF (1 mM) and MAL (1 mM) were used in these tests. All reactions were conducted under the condition of 50 mM HEPES buffer pH7.5, 25°C, Pro-Gly as substrate.

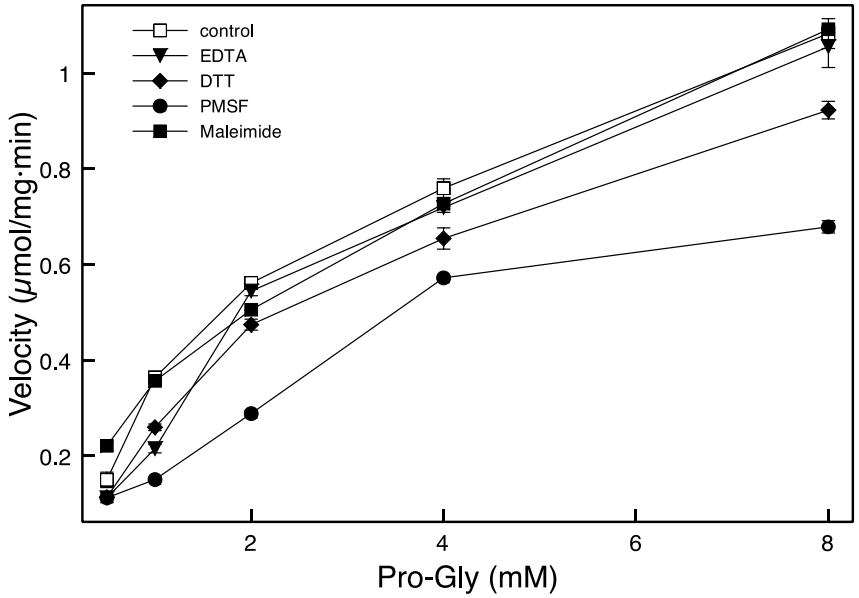

Fig. 5-21 Inhibition of r-PepR2. Inhibitors of EDTA (5 mM), DTT (1 mM), PMSF (1 mM) and MAL (1 mM) were used in these tests. All reactions were conducted under the condition of 50 mM HEPES buffer pH8.0, 30°C, Pro-Gly as substrate.

Table 5-9 Summary of r-PepR1 inhibition test

	k_{cat} (min^{-1})	K_m (mM)	k_{cat}/K_m (min^{-1}·mM^{-1})	Relative activity (%)
Control[1]	48.5 ± 0.2	6.6 ± 0.1	7.3 ± 0.2	100[2]
EDTA (5 mM)	8.2 ± 0.2	1.8 ± 0.2	4.6 ± 0.2	62
DTT (1 mM)	14.3 ± 0.1	2.5 ± 0.1	5.8 ± 0.1	79
PMSF (1 mM)	13.4 ± 0.2	2.5 ± 0.3	5.4 ± 0.2	73
MAL (1 mM)	32.2 ± 0.1	4.4 ± 0.3	6.5 ± 0.1	88

[1] All reactions were conducted under the condition of 50 mM HEPES buffer pH7.5, 25°C, Pro-Gly as substrate.

[2] The activity of control without inhibitor was normalized to 100%, and the relative activities of the inhibitor tests were calculated accordingly.

Table 5-10 Summary of r-PepR2 inhibition test

	k_{cat} (min^{-1})	K_m (mM)	k_{cat}/K_m (min^{-1}·mM^{-1})	Relative activity (%)
Control[1]	41.9 ± 0.2	5.8 ± 0.1	7.3 ± 0.2	100[2]
EDTA (5 mM)	21.7 ± 0.1	3.8 ± 0.1	5.6 ± 0.1	77
DTT (1 mM)	25.3 ± 0.2	4.5 ± 0.2	5.6 ± 0.1	76
PMSF (1 mM)	20.6 ± 0.3	5.3 ± 0.6	3.9 ± 0.3	53
MAL (1 mM)	28.4 ± 0.1	4.2 ± 0.3	6.8 ± 0.1	93

[1] All reactions were conducted under the condition of 50 mM HEPES buffer pH8.0, 30°C, Pro-Gly as substrate.

[2] The activity of control without inhibitor was normalized to 100%, and the relative activities of the inhibitor tests were calculated accordingly.

5.4.9 Native molecular mass

5.4.9.1 Dynamic light scattering

Dynamic light scattering (DLS) measures Brownian motion and relates this to the size of the protein particles. Principle of DLS is briefly demonstrated as follows (Wettig *et al.*, 2002 and 2003). The protein particles are illuminated with a laser, and the intensity fluctuations in the scattered light are recorded for a time length. As a consequence of Brownian motion (diffusion), the protein particles in the solution are always moving around. The scattered light from the moving protein particles is constantly changing with time. Thus the recorded information contains the time scale (named as delay time within a unit of micro-second) and the movement of the scattered light showing the fluctuation of the scattered light intensity around average values. The frequency of fluctuation can be converted into the particle sizes based on the Stokes-Einstein Equation (2) where D_T is translation diffusion coefficient, k is Boltzmann constant 1.38×10^{-23}, T is temperature in degree Kevin, η is solvent viscosity, and R_H is hydrodynamic radius.

$$D_T = \frac{kT}{6\pi\eta R_H} \qquad \text{Equation (2)}$$

The Equation shows the relationship between the size of a particle (the native molecular mass of prolinase in this study) and the speed of movement (frequency of the fluctuation). Generally, small particles move more quickly than large particles based on the theory of Brownian motion, indicating that the DLS intensity fluctuation of small particles are with higher frequency than large particles. Therefore, the frequency of the intensity fluctuations are size-dependent, and can be further calculated for the diffusion coefficient and the radius (termed as hydrodynamic radius) of the protein particle. The hydrodynamic radius is utilized to calculate the molecular weight. The calculated molecular weight (MW) is the power to the hydrodynamic radius (R_H) times the constant of the hydrodynamic radius factor (The formula is: MW (kDa) = [R_H Factor * R_H (nm)]^{Power}).

In the present study, DLS was employed to determine native molecular mass of r-PepR1 and r-PepR2. This method provided an accurate measurement of the average size of prolinase particles in solution. The intensity fluctuations of r-PepR1 and r-PepR2 were digitally processed into diffusion coefficients using Dynamics v.5.26.60 software package (Protein Solution Inc.). The correlation between the diffusions coefficients and the delay times of r-PepR1 and r-PepR2

were plotted in Fig. 5-22. The correlation curve was an indicator to determine whether the signal was correlated and to compare the size of the particles based on the diffusion (Goldburg, 1999). The results implicated that both r-PepR1 and r-PepR2 were correlated with the typical exponential decay. Conversely, uncorrelated diffusion coefficients would add up to roughly the same number and would look like random fluctuation around the baseline (Schillen *et al*., 1994). The correlation curve of r-PepR1 decayed at a slower rate than r-PepR2, indicating that r-PepR1 diffused slower than r-PepR2. It also meant that the particle size of r-PepR1 was larger than r-PepR2.

Hydrodynamic radius of r-PepR1 and r-PepR2 were then calculated from the Stokes-Einstein Equation. However, some of hydrodynamic radius data were filtered out according its SOS value (sum of square) (Tanner *et al*., 1982). The SOS was a quantitative value representing the residual and the goodness of fit. The hydrodynamic radius with the SOS value between 500 to 1000 was used for next step calculation of molecular mass. The hydrodynamic radius with the SOS value outside of 500 to 1000 was regarded as outliers. These outliers were bad correlations probably arising from the presence of dust or partial aggregation (Tanner *et al*., 1982; Jansson *et al.*, 2004). All of the hydrodynamic radiuses of r-PepR1 and r-PepR2 were plotted in Fig. 5-23 and Fig. 5-24. The hydrodynamic radius obtained from program Dynamics v.5.26.60 were plotted as x-axis. The y-axis was the calculated molecular weight using the formula MW (kDa) = $[R_H \text{ Factor} * R_H \text{ (nm)}]^{\text{Power}}$. In this study, the constant of the hydrodynamic radius factor (R_H Factor) was 1.68, and the power was 2.3398. Recombinant prolinase r-PepR1 was determined to have a native molecular mass of 156.5 kDa. The result implicated that r-PepR1 was a tetramer with a molecular mass approximately four-times of its monomer (39.2 kDa). Likewise, r-PepR2 was measured to have a native molecular mass of 128.2 kDa. It was also about four-times of its monomer (34.6 kDa) as a tetramer.

Both r-PepR1 and r-PepR2 were shown as tetramers by DLS. Nevertheless, there were some limitations of DLS including that 1) the shape of the protein molecules affected measurements of the hydrodynamic radius. As in DLS, the shape of particle was hypothetically considered to be hard sphere rather than coil or rod. 2) The dust or other impurities might significantly affect the light scattering intensity at low concentration of buffer (Muschol and Rosenberger, 1995). Therefore, the native molecular masses of r-PepR1 and r-PepR2 were further confirmed with gel filtration.

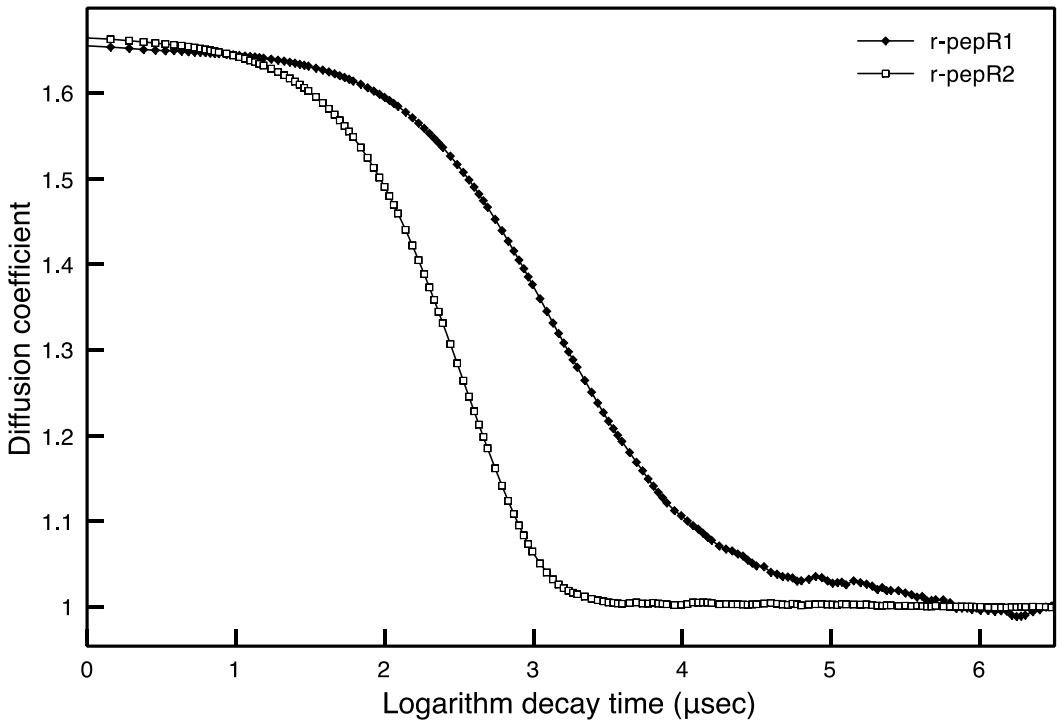

Fig. 5-22 Correlation curves of r-PepR1 and r-PepR2. Sample was prepared with 20 mM sodium phosphate pH8.0 at 25°C. Data was analyzed with program Dynamics v.5.26.60.

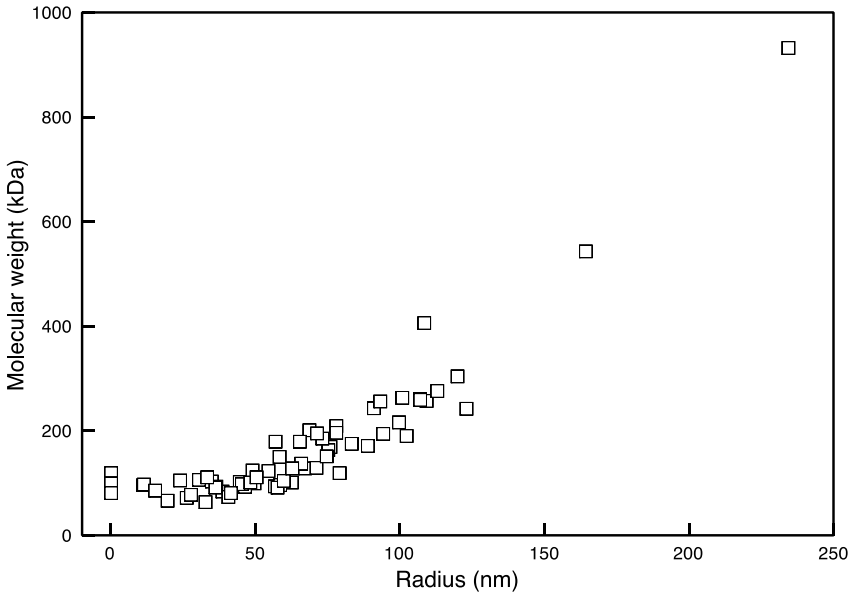

Fig. 5-23 Calibration curves of r-PepR1 molecular weight versus hydrodynamic radius. The native molecular mass of r-PepR1 was measured to be 156.5 kDa being a tetramer. Sample was prepared with 20 mM sodium phosphate pH8.0 at 25°C.

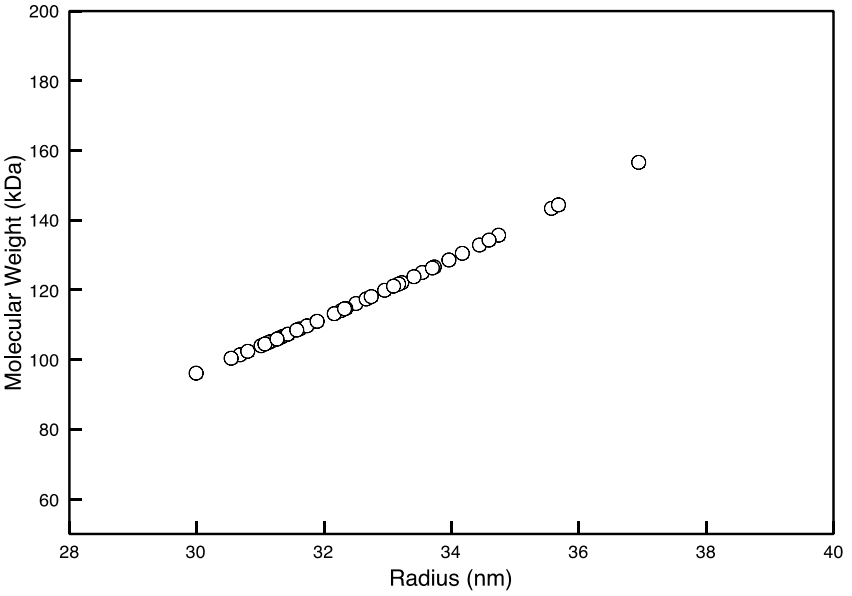

Fig. 5-24 Calibration curves of r-PepR2 molecular weight versus hydrodynamic radius. The native molecular mass of r-PepR2 was measured to be 128.2 kDa being a tetramer. Sample was prepared with 20 mM sodium phosphate pH8.0 at 25°C.

5.4.9.2 Gel filtration

Gel filtration (known as size exclusion chromatography) was applied to determine recombinant prolinase molecular weights for estimation of native molecular masses. In the present study, proteins weight standards consisted of bovine thyroglobulin (MW 670,000); bovine γ-globulin (MW 158,000); chicken ovalbumin (MW 44,000); horse myoglobin (MW 17,000); and Vitamin B_{12} (MW 1,350). A calibration curve was calculated by plotting the elution volumes of known standard proteins versus the logarithm of their molecular weight. The R square of the calibration curve was 0.96 with high correlation. As shown in the gel filtration chromatogram (Fig. 5-25), r-PepR1 was eluted between protein peaks of γ-globulin and ovalbumin. The peak of r-PepR1 was observed close to the γ-globulin peak (Fig 5-28). Molecular weight of r-PepR1 was calculated as 144.7 kDa, which was approximately four-times of its monomer (summarized in Table 5-11). It corresponded to the result from DLS (this study) with a native molecular mass of 156.8 kDa being a tetramer. Likewise, the molecular weight of r-PepR2 (Fig. 4-26) was calculated as 124.8 kDa. It agreed with the result from DLS (Chapter 5.4.9.1) with a native molecular mass of 128.2 kDa being a tetramer. The most likely causes of error in protein molecular weight estimation by gel filtration were 1) the inaccurate judgment of elution volumes, 2) different elution times of the same protein in different runs of gel filtration chromatograph, 3) different shapes of various proteins. To calculate the accuracy of using each method, the tested molecular weight (MW) was divided by theoretical tetramer MW. The estimated MW of r-PepR2 using DLS was 128.2 kDa and its theoretical MW is 138.4 kDa (four times of 34.6 kDa of monomer). Its accuracy was estimated as the ratio between them, showing that the accuracy was 92.6% for r-PepR2. Similarly the accuracy of the MW determined with DLS was estimated as 99.8% for r-PepR1. The deviation of DLS method was as much as 7.4%. For the method of gel filtration chromatography, the accuracy of the molecular weight estimation of r-PepR1 and r-PepR2 was 92.3% and 90.2%, respectively, with a deviation of 9.8%. These deviations were corresponded to Andrews's study (1964). The deviation of molecular weight of the unknown protein and the known ones estimated from the elution time or volumes of gel filtration chromatography were approximate ±10% (Andrews, 1964). The result also agreed to the common statement that DLS was more accurate than gel filtration chromatography (Diaz *et al.*, 2004). Confirmed with two methods, we concluded that both prolinases had homotetrameric structures (summarized in Table 3-14).

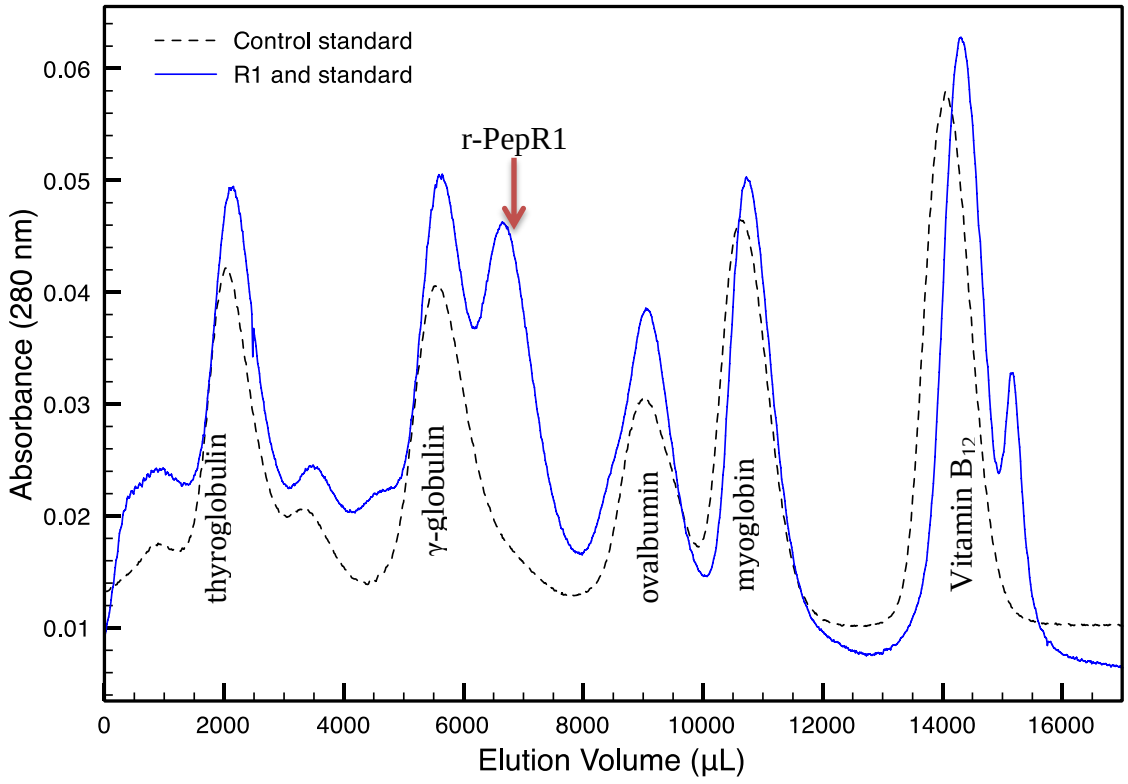

Fig. 5-25 Elution diagram for determination of r-PepR1 native molecular mass against standard proteins. Blue solid line was r-PepR1 with standard proteins. Black dash line was standard proteins with water as control. The peak pointed at with a red arrow was r-PepR1. Five standard proteins were used in this study: bovine thyroglobulin (MW 670,000), bovine γ-globulin (MW 158,000), chicken ovalbumin (MW 44,000), horse myoglobin (MW 17,000); and Vitamin B_{12} (MW 1,350). The native molecular mass of r-PepR1 was calculated to be 144.7 kDa as a tetramer.

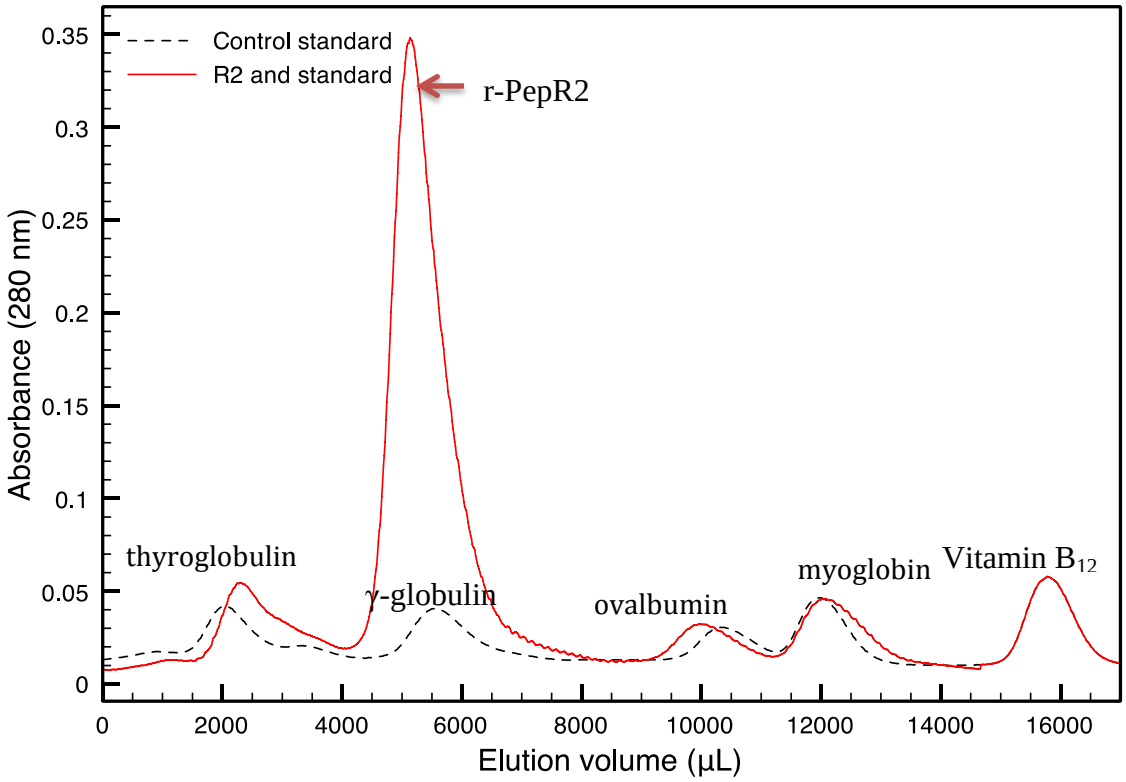

Fig. 5-26 Elution diagram for determination of r-PepR2 native molecular mass against standard proteins. Red solid line was r-PepR2 with standard proteins. Black dash line was standard proteins with water as control. The peak pointed at with a red arrow was r-PepR2 sample. Five standard proteins were used in this study: bovine thyroglobulin (MW 670,000), bovine γ-globulin (MW 158,000), chicken ovalbumin (MW 44,000), horse myoglobin (MW 17,000); and Vitamin B_{12} (MW 1,350). The native molecular mass of r-PepR2 was calculated to be 124.8 kDa as a tetramer.

Table 5-11 Native molecular weight determined from DLS and gel filtration

	Monomer MW	DLS[1]	Gel Filtration[2]
r-PepR1	39.2 kDa	156.5 kDa	144.7 kDa
r-PepR2	34.6 kDa	128.2 kDa	124.8 kDa

[1] The accuracy of r-PepR1 and r-PepR2 using DLS method was 99.8% and 92.6%, respectively. The deviation was as much as 7.4%.

[2] The accuracy of r-PepR1 and r-PepR2 using gel filtration chromatography was 92.3% and 90.2%, respectively. The deviation was as much as 9.8%.

5.4.10 Characterization of protein secondary structure

Circular dichroism spectroscopy (CD) was applied to investigate the secondary structure of recombinant prolinases. CD spectra were measured when protein molecule absorbed the left and right circularly polarized light to different extents. In the present study, the CD spectra of r-PepR1 and r-PepR2 were tested on the Far-UV range of 190 to 260 nm (Fig. 5-27). The analysis of the CD spectra was based on a set of reference proteins with known structures and the combination of individual secondary structure components (α-helices, β-sheets and random coils) (Pelton and McLean, 2000). Typically, α-helices rich proteins had negative signal near 208 nm and 222 nm but positive signal near 193 nm. The CD spectra of β-sheets displayed negative signal near 216 nm while positive signal between 195 nm and 200 nm. Random coils had negative signal near 195 nm whereas low signal at the wavelength greater than 210 nm. CD spectra were collected between 190 and 260 nm for both r-PepR1 and r-PepR2 (Fig 5-29). The observed spectra were analyzed to estimate the contents of each secondary structure with the program CDNN (Bohm *et al.*, 1992) and results were summarized in Table 5-12. r-PepR1 showed the secondary structure with a ratio of 23.1% of α-helices, 37.9% of β-sheets, 19.9% of β-turns and 34.0% of random coils. r-PepR2 had 19.2% of α-helices, 54.1% of β-sheets, 15.6% of β-turns and 21.2% of random coils.

Table 5-12 Estimated percentages of protein secondary structure components of r-PepR1 and r-PepR2 from CD spectra

	α-helix	Antiparallel	Parallel	β-turn	Random Coil
PepR1[1]	23.1%	27.8%	10.1%	19.9%	34.0%
PepR2	19.2%	46.5%	7.6%	15.6%	21.2%

[1] Recombinant prolinase r-PepR1 and r-PepR2 were prepared in 20 mM sodium phosphate buffer pH8.0 at 20°C.

(A)

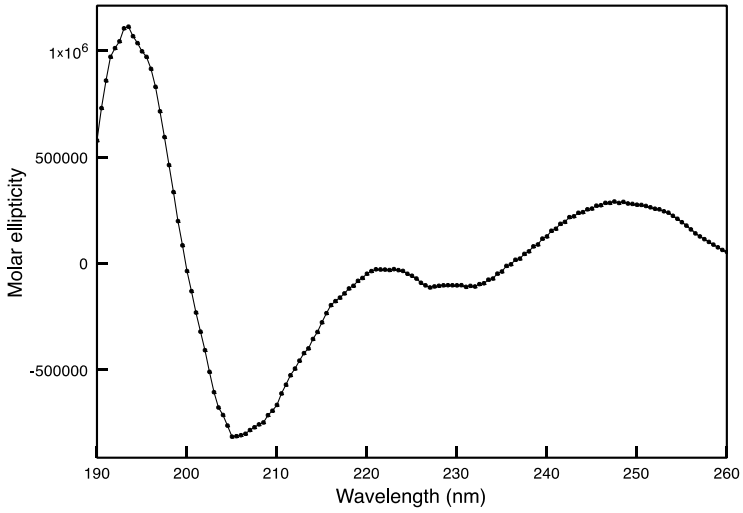

(B)

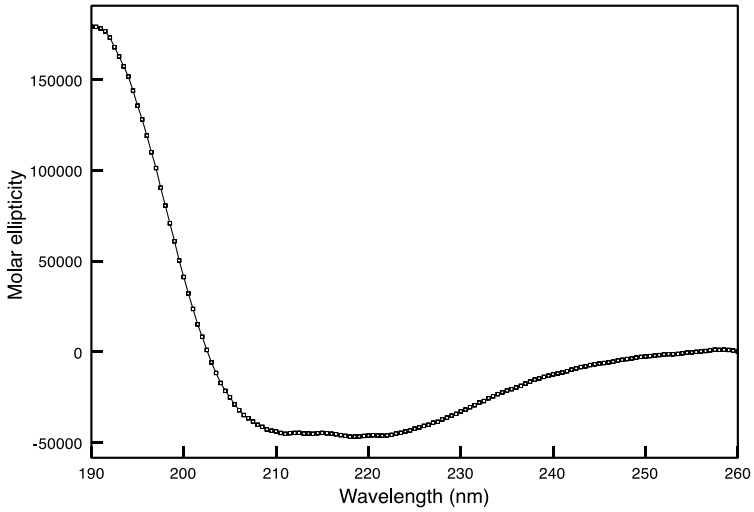

Fig. 5-27 CD spectra of recombinant prolinases for determination of protein secondary structure. (A) r-PepR1 (B) r-PepR2. Both r-PepR1 and r-PepR2 were prepared in 20 mM sodium phosphate buffer pH8.0 at 20°C. CD data in the range of 190 to 260 nm was used. Each data point was detected four times to obtain the mean value as in the plots.

5.4.11 Characterization of unfolding by CD thermal denaturation

Thermal denaturation of proteins is defined as the transition of folded to unfolded structure. At low temperatures, proteins are folded and have highly asymmetric secondary structural components. At high temperatures, proteins lose the highly organized structures because of unfolding, resulting in the loss of CD signal. The unfolding is occasionally irreversible, and it can explain incomplete recovery of the CD signal at high temperature in the thermal unfolding curve. In this research, the unfolding of prolinase was then characterized for T_M (the midpoint temperature of the unfolding transition) using the change in ellipticity of CD signal. As an index of unfolding, both CD signals of r-PepR1 and r-PepR2 were recorded at 222 nm from temperature 20°C to 85°C (Fig. 5-28). This wavelength represents α-helical protein contents. The CD data was transformed into α (the fraction folded at any Kelvin temperature). The α was calculated from the equation of $\alpha = (\theta_t - \theta_U)/(\theta_F - \theta_U)$, where θ_t was the observed ellipticity at any Kelvin temperature, θ_F was the ellipticity of the fully folded form and θ_U was the ellipticity of the unfolded form (Greenfield, 2006). T_M was defined as the temperature where α equaled 0.5. The T_M of r-PepR1 was determined to be 302.30 ± 28.13 K, which approximated 29°C. The T_M of r-PepR2 was 321.49 ± 0.06 K and approximated 48°C. The T_M values indicated that r-PepR1 was not stable at room temperature having a relatively low T_M, whereas r-PepR2 was more stable than r-PepR1. This may show their cooperative contribution in proline-containing peptides in a wider range of temperature.

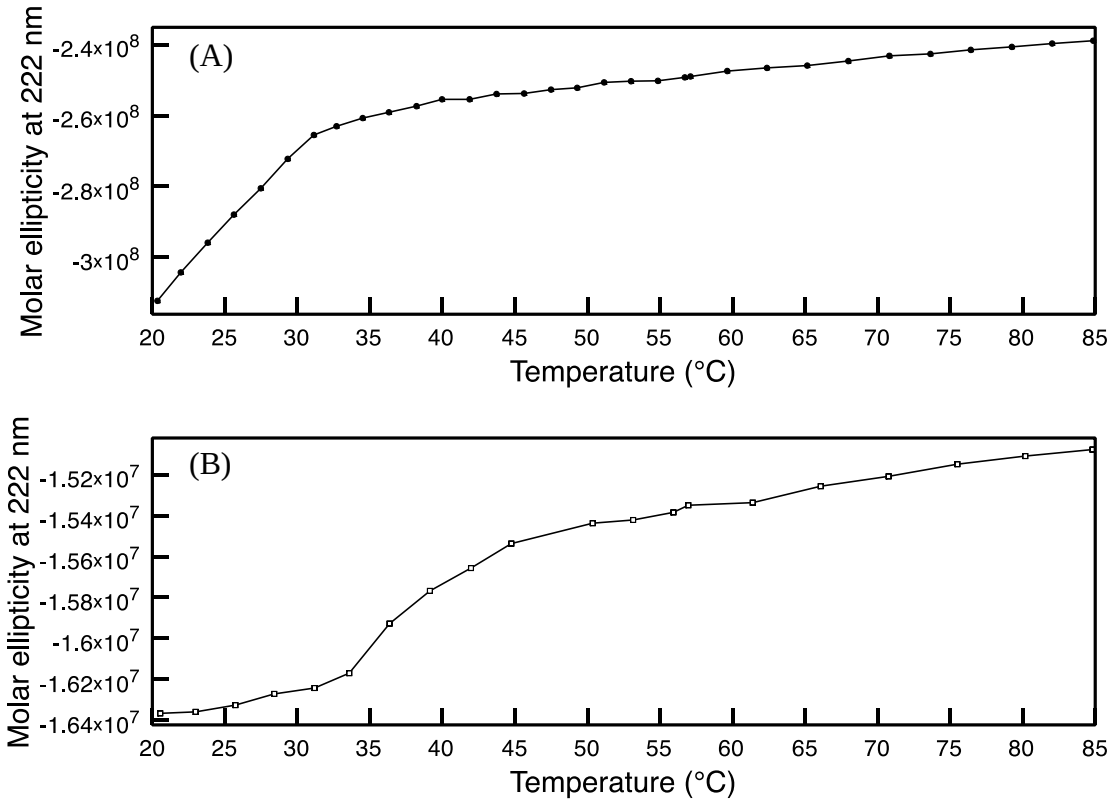

Fig. 5-28 CD thermal unfolding curve of recombinant prolinases. (A) T_M of r-PepR1 was estimated to be 29°C, (B) T_M of r-PepR2 was estimated to be 48°C. Both r-PepR1 and r-PepR2 were prepared in 20 mM sodium phosphate buffer pH8.0. Temperature was increased from 20°C to 85°C. CD data was recorded at a single wavelength of 222 nm.

5.4.12 Three-dimensional structure prediction of prolinase

The deduced protein sequence from *Lactobacillus plantarum* prolinase-coding gene *pep*R1 and *pep*R2 were submitted to the JICSAW server (Bates *et al.*, 1999, 2001, and 2002) and I-TASSER server (Zhang, 2008; Roy *et al.*, 2010 and 2012). Results from the two servers reinforced one another in an attempt to predict PepR1 and PerR2 molecular structures. PepR1 was predicted to have the highest structural similarity with the known structure of *Mycobacterium smegmatis* proline iminopeptidase (EC 3.4.11.5). PepR2 was predicted to have the highest structural similarity with the known structure of *Thermoplasma acidophilum* proline iminopeptidase (EC 3.4.11.5). Predicted models of PepR1 and PepR2 are displayed in Fig. 5-29.

The likeliness of models is judged by indicative factors, including energy minimization of molecule, C-score, TM-score, RMSD, number of decoys and cluster density, and these values for prolinase models are summarized in Table 5-13. C-score is a confidence score for estimating the quality of the predicted model. C-score is calculated on the basis of the significance of threading template alignments and the convergence parameters of the structure assembly simulations (Zhang, 2008). C-score has a typical range of -5 to 2; where the larger the C-score shows the higher confidence. In the present study, C-scores of PepR1 and PepR2 using model *Thermoplasma acidophilum* proline iminopeptidase and *Mycobacterium smegmatis* proline iminopeptidase were 1.03 and 1.07, respectively, indicating the models with high confidence. TM-score is defined to assess the topological similarity between two structures. Both of TM-scores of PepR1 and PepR2 were larger than 0.5, which signified both models with correct topology. The TM-score larger than 0.5 was used to determine the structure class/protein family of the predicted query protein structure. A TM-score less than 0.17 would implicate a random similarity. RMSD is calculated from the average distances of all residue pairs with an equal weight (Kabsch, 1976). The RMSD between two prolinases was 5.45 Å. Values of RMSD of PepR1 and PepR2 were low, which indicated the modeling errors were small. Number of decoys is the number of structural decoys used in generating the model. The cluster density is the number of structure decoys at a unit of space in the cluster. Both of the cluster density of PepR1 and PepR2 were high, implicating that the structures occurred often in the simulation trajectory and were high quality fitted model. The results above agreed with that *L. plantarum* prolinases (PepR1 and PepR2) belonged to proline peptidase family PepI/PepL/PepR, having the most similar three-dimensional structure with PepI.

Table 5-13 Factors for protein structure modeling

	PepR1	PepR2
Model	*Thermoplasma acidophilum* proline iminopeptidase (PepI)	*Mycobacterium smegmatis* proline iminopeptidase (PepI)
Energy	-391.20	-413.04
C-score	1.03	1.07
TM-score	0.85 ± 0.08	0.86 ± 0.07
RMSD	4.1 ± 2.8 Å	4.0 ± 2.7 Å
No. of decoys	9432	10200
Cluster density	0.9091	0.9346

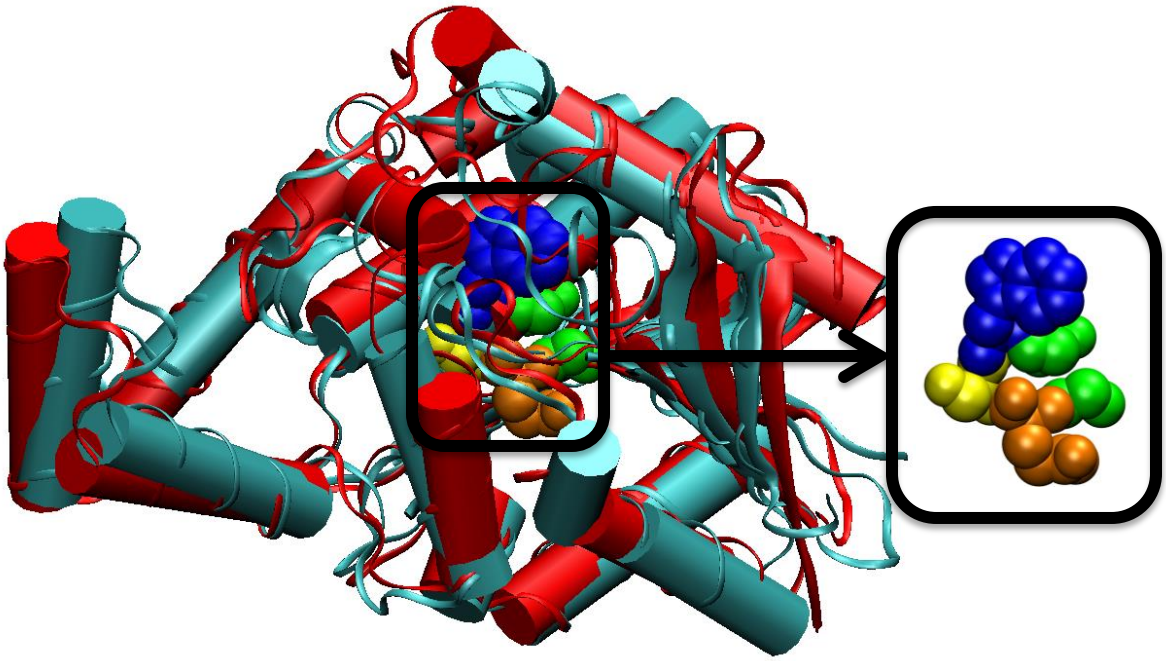

Fig. 5-29 Superimposed protein structure of prolinase PepR1 as well as PepR2 and their motif GQSWGG. PepR1 is red, PepR2 is cyan. Protein secondary structure of α-helix is displayed in the shape of cylinder, and β-sheet is in the shape of arrow. Motif GQSWGG residues are enlarged, with residue G (glycine) in green, residue Q (glutamine) in orange, residue S (serine) in yellow, residue W (tryptophan) in blue.

6 DISCUSSIONS

Prolinase (designate as PepR in bacteria) was first detected by Grassmann *et al.* (1932) and subsequently purified to varying degrees from porcine (Davis and Smith, 1953; Mayer and Nordwig, 1973), bovine kidney (Akrawi and Bailey, 1976 and 1977), human organs (Priestman and Butterworth, 1982 and 1985; Myara and Stalder, 1986; Miech *et al.*, 1988) and yeasts (Shao *et al.*, 1997; Luoma, 2001; Varmanen *et al.*, 1996 and 1998). Microbial PepR has been identified only in species of the genus *Lactobacillus* and it seems to be highly conserved in *Lactobacillus* with 65 to 75% identity (Champomier-Verges *et al.*, 2002). Generally, most of *Lactobacilli* have one gene corresponding to PepR; whereas *Lactobacillus plantarum* WCSF1 has two putative prolinases (PepR1 and PepR2).

Lactobacillus plantarum PepR1 and PepR2 were found to share 55.5% of DNA identity and their amino acid sequence shared 48.5% identity and 67% similarity, implicating their distance. Proteins with similar sequences adopt similar structures (Zuckerkandl and Pauling, 1965). Most protein pairs with more than 30% identical residues were found to be structurally similar (Sander and Schneider, 1991). Similarity hints that they might descent from a common ancestor. Homology search of the DNA sequences of *pep*R1 and *pep*R2 in Genbank database shows that *pep*R1 has 99% similarity with *pep*R from *Lactobacillus plantarum* 16 (Accession Number: CP006033.1) and *pep*R *Lactobacillus plantarum* ZJ316 (Accession Number: CP004082.1); whereas *pep*R2 has 99% similarity with *pep*R from *Lactobacillus plantarum* JDM1 (Accession Number: CP001617.1). In terms of amino acid identity, PepR1 shares 84%, 84%, and 83% identities with PepR from *Lactobacillus zeae* ATCC393 (Accession Number: BAF85818.1), PepR from *Lactobacillus rhamnosus* ATCC14957 (Accession Number: BAF85816.1), PepR from *Lactobacillus zeae* DSM20178 (Accession Number: BAF85817.1), respectively; PepR2 shares 51% with PepR from *Lactobacillus rhamnosus* (Accession Number: BAF85816.1) as well as PepR from *Lactobacillus zeae* (Accession Number: BAF85818.1 and BAF85817.1). Both of PepR1 and PepR2 have high amino acid sequence identities with iminopeptidase (PepI) as well

as aminopeptidase (PepL). PepR1 and PepR2 sharing low sequence identity can be assumed to have arisen by divergent evolution from the same ancestor. The divergent evolution may have lead PepR1 and PepR2 to becoming highly specific for their respective substrates and their substrate-binding pockets becoming different. However, their catalytic reactions remain similar, which may be due to some conserved residues in their active sites. Moreover, evolutionary pressure of the two putative prolinases not only contributes to diversity of catalytic activities but also adaptation in different pH and temperature niches. Thus, the evolutionary pressure may result in two forms of prolinases with compatible enzyme properties in PepR1 and PepR2.

In mammalian, it has been reported at least two forms of prolinases in human prostate (Masuda *et al.*, 1994), human skin fibroblasts (Butterworth and Priestman, 1982), human erythrocyte (Wang *et al.*, 2004), human leukocytes (Kodama *et al.*, 1989), and bovine kidneys (Neuman and Smith, 1951; Sarid *et al.*, 1962); whereas two forms of prolinases in microorganism have not been reported or investigated yet. The two forms of prolinases in human differ from each other in their molecular weights, their responses to preincubation with Mn^{2+}, their substrate specificities, the optimal pH, and thermal stability (Kodama *et al.*, 1989). Two forms of prolinases are clearly two isozymes, although the reason of two forms of prolinases presenting in human remains unknown. Regulatory mechanisms have been investigated on other isozymes (for instance, isozymes of lactate dehydrogenase (LDH)), which hint a reason to the presence of two forms of prolinase. Because of the enzyme regulatory mechanism, isozymes of LDH are expressed at different stages of development and in different tissues but having the same catalysis reaction. It may be due to regulatory mechanism of the two isozymes to supply prolinase activities under different conditions (or stimuli).

Prolinase (PepR) has been categorized using BLASTP analysis, multiple sequence alignments (MSA) and three-dimensional structure alignment (Liu *et al.*, 2010). These analyses show prolinase belongs to the prolyl oligopeptidase family (S33 family) of PepI/PepL/PepR (PepI: iminopeptidase, PepL: aminopeptidase). The family shares a consensus catalytic motif of GXSXGG, and this family is included in the clan of SC (serine carboxypeptidase), having the active site residues Ser-His-Asp in the sequence (Orengo *et al.*, 2013). The active site Ser occurs within the motif Gly-Xaa-Ser-Xbb-Gly, where Xaa can by any residue and Xbb is usually hydrophobic (Albertson and Koomey, 1993; Yoshimoto and Tsuru, 1985). Moreover, a hierarchical and structure-based classification of peptidases through MEROPS analyses indicates

close relationships of PepR (prolinase from *Lactobacillus*) to PepI (bacterial iminopeptidase from various species). (The MEROPS is an online database for peptidases and their inhibitors (Rawling and Barrett, 1993; Rawling *et al.*, 2004; http://merops.sanger.ac.uk).) The distances between peptidases are indicated in the indices of their MEROPS ID number. *Lactobacillus plantarum* WCFS1 PepR1 and PepR2 belong to the group of PepR (all *Lactobacillus*-type prolinases). Thus, both PepR1 and PepR2 have the MEROPS ID S33.004, whereas PepI is S33.001. The close MEROPS IDs of PepI and PepR1 as well as PepR2 indicate that they have a common ancestor, based on either the tertiary structures of them are similar or the active site residues are in the same order in the sequence (Rawlings *et al.*, 2008). It agrees with the present study that PepR1 and PepR2 have the most similar tertiary structures with PepI in computer modeling. The identification of the family and the clan of prolinase will assist better understanding of *L. plantarum* PepR1 as well as PepR2 for their similarity with the other members in the same family and clan, and their possible proteolytic mode. Peptidases under the category of clan SC, family S33 contains mainly exopeptidases that act at the N-terminus of peptides, preferably (but not exclusively) a Pro at N-terminal. The peptidases are usually serine proteases as their proteolytic mode. It agrees with Orengo's study (2013) that the peptidases have a catalytic triad of serine, histidine and aspartate in common: serine acts as a nucleophile, histidine as a base and aspartate as an electrophile. Most of these peptidases share similarity mechanisms, however, some exceptions exist as not being serine proteases. One of the exceptions is PepL (*Lactobacillus delbrueckii*), which is a metal-ion-activated enzyme (Bryce and Rabin, 1964). This may be an explanation for PepR1 and PepR2 within the same group but PepR1 was suggested as a metallo-protease in this research. PepL is also found to have multiple forms in *Drosophila melanogaster* (Beckman *et al.*, 1964) and *Pinus attenuate* (Conkle, 1971), which sheds the light on PepR possibly having two forms with different catalytic modes.

The studies in this thesis showed that PepR1 and PepR2 share similarity in their secondary structure, tertiary structure (also known as three-dimensional structure), and they are homotetrameric in their quaternary structure. Both of r-PepR1 and r-PepR2 from the present study showed a higher ratio of β-sheets (r-PepR1 37.90% and r-PepR2 54.10%) over other secondary components using CD test. The high ratio of β-sheets (54.10%) in r-PepR2 may contribute to the stability of the enzyme. β-sheets are more stable than helical regions of an enzyme at high temperature by investigating the folding and folding mechanism of β-lactamse

and RNase A (Vijayakumar *et al.*, 1993; Udgaonkar and Baldwin, 1990 and 1988). The stability of β-sheets is attributed in the hydrogen bonds. It was shown in Vijayakumar *et al.* study (1993) that the hydrogen bonds within the β-sheets region are protected to a greater extent than in the helical region and the protection factor is observed to increase with time from the start of folding. Compare with r-PepR2, r-PepR1 showed lower thermal stability (48 vs. 29°C) and lower β-sheet contents (54.1 vs. 37.9%). Although β-sheet content rules the stability of proteins and the stability is affected by the environment and experimental conditions (Vijayakumar *et al.*, 1993), the contents of β-sheets may be a reason of the less stable characteristic of r-PepR1. β-sheets are known in two arrangements: antiparallel and parallel. In the antiparallel arrangement, the hydrogen bonds are aligned directly opposite each other, making for short, strong and stable bonds. Contrarily, the parallel arrangement is less stable because the geometry of the individual amino acid molecules forces the hydrogen bonds to occur at an angle, making them long and thus weak (Perczel *et al.*, 2005). The antiparallel arrangement was 46.5 % of the total secondary structure of r-PepR2, whereas it is only 27.8% in r-PepR1, The contents of antiparallel in r-PepR1 is not significantly higher than the other components. The lower antiparallel β-sheet contents may be a factor of less stable nature of PepR1 compared with PepR2.

In the three-dimensional structural aspect, PepR1 and PepR2 have similar overall topology based on the homology model construction. r-PepR1 and r-PepR2 were evaluated to be homotetrameric in this study, corresponded to a previous finding. In the study of Shao *et al.* (1997), the PepR from *Lactobacillus helveticus* CNRZ32 has a native molecular mass of 125 kDa almost four-times of its subunits of 33 kDa. These structural similarities along with their Pro-Xaa hydrolytic capability can provide an evidence that both of these putative prolinases are truly prolinases. Their divergence in local regions of their structures provides them with important prerequisites to evolve and confer their differences on their characteristics.

In the characteristics aspects, r-PepR1 and r-PepR2 hydrolyze dipeptides having the N-terminal proline residue and broad specificity at the C-terminal including small residue (Gly), hydrophobic residue (Leu, Pro, Met), acid residue (Glu), nucleophilic residue (Ser), basic residue (Arg), and aromatic residue (Phe). While both enzymes can hydrolyze Pro-Xaa in general, the preferences towards the C-terminal residue are differed between them. r-PepR1 has the highest catalytic efficiency towards Pro-Met, whereas r-PepR2 prefers Pro-Gly. Previous studies also show that prolinase is a strict dipeptidase only hydrolyzing dipeptides but with a broad substrate

specificity (hydrolyzing some of dipeptides not containing the N-terminal proline residue) (Reith and Neidle, 1979; Priestman and Butterworth, 1985). The optimal pH for prolinase activity is normally found in the range pH7.5-8.3 at weak alkali condition (Masuda *et al.*, 1994). And the optimal temperature of reaction often reflects the optimal temperature for growth of the microorganism from which the prolinase originated (Gonzales and Robert-Baudouy, 1996). The optimal pH and temperature are agreed with the present study that r-PepR1 has the optimal activity at pH7.5 and at 25°C, while r-PepR2 at pH8.0 and at 30°C. r-PepR1 has the low optimal temperature related to its thermal stability, because it starts unfolding at 29°C (T_M).

The inhibition tests suggest that r-PepR1 is metallo-protease found by 38% reduced activity with 5 mM EDTA. In a metallo-protease, the metal resembles protons and they are electrophiles that they are able to accept an electron and form a chemical bond. EDTA inhibits metallo-protease by chelating with the metal (Lombardi *et al.*, 2011). The inhibition tests also suggest that r-PepR2 is in a serine-protease proteolytic mode found by 47% reduced activity with 1 mM PMSF. A serine protease usually has a catalytic triad Ser-His-Asp, where His acts as a base, a proton acceptor and remove the proton from the hydroxyl group of Ser in the triad. The deprotonation makes the serine residue more reactive and the deprotonated side chain attacks the carbon atom in a peptide bond of the substrate in nucleophilic manner. The negative charge of carboxylic acid group of Asp then stabilizes the positive charge given by protonation on the side chain of His (Blow *et al.*, 1969; Allen, 2010; Stroud, 1974). The active site of serine protease contains other resides that complete the catalytic triad or tetrad (Rawlings and Barrett, 1993) and their function mainly consists of polarizing hydroxyl group on Ser in order to allow the initial nucleophilic attack (Gonzales and Robert-Baudouy, 1996). PMSF reacts with the hydroxyl group of Ser and inhibits the binding between substrate and the serine proteases catalytic triad. Inhibition of PMSF suggests that r-PepR2 has a serine residue in the enzyme active site being a serine protease.

These observations suggested that pepR1 and PepR2 have different modes of catalysis despite of their similarity in the structures. The past research in prolinases showed that there are two different types of prolinase catalysis: metallo enzyme and serine proteinases. Prolinase from human kidney and swine kidney are activated with Mn^{2+} or Cd^{2+} as a metallo-protease (Butterworth and Priestman, 1982; Neuman and Smith, 1951; Sarid *et al.*, 1962), and the zinc protease PepR is found from *Mycobacterium tuberculosis* H37Rv (GenBank Accession Number:

NC000962.3). In contrast, prolinase from *Lactobacillus helveticus* and *Lactobacillus rhamnosus* are serine enzymes (Varmanen *et al.*, 1996 and 1998; Shao *et al.*, 1997; Dudley and Steele, 1994). These serine proteases have been further confirmed by genetic mutagenesis by replacing the serine residue in the catalytic triad. The results show that the prolinases from *L. helveticus* and *L. rhamnosus* have an identical catalytic site (GQSWGG) and the serine residue (Ser_{111}) is essential for catalysis. The enzyme catalytic mechanisms of PepR1 and PepR2 are not completely clear yet, but it suggests that PepR1 and PepR2 may evolve from different ancestral enzymes as evident in the differences found between human and bacterial prolinases. More investigations are required for further confirming the proteolytic modes of these two prolinases. The dependency of metal for prolinase isozymes activities may arise from the distinct feature of *L. plantarum.* The distinct feature of *L. plantarum* is the definite requirement for manganese (Goossens *et al.*, 2003). Manganese in *L. plantarum* serves as a prototypical biological role including structuring, activation of enzymes and so on. *L. plantarum* can tolerate up to 35 mM of Mn^{2+} and the concentrations of Mn^{2+} are different in extracellular and intracellular (Archibald and Fridovich, 1982; Hastings *et al.*, 1986). The intracellular accumulation of up to 35 mM of Mn^{2+} is regulated by a highly specific, high affinity, high velocity transport system (Hao *et al.*, 1999). The different concentrations of Mn^{2+} in *L. plantarum* may lead to the presence of two forms of prolinases being metal-dependent and metal-independent proteases.

Lactobacillus plantarum PepR1 and PepR2 are different to each other on their DNA sequences (only 55.5% identity), substrate specificity, the optimaml temperature and pH, enzyme kinetics with different K_m and k_{cat} values, thermal stability, proteolysis mode; whereas they have similarity in their secondary, tertiary and quaternary structures, and have the same enzymatic functionality (hydrolysis of Pro-Xaa). The features above suggest them to be multiple forms of prolinase and they could be defined as isozymes (Weeden and Wendel, 1990). The presence of two forms of prolinases may arise from the evolution and owing to unknown regulatory properties. Generally, the presence of isozymes is to allow fine adjustment of metabolism to meet the need of different development stages, and allow the use of the enzyme based on its environment (Berg *et al.*, 2002). The multiplicity of prolinase isozymes may also due to their distribution in the subcellular compartment. They might be cytosolic, mitochondrial, or plastid isozymes that are encoded by different locus (like glutamate dehydrogenase isozymes) (Cammaerts, 1983). The presence of prolinase isozymes may also preserve the functionality of

prolinase in case of the genetic problems by expressing the isozymes from two genetic loci (*pep*R1 and *pep*R2). Also as shown through the differences in catalytic modes, the multiplicity of prolinase isozymes may be due to evolution and have them change to improve their catalytic abilities to an extent in which they only share poor sequence homology. The prolinase isozymes exhibit widely divergent kinetic characteristics showing different preference towards various substrates, which consist in broadening the substrate specificity as prolinase. With a wider range of optimum temperature, pH and thermal stability, prolinase isozymes can complementarily and cooperatively contribute in maintaining the functionality of prolinase under different environments.

7 CONCLUSION

This research has revealed that putative *L. plantarum* PepR1 and PepR2 are truly prolinase cleaving iminodipeptides with the N-terminal proline. They can be applied in fermented foods manufacture for debittering, using the investigated fundamental information including the optimal conditions for enzyme activities, substrate specificities, kinetic parameters, proteolysis modes, enzyme structures (secondary, tertiary and quaternary structures). This research also showed several interesting characteristics of *L. plantarum* prolinases PepR1 and PepR2. They might be isozymes with structural similarity and the same enzymatic functionality but different characteristics. Depending on the environmental conditions, the proline recycling can be mediated through different characteristics of the two isozymes. These isozymes work together to hydrolyze bitter peptides as well as to compensate prolidase deficient activity with broader specificity, broader pH and temperature for their activities. The multicity characteristic of *L. plantarum* prolinases would contribute to reduce bitterness in fermented foods manufacture with higher efficiency.

8 PROSPECTIVE RESEARCH

For further research, the pure recombinant prolinases should be crystallized and analyzed for their structures by X-ray diffraction. The three-dimensional structure of recombinant prolinases would assist in better understanding the catalytic mechanisms of the enzymes. After obtaining the elaborate structural information, the protein molecules can be specifically altered by site-directed mutagenesis for confirming the active site of the recombinant prolinases in order to examine the suggestions of the proteolysis modes indicated in this study. The confirmation of the active site will elucidate the details of the catalytic mechanisms of the recombinant prolinases. It would be interesting to investigate the modes of proteolysis since the results in this research and other prolinase studies have not showed an unquestionable answer to it. The two prolinases provide a broader range of working pH, temperature, and substrate preferences, thus it could be applied as a treatment for prolidase deficiency patients as enzyme supplementation. Moreover, the role of PepR protein in growth and physiology or its possible biosynthesis and regulation in microbial is not clear. Previous observation showed that PepR was not a limiting enzyme for growth of *Lactobacillus helveticus* CNRZ32 in milk (Shao *et al.*, 1997). Investigation can be aimed at regulations of *pep*R1 and *pep*R2 transcription in response to growth conditions, and understanding the possible role of *pep*R1 and *pep*R2 in proline metabolism during growth and survival in the host which can explain the present of two forms of prolinases in *L. plantarum* WSCF1.

9 REFERENCES CITED

Allen, K. 2010. Acids and bases. Nature Chem. Biol. 10:1038-1043.

Albertson, N.H., and Koomey, M. 1993. Molecular cloning and characterization of a proline iminopeptidase gene from *Ineisseria gonorrhoeae*. Molecular. Micro. 9:1203-1211.

Akrawi, A.F., and Bailey, G.S. 1976. Purification and specificity of prolyl dipeptidase from bovine kidney. Biochim. Biophys. Acta. 422:170-178.

Akrawi, A.F., and Bailey, G.S. 1977. The separation of prolyl dipeptidase from other dipeptidases of bovine kidney. Biochem. Soc. Trans. 5:272-274.

Andrews, P. 1964. Estimation of the molecular weights of proteins by Sephadex gel-filtration. J. Biol. Chem. 91:222-233.

Archibald, F.S., Fridovich, I. 1982. Investigations of the state of manganese in *Lactobacillus plantarum*. Arch. Biochem. Biophys. 215:589-590.

Bates, P. A., Kelley, L.A., MacCallum, R.M., Sternberg, M.J.E. 2001. Enhancement of protein modeling by human intervention in applying the automatic programs 3D-JIGSAW and 3D-PSSM. Pro.: Str. Func. and Gene. 5:39-46.

Bates, P.A., Sternberg, M.J.E. 1999. Model building by comparison at CASP3: using expert knowledge and computer automation. Pro.: Str. Func. and Gene. 3:47-54.

Bates, P.A., Contreras-Moreira, B. 2002. Domain Fishing: a first step in protein comparative modeling. Bioinfo. 18:1141-1142.

Beckman, L., Scandalios, J.G., Brewbaker, J.L. 1964. Genetics of leucine aminopeptidase isozymes in maize. Gene. 50:899-904.

Berg, J.M., Tymoczko, J.L., Stryer, L. 2002. Isozymes provide a means of regulation specific to distinct tissues and developmental stages. Biochem. 5th Edit. New York. pp. 1137-1145.

Blow, D.M., Birkthoft, J.J., Hartley, B.S. 1969. Role of a buried acid group in the mechanism of action of chymotrypsin. Nature. 221"337-340.

Bohm, G., Muhr, R., Jaenicke, R. 1992. Quantitative analysis of protein far UV circular dichroism spectra by neural networks. Pro. Eng. 5:191-195.

Butterworth, J., and Priestman, D. 1982. Fluorimetric assay for prolinase and partial characterization in cultured skin fibroblasts. Clin. Chim. Acta. 122:51-60.

Butterworth, J., and Priestman, D. 1985. Prolinase and non-specific dipeptidase of human kidney. Biochem. J. 231:689-694.

Cader, S., Gouzy-Darmon, C., Petres, S., Piesse, C., Pham, V.L., Beinfeld, M.C., Cohen, P., Foulon, T. 2004. Expression and purification of rat recombinant aminopeptidase B secreted from baculovirus-infected insect cells. Pro. Expr. Purif. 36:19-30.

Cammaerts, D. 1983. A study of the polymorphism and the gentic control of the glutamate dehydrogenase isozymes in *Arabidopsis thaliana.* Plant Sci. Lett. 31:1-65.

Champomier-Verges, M. Marceau, A., Mera, T., Zagorec, M. 2002. The *pep*R gene of *Lactobacillus sakei* is positively regulated by anaerobiosis at the transcriptional level. App. And Environ. Microbial. 68:3873-3877.

Chant, A., Kraemer-Pecore, C.M., Watkin, R., Kneale, G.G. 2005. Attachment of a histidine tag to the minimal zinc finger protein of the *Aspergillus nidulans* gene regulatory protein AreA causes a conformational change at the DNA-binding site. Pro. Expr. Purif. 39:152-159.

Chen, H., Xu, Z., Xu, N., Cen, P. 2005. Efficient production of a soluble fusion protein containing human beta-defensin-2 in *E. coli* cell free system. J. Biotechnol. 115:307-315.

Conkle, M.T. 1971. Inheritance of alcohol dehydrogenase and leucine aminopeptidase isozymes in knobcone pine. Forest. Sci. 17:190-194.

Damina, F., Cunningham, B.O. 1997. Proline specific peptidases. Bioch. Biophy.Acta. 1343:160-186.

Danson, M.J., Hough, D.W., Russell, R.J.M., Taylor, G.L., Pearl, L. 1996. Enzyme thermostability and thermoactivity. Pro. Eng. 9:629-630.

Diaz, A., Taylor, C., Rodriguez, A., Pajon, R., Espinosa, R., Silva, R. 2004. Estimating molecular mass of the complex formed by the B transferrin binding protein (TbpB, Strain CU385) from *Neisseria meningitidis* and human transferrin using gel filtration chromatography and dynamic light scattering. Biotech. Appl. 21:153-157.

De Vries, E.G.E., de Hooge, M.N., Gietema, J.A., de Jong, S., Ferreira, C.G. 2003. Apoptosis: tager of cancer therapy. Clin Cancer. Res. 9:912.

Dudley, E.G. and Steele, J.L. 1994. Nucleotide sequence and distribution of the *pep*PN gene from *Lactobacillus helveticus* CNRZ32. FEMS Microbio. Lett. 119:41-45.

Duve, H., Johnsen, A.H., Scott, A.G., Thorpe, A. 1995. Regul. Pept. 57:237-245.

Dyson, M.R., Shadbolt, S.P., Vincent, K.J., Perera, R.L., McCafferty, J. 2004. Production of soluble mammalian proteins in *Eschrichia coli*: identification of protein features that correlate with successful expression. BMC. Biotechnol. 4:32.

Eisenhauer, D.A., McDonald, J.K. 1986. J. Biol. Chem. 261:8859-8865.

Fonda, I., Kenig, M., Gaberc-Porekar, V., Pristovaek, P., Menart, V. 2002. Attachment of histidine tags to recombinant tumor necrosis factoralpha drastically changes its properties. J. Sci. World. 15:1312-1325.

Fox, P.F. 1989. Proteolysis during cheese manufacture and ripening. J. Dairy Sci.. 72:1379 –1400.

Fox, P.F., and Law, J. 1991. Enzymology of cheese ripening. Food Biotechnol. 5**:**239–262.

Fox, P.F., and McSweeney, P. 1996a. Chemistry, biochemistry and control of cheese flavour. In Proceedings of the 4th Cheese Symposium, pp 135–159.

Fox, P.F., Wallace, J.M., Morgan, S., Lynch, C.M., Niland, E.J., and Tobin, J. 1996b. Acceleration of cheese ripening. Antonie van Leeuwenhoek. 70, 271-297.

Fox, P.F., and Wallace, J.M. 1997. Formation of flavour compounds in cheese. Ad. Appl. Micro. 45:17– 85.

Fukasawa, K., Fkasawa, K.M., Hiraoka, B.Y., Harada, M. 1983. Biochim. Biophys. Acta. 745:6-11.

Goldburg, W.I. 1999. Dynamic light scattering. Am. J. Phys. 67:1156-1160.

Gonzales, T., Robert-Baudouy, J. 1996. Bacterial aminopeptidases: properties and functions. FEM Micro. Rev. 18:319-344.

Goossens, D., Jonkers, D., Stobberingh, E., van den Bogaard, A., Russel, M., Stockbrugger, R. 2003. Probiotics in gastroenterology: indications and future perspectives. Scand. J. Gastroenterol. Suppl. 1:15-23.

Grappin, R., Rank, T.C., and Olson, N.F. 1985. Primary proteolysis of cheese proteins during ripening. J. Dairy Sci. 68:531–540.

Grassmann, W., Schoenebeck, O.V., Auerbach, G. 1932. Uber die enzymatische Spaltbarkeit der Prolinpeptide. II. Hoppe-Seyler's Z. Physiol. Chem. 210:1-14.

Greenfield, N.J. 2006. Using circular dichroism collected as a function of temperature to determine the thermodynamics of protein unfolding and binding interactions. NIH Public Access. 1:2527-2535.

Hammarstrom, M., Hellgren, N., van Den Berg, S., Berglund, H., Hard, T. 2002. Rapid screening for improved solubility of small human proteins produced as fusion proteins in *Escherichia coli*. Pro. Sci. 11:313-321.

Hao, Z., Chen, S., Wilson, D.B. 1999. Cloning, expression, and characterization of cadmium and manganese uptake genes from *Lactobacillus plantarum.* Appl. Environ. Microbiol. 65:4746-4752.

Hastings, J.W., Holzapfel, W.H., Niemand, J.G. 1986. Radiation resistance of *lactobacilli* isolated from radurized meat relative to growth and environment. Appl. Environ. Microbiol. 52:898-901.

Ishibashi, N., Ono, I., Kato, K., Shigenaga, T., Shinada, I., Okai, H., and Fukui, S. 1987. Role of the Hydrophobic Amino Acid Residue in the Bitterness of Peptides.

Ishibashi, N., Kubo, T., Chino, M., Fukui, H., Shinoda, I., Kikuchi, E., Okai, H., Fukui, S. 1988. Taste of Proline-containing Peptides. Agric. Biol. Chem. 52:95-98.

Jaenicke, R. 1996. Stability and folding of ultrastable proteins: eye lens crystallins and enzymes from thermophiles. FASEB. J. 10:84-92.

Jansson, J., Schillen, K., Olofsson, G., Silva, R.C., Loh, Watson. 2004. The interaction between PEO-PPO-PEO triblock copolymers and ionic surfactants in aqueous solution studied using light scattering and calorimetry. J. Phys. Chem. 108:82-92.

Jenny, R.J., Mann, K.G., Lundblad, R.L. 2003. A critical review of the methods for cleavage of fusion proteins with thrombin and factor Xa. Pro. Expr. Purif. 31:1-11.

Kabsch, W. 1976. Asolution for the best rotation to relate two sets of vectors. Acta Cryst. 32:922-923.

Keast, R.S.J., and Roper, J. 2007. A complex relationship among chemical concentration, detection, threshold, and suprathreshold intensity of bitter compounds. Chem. Senses. 32:245-253.

Kenig, M., Peternel, S., Gaberc-Porekar, V., Menart, V. 2005. Influence of the prtein oligomericity on final yield after affinity tag removal of recombinant proteins. J. Chromatogr. 1101:293-306.

Kim, K.M., Yi, E.C., Baker, D., Zhang, K.Y. 2001. Post-translational modification of the N-termianl His-tag interferes with the crystallization of the wild-type and mutant SH3 domains from chicken src tyrosine kinase. Acta Crystallogr. D. Biol. Crystallogr. 57:759-762.

Kirimura, J., Shimizu, A., Kimizuka, A., Ninomiya, T., Katsuya, N. 1969. The contribution of peptides and amino acids to the taste of fodd-stuffs. J. Agric. Food Chem. 17:689-695.

Kodama, H., Ohhashi, T., Ohba, C., Ohno, T., Arata, J., Kubonishi, I., Miyoshi, I. 1989. Characteristics and partial purification of prolidase and prolinase from leukocytes of a normal human and a patient with prolidase deficiency. Clin. Chim. Acta. 180:65-72.

Kwon, S.Y., Choi, Y.J., Kang, T.H., Lee, K.H., Cha, S.S., Kim, G.H., Lee. H., Kim, K.T., Kim, K.J. 2005. Highly efficient protein expression and purification using bacterial hemoglobin fusion vector. Plasmid. 53:274-282.

Lombardi, P.M., Cole, K.E., Dowling, D.P., Christianson, D.W. 2011. Structure, mechanism, and inhibition of histone deacetylases and related metalloenzymes. Curr. Opin. Struct. Biol. 21:735-743.

Light, A., Smith, E.L. 1963. In the proteins, 2nd ed., vol. l, p. 2. Ed. by Neurath, H. New York: Academic Press Inc.

Liu, M., Bayjanov, J.R., Renckens, B., Nauta, A., Siezen, R. 2010. The proteolytic system of lactic acid bacteria revisited: a genomic comparison. BMC. Genomics. 11:1471-2164.

Martins, J.T., Li, D.J., Baskin, L.B., Jialai, I., Keffer, J.H. 1996. Comparison of cardiac troponin I and lactate dehydrogenase isoenzymes for the late diagnosis of myocardial injury. American J. of Clin. Pathol. 106:705-708.

Masuda, S., Watanabe, H., Morioka, M., Fujita, Y., Ageta, T., Kodama, H. 1994. Characteristics of partially purified prolidase and prolinase from the human prostate. Acta Med Okayama. 48:173-179.

Mayer, A., Sharma, S.K., Tolner, B., Minton, N.P., Purdy, D., Amlot, P., Tharakan, G., Begent, R.H.H., Chester, K.A. 2004. Modifying an immunogenic epitope on a therapeutic protein: a step towards an improved system for antibody-directed enzyme prodrug therapy (ADEPT). Br. J. Cancer. 90:2402-2410.

Mayer, H., and Nordwig, A. 1973. The cleavage of prolyl peptides by kidney peptidases. Detection of a new peptidase capable of removing N-terminal proline. Hoppe-Seyler's Z. Physiol. Chem. 354:380-383.

Mcdonald, J.K., Callahan, P.X., Ellis, S., Smith, R.E., Barret, A.J., Dingle, T.J. 1971. Tissue Proteinases, Northholland, Amsterdam. pp.69-107.

McSweeney P. 2004. Biochemistry of cheese ripening. Inter. J. of Dairy Technol. 57:2-3.

Morel, F., Lamarque, M., Bissardon, I., Atlan, D., Galinier, A. 2001. Autoregulation of the biosynthesis of the CcpA-like protein, PepR1, in *Lactobacillus delbrueckii* subsp *bulgaricus*. J. Mol. Microbiol. Biothechnol. 3:63-66.

Muschol, M., Rosenberger, F. 1995. Interactions in undersaturated and supersaturated lysozyme solutions: Static and dynamic light scattering results. J. Chem. Phys. 103:10424-10432.

Nallamsetty, S., Waugh, D.S. 2005. Solubility-enhancing proteins MBP and NusA play a passive role during the folding of their fusion partners. Prot. Expr. Purif.

Neuman, R.E., Smith, E.L. 1951. Synthesis of proline and hydroxyproline peptides; their cleavage by prolinase. J. Biol. Chem. 193:97-111.

Nomura, K. 1986. FEBS. Lett. 209:235-238.

Orengo, C., Bateman, A., Uversky, V. 2013. Protein families: relating protein sequence, structure, and function. 1:302-303.

Pelton, J.T., McLean, L.R. 2000. Spectroscopic methods for analysis of protein secondary structure. Analyt. Bioch. 277:167-176.

Perczel, A., Gaspari, Z., Csizmadia, I.G. 2005. Structure and stability of β-pleated sheets. J. of Comput. Chem. 26:1155-1168.

Rajan, S.S., Lackland, H., Stein, S., Denhardt, D.T. 1998. Presence of an N-terminal polyhistidine tag facilitates stbale expression of an otherwise unstable N-terminal domain of mouse tissue inhibitor of metalloproteinase-1 in *Escherichia coli*. Pro. Expr. Purif. 13:67-72.

Rank T.C., Grappin R. and Olson N.F. 1985. Secondary proteolysis of cheese during ripening: a review. J. Dairy Sci. 68:801–805.

Rawlings, N.D., Barrett, A.J. 1993. Evolutionary families of peptidases. Biochem. J. 290:205-218.

Rawlings, N.D., Tolle, D.P., Barrett, A.J. 2004. Evolutionary families of peptidase inhibitors. Biochem. J. 378:705-716.

Rawlings, N.D., Morton, F.R., Kok, C.Y., Kong, J., Barrett, A.J. 2008. MEROPS: the peptidase database. Nucleic Acids Res. 36:320-325.

Reith, M.E.A., and Neidle, A. 1979. The isolation of two dipeptide hydrolases from mouse brain cytoplasm. Biochem. Biophys. Res. Commun. 90:794-800.

Roy, A., Kucukural, A., Zhang, Y. 2010. I-TASSER: a unified platform for automated protein structure and function prediction. Nature Protocals. 5:725-738.

Roy, A., Yang, J., Zhang, Y. 2012. Cofactor: an accurate comparative algorithm for structure-based protein function annotation. Nucl. Acids Res. 40:471-477.

Sander, C., and Schneider, R. 1991. Database of homology-derived protein structures and the structural meaning of sequence alignment. Proteins. 9:56-68.

Sarid, S., Berger, A., Katchalski, E. 1962. Proline iminopeptidase II. Purification and comparison with iminodipeptidase (prolinase). J. Biol. Chem. 237:2207-2212.

Schillen, K., Brown, W., Johnsen, R.M. 1994. Micellar sphere-to-rod transition in an aqueous triblock copolymer system. A dynamic light scattering study of translational and rotational diffusion. Macromol. 27:4825-4832.

Shao, W., Yuksel, G.U., Dudley, E.G., Parkin, K.L., Steele, J.L. 1997. Biochemical and Molecular Characterization of PepR, a Dipeptidase, from *Lactobacillus helveticus* CNRZ32. Appl. Envir. Micro. Sept. pp. 3438-3443.

Shi, S., Xue, J., Fan, K., Kou, G., Wang, H., Guo, Y. 2007. Preparation and characterization of recombinant protein ScFv(CD11c)-TRP2 for tumor therapy from inclusion bodies in *Escherichia coli*. Pro. Expr. Purif. 52:131-138.

Shinoda, I., Tada, M., Okai, H., Fukui, S. 1986. Bitter taste of H-Pro-Phe-Pro-Gly-Ile-Pro-OH corresponding to the partial sequence (positions 61-67) of bovine β-casein and related peptides. Agr. Biol. Chem. 50:1247-1254.

Smyth, D.R., Mrozkiewicz, M.K., McGrath, W.J., Listwan, P., Kobe, B. 2003. Crystal structures of fusion proteins with large-affinity tags. Pro. Sci. 12:1313-1322.

Sousa M.J., Ardo Y. and McSweeney P. 2001. Advances in the study of proteolysis in cheese during ripening. Inter. J. Dairy Sci. 11:327–345.

Strong, F.C. 1952. Theoretical basis of Bouguer-Beer Law of radiation absorption. Anal. Chem. 24:338-342

Stroud, R.M. 1974. A family of protein cutting enzymes. Sci. Am. 231:74-88.

Sun, Q.M., Chen, L.L., Cao, L., Fang, L., Chen, C., Hua, Z.C. 2005. An improved strategy for high-level production of human vasostatin 120-180. Biotechnol. Prog. 21:1048-1052.

Tamura, M., Mori, N., Miyoshi, T., Koyama, S., Kohri, H., Okai, H. 1990. Practical debittering using model peptides and related compounds. Agr. Biol. Chem. 54:41-51.

Tang, W., Sun, Z.Y., Pannell, R., Gurewich, V., Liu, J.N. 1997. An efficient system for production of recombinant urokinase-type plasminogen activator. Pro. Expr. Purif. 11:279-283.

Tanner, R.E., Herpigny, B., Chen, S.H., Rha, C.K. 1982. Conformational change of protein sodium dodecylsulfate complexes in solution: A study of dynamic light scattering. J. Chem. Phys. 76:3866-3869.

Troll, W., Lindsley, J. 1955. A photometric method for the determination of proline. J. Biol. Chem. 215:655-660.

Udgaokar, J.B., and Baldwin, R.L. 1998. NMR evidence for an early frame work intermediate on the folding pathway of ribonuclease A. Nature. 335:694-699.

Udgaokar, J.B., and Baldwin, R.L. 1990. Early folding intermediate of ribonuclease A. Proc. Natl. Acad. Sci. USA. 87:8197-8201.

Upadhyay V.K., McSweeney P., Magboul A. and Fox P.F. 2004. Proteolysis in cheese during ripening. In Cheese: Chemistry, Physics and Microbiology. Vol 1: General Aspects, 3rd edn, pp 391–434.

Vijayakumar, S., Vishveshwara, S., Ravishanker, G., Beveridge, D.L. 1993. Differential stability of β-sheets and α-helices in β-lactamase: a high temperature molecular dynamics study of unfolding intermediates. Biophys. J. 65:2304-2312.

Wang, W., Liu, G., Yamashita, K., Manabe, M., Kodama, H. 2004. Characteristics of prolinase against various iminodipeptides in erythrocyte lysates from a normal human and a patient with prolidase deficiency. Clin. Chem. Lab. Medic. 42:1102-1108.

Weeden, N.F., and Wendel, J.F. 1990. Genetics of plant isozymes. Isozymes in plant biology. in Soltis, D.E., and Soltis, P.S. eds. Chapman and Hall. London. pp.46-72.

Wettig, S.D., Novak, P., Verrall, R.E. 2002. Thermodynamic and aggregation properties of Gemini surfactant with hydroxyl substituted spacers in aqueous solutions. Langmuir. 18:5354-5359.

Wettig, S.D., Li, X., Verrall, R.E. 2003. Thermodynamic and aggregation properties of Gemini surfactant with epoxylated substituted spacers in aqueous solutions. Langmuir. 19:3666-3670.

Wilk, S. 1983. Life Sci. 33:2149-2157.

Wren, J.J., Wiggall, P.H. 1964. An improved colorimetric method for the determination of proline in the presence of other ninhydrin-positive compounds. J. Biol. Chem. 94:216-220.

Yaron, A., Naider, F. 1993. CRC Crit. Rev. Biochem. Mol. Biol. 28:31-81.

Yoshimoto, T., and Tsuru, D. 1985. Proline iminopeptidase from *Bacillus coagulans*: purification and enzymatic properties. Biochem. J. 97:1477-1485.

Zhang, Y. 2008. I-TASSER server for protein 3D structure prediction. BMC. Bioinfo. 9:40.

Zuckerkandl, E., and Pauling, L. 1965. Evolutionary divergence and convergence in proteins. Academic Press, New York. Bryson, V., and Vogel, H.J. (eds). pp. 97-166.